The Dissertation Committee for Jaemin Lee Certifies that this is the approved version of the following dissertation:

Loss of FlhE in the flagellar Type III secretion system allows proton influx into *Salmonella* and *Escherichia coli*

Committee:

Rasika M. Harshey, Supervisor

George Georgiou

Marvin Whiteley

Yan Jessie Zhang

M. Stephen Trent

Loss of FlhE in the flagellar Type III secretion system allows proton influx into *Salmonella* and *Escherichia coli*

by

Jaemin Lee, B.S

Dissertation

Presented to the Faculty of the Graduate School of

The University of Texas at Austin

in Partial Fulfillment

of the Requirements

for the Degree of

Doctor of Philosophy

The University of Texas at Austin

August 2012

Dedication

I would like to dedicate this dissertation to my Lord and Savior Jesus Christ, who guided me through these years of Graudate School as a part of his greater plan. Also, he continued to provide me strength to finish my work. I also dedicate this dissertation to my loving parents for their encouragement and continuous prayer support.

Acknowledgements

First of all, I would like to thank my advisor Dr. Rasika Harshey for her continuous support and guidance through my graduate training. Her aggressive scientific mind and enthusiasm for research are responsible for my professional development. It has been a great experience for me to work with a scientist like her. I also thank Dr. Art Monzingo for his great help with the protein crystallization. I extend my gratitude to my committee members, Dr. George Georgiou, Dr. Marvin Whiteley, Dr. Stephen Trent, and Dr. Yan Jessie Zhang for their time and advice.

I am grateful for the friendship and scientific discussions from past and present members in Dr. Harshey's and Dr. Jayaram's laboratories. I would like to especially thank Dr. Qingfeng Wang for helping me learn basic skills for the swarming and microarray, Dr. Jon Partidge and Vincent Nieto for their discussions and help with editing and Dr. Rudra Saha for his discussion about the protein crystallization.

I would to thank my friends Bomsoo Cho and Jae Sook Park for their great friendship. I also want to thank Yonghwan Kim for helping me to get settled in Austin and Suk Ho Eun for helping me get through core courses. Special thanks to my pastor David Dae-young Kim and his wife Myoung-sook Kim, and my friend Jihyun Kim for their love and prayers.

Finally, I would like to thank my parents for their love and support through my life and for their continuous prayer. I also thank my sisters and brothers-in a law for their love and encouragement.

Loss of FlhE in the flagellar Type III secretion system allows proton influx into *Salmonella* and *Escherichia coli*

Jaemin Lee, Ph.D.

The University of Texas at Austin, 2012

Supervisor: Rasika M. Harshey

flhE belongs to the *flhBAE* flagellar operon in Enterobacteria, whose first two members function in Type III secretion (T3S). In *Salmonella enterica*, absence of FlhE affects swarming but not swimming motility. Based on a chance observation of a 'green' colony phenotype of *flhE* mutants on pH indicator plates containing glucose, I have established that this phenotype is associated with lysis of flagellated cells in an acidic environment created by glucose metabolism. The *flhE* mutant phenotype of *Escherichia coli* is similar overall to that of *S. enterica,* but is seen in the absence of glucose and unlike in *S. enterica*, causes a substantial growth defect. *flhE* mutants have a lowered cytoplasmic pH in both bacteria, indicative of a proton leak. GFP reporter assays indicate that the leak is dependent on the flagellar system, is present before the T3S system switches to secretion of late substrates, but gets worse after the switch and upon filament assembly, leading to cell lysis. I show that FlhE is a periplasmic protein, which co-purifies with flagellar basal bodies. Also, co-localization of fluorescent fusion proteins suggests a plausible interaction between FlhE and FlhA, implicated in channeling protons

for PMF-driven secretion. These results imply that FlhE may act as a plug or a chaperone to regulate proton flow through the flagellar T3S system. I have obtained crystals of the FlhE protein. X-ray data show that the FlhE crystal belongs to space group $P2_12_12_1$ and is diffracted to 2.02 Å. Completion of this study will contribute to a better understanding of the proposed role of FlhE.

Table of Contents

List of Tables

List of Figures

CHAPTER 1: Introduction

1.1 FLAGELLAR STRUCTURE

Many wild-type strains of *Escherichia coli* (*E. coli*) and *Salmonella enterica* serovar Typhimurium (*S. enterica or Salmonella*) are motile. Their motility is facilitated by flagellar rotation. The flagellar structure and its assembly have been intensively studied (Macnab, 2003; Harshey, 2011). The number of flagella is varied, but is typically around 6 to 8 per cell, distributed randomly over the cell surface in a 'peritrichous' pattern (Fig. 1.1A). Each flagellum consists of three main parts, the basal body, the external hook, and the filament, made of approximately 25 different proteins with varying stoichiometries ranging from a few to several thousand subunits (Fig. 1.1B).

The basal body is a complex structure, embedded within the cell surface (DePamphilis & Adler, 1971). It consists of several rings either attached to or surrounding a central membrane-spanning rod. The moving rotor and stationary stators constitute the motor. The moving parts of the basal body include the cytoplasmic C ring, the MS ring in the cytoplasmic membrane, and the periplasmic rod. The non-moving parts include the force-generating stators (Mot proteins) surrounding the MS ring, and the L and P rings. Stators conduct protons, delivering them at the rotor-stator interface near the C ring, thus powering rotation by proton motive force (PMF) (Minamino & Namba, 2008; Paul et al, 2008). The C ring functions in both motor rotation and rotor switching. The rod is 25 nm long and extends from the MS ring to the outer membrane. Several

proteins make up its discrete proximal and distal portions. The rod functions as a drive shaft to transmit torque generated at the rotor-stator interface to the external filament. The L and P rings, located in the outer membrane and the peptidoglycan layer, respectively, function as a bushing complex, forming a pore through which the rod exits the outer membrane.

The hook is a 55 nm long curved structure that serves as a flexible joint connecting the basal body to the filament. It is built from a single protein FlgE (Jones et al, 1990; Hirano et al, 1994). The hook is shorter and less rigid than the filament (Block et al, 1989).

The filament is helical (left-handed under normal conditions), and is assembled from thousands of subunits of a single protein flagellin, capped at its tip by a structure made of the FliD protein. *E. coli* only makes a single flagellin protein FliC, whereas *Salmonella* has two types of flagellins, FljB and FliC, whose expression is alternately controlled by flagellar phase variation (Bonifield & Hughes, 2003). The biological significance of the alternate forms is not known. The FliD cap permits the correct folding and polymerization of secreted flagellin subunits (Ikeda et al, 1996). Two hook-associated proteins or HAPs (FlgK and FlgL) form a short hook-filament junction and work as structural adaptors between the flexible hook and the rigid filament (Ikeda et al, 1989). In the absence of either the HAP proteins or FliD, filament assembly fails, and flagellin subunits are secreted into the medium (Homma et al, 1984). The filament has a diameter of ~20 nm, and its size varies, ranging from 5 to 10 μm (Brumell & Grinstein,

2004; Di Tommaso et al, 2011). The high rigidity and the helical shape of the filament allows it to function as a propeller (Fujime et al, 1972).

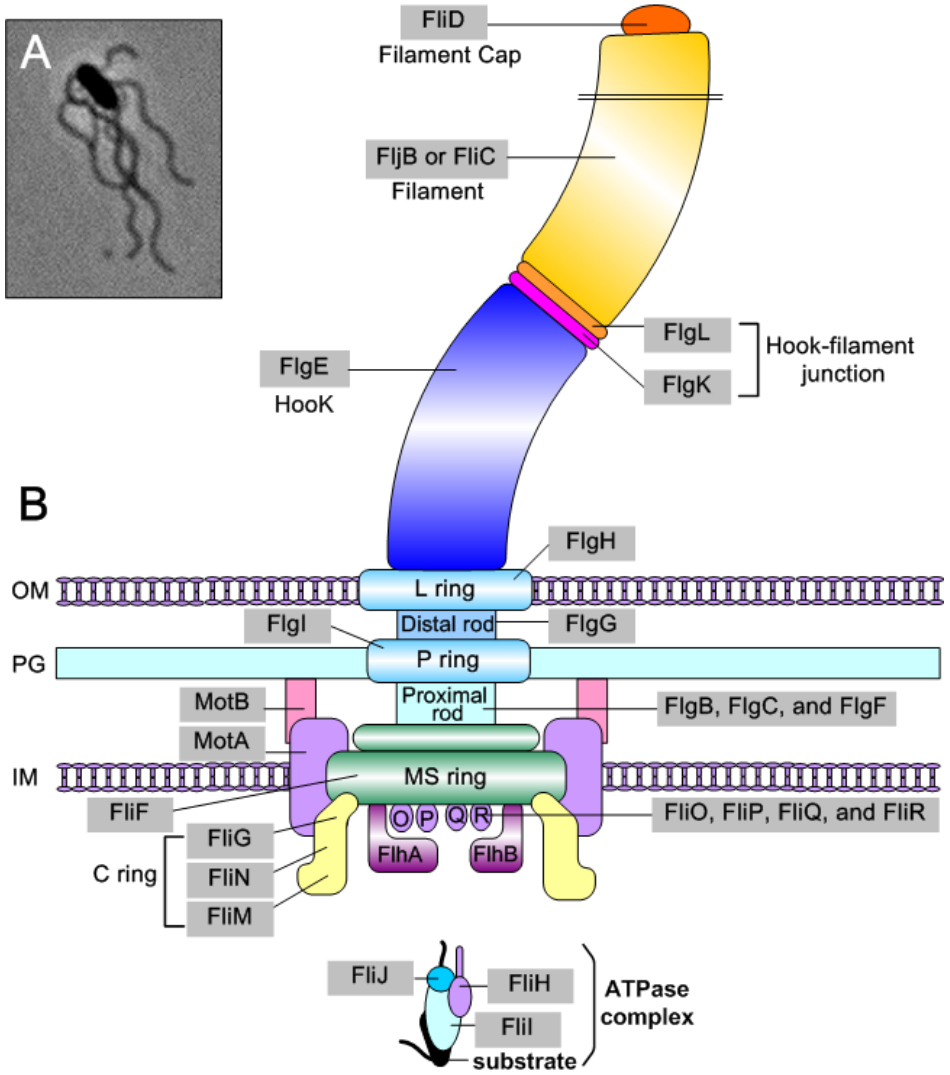

Fig. 1.1. The flagellum of *S. enterica*. **A**. A single bacterium with peritrichous flagella visualized by silver staining. **B**. Schematic of the flagellar structure. The basal body constitutes that part of the flagellum which is embedded in the membrane, including the attached cytoplasmic C ring. The hook and filament are external to it. The rod cap (FlgJ) and the hook cap (FlgD), which are transiently associated during rod and hook polymerization, respectively, are not shown. FliK (not shown) is secreted during rod-hook polymerization and functions as a molecular ruler. See text for other details. OM, outer membrane; PG, peptidoglycan; IM, inner or cytoplasmic membrane.

1.2 FLAGELLAR GENE HIERARCHY

The *Salmonella* flagellar regulon includes more than 60 genes, organized in a transcriptional hierarchy based on 3 promoter classes - P_{class1}, P_{class2}, and P_{class3} (Chilcott & Hughes, 2000; Frye et al, 2006) (Fig. 1.2). The regulation of these promoter classes is temporal and is responsive to flagellar assembly (Karlinsey et al, 2000). Among Gram-negative enteric bacteria with peritrichous flagella, this system is well conserved.

The P_{class1} promoter genes are under control of global regulatory signals and encode the master flagellar operon *flhDC* (Kutsukake, 1997). $FlhD_4C_2$ forms the master transcriptional activator complex (Wang et al, 2006b). This complex, together with a sigma factor (σ^{70}), transcribes the P_{class2} promoter genes (Kutsukake et al, 1990; Liu & Matsumura, 1994), which encode the structural subunits of the hook and basal body (HBB), and two regulatory proteins FlgM and FliA (σ^{28}). FlgM is an anti-σ^{28} protein that binds and sequesters the sigma factor (Kutsukake et al, 1994). After hook synthesis is completed, FlgM is secreted outside the cell through the HBB structure, releasing σ^{28} to activate P_{class3} promoter genes (Hughes et al, 1993). P_{class3} or late flagellar genes include those for the filament, Mot proteins, and chemotaxis proteins (Aldridge et al, 2006b).

1.3 TRANSCRIPTIONAL REGULATION

The master $FlhD_4C_2$ regulator controls its own synthesis by inhibiting the P_{class1} promoter (Kutsukake, 1997) (Fig. 1.2). Activation of P_{class2} by $FlhD_4C_2$ sets up the σ^{28}-FlgM interaction important for controlling the expression of P_{class3} genes (Saini et al, 2011). However, a recent model predicts that P_{class3} activity is not as a direct consequence

of the transcriptional hierarchy, but is rather due to the rate of FlgM secretion. The cell uses FlgM secretion as a proxy measure for estimating HBB numbers, setting up a regulatory circuit that continuously tunes the timing and magnitude of P_{class3} activity, thereby controlling flagella numbers.

In addition to the transcriptional factors, other proteins that fine-tune flagellar gene expression include the flagellar chaperones FlgN and FliT, a transcriptional factor FliZ, and an EAL domain protein YdiV (Fig. 1.2). FlgN is a chaperone for the HAP proteins FlgK and FlgL, which aids in the secretion of these proteins (Bennett et al, 2001). FlgN also increases the translation of FlgM from P_{class3} transcript. The regulatory function of FlgN is suppressed when the secretion of FlgK and FlgL is inhibited (Tapley et al, 2010). FliT is a chaperone for FliD, and also works as a negative regulator of $FlhD_4C_2$ by binding to $FlhD_4C_2$ and inhibiting its function (Yamamoto & Kutsukake, 2006). FliZ, a P_{class2} protein, activates the P_{class1} promoter by regulating $FlhD_4C_2$ protein levels positively in a post-translation manner (Saini et al, 2008). YdiV, a protein with an EAL domain signature generally associated with a cyclic-di-GMP phosphodiesterase function (Simm et al, 2004), works as a negative regulator for flagellar gene expression by inhibiting $FlhD_4C_2$ binding to the P_{class2} promoter and targeting it for ClpXP degradation (Muller & Sinn, 1977; Takaya et al, 2012).

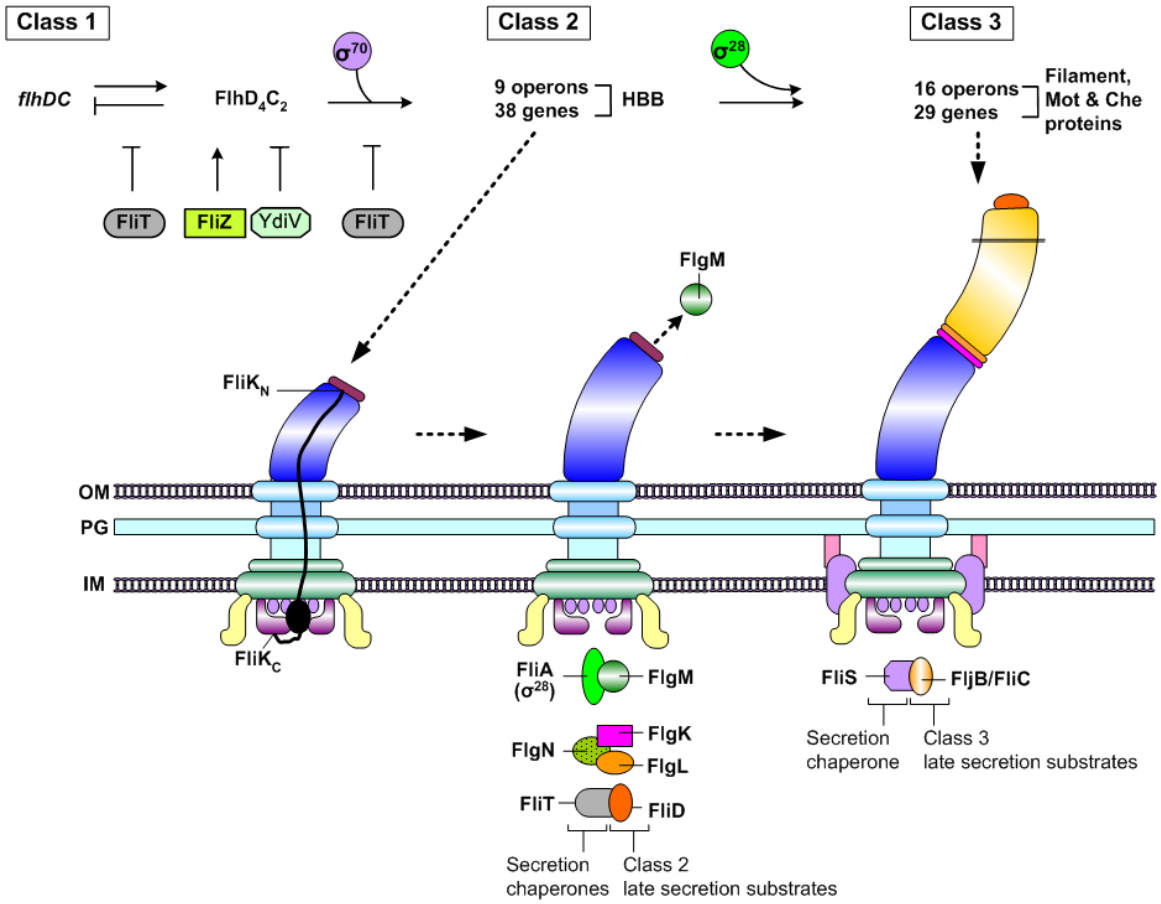

Fig. 1.2. Hierachy of flagellar gene regulation in *S. enterica*. See text for details. Adapted from Harshey, 2012.

1.4 FLAGELLAR ASSEMBLY

1.4.1 Flagellar assembly pathway

Following the transcription regulatory cascade described above, flagellum assembly begins inside the cell (Fig. 1.3). Integral flagellar membrane components comprising the MS (FliF), L (FlgI) and P (FlgH) rings, flagellar Type III secretion (T3S) complex (FlhA, FlhB, FliO, FliP, FliQ, and FliR), as well as stators (MotA, MotB) are all thought to self-assemble or be incorporated at their functional sites through export via the general secretory pathway Sec of *E. coli* (Macnab, 2003). All other flagellar components located beyond the cytoplasmic membrane are exported by the flagellar T3S system (Macnab, 2003). Table 1.1 lists the function and location of all flagellar components.

The first step in flagellar assembly is thought to be formation of the MS ring in the inner membrane, because the MS ring protein FliF was observed to self-assemble when overexpressed (Ueno et al, 1992; Katayama et al, 1996). This view may have to be revised based on the results of a recent study, where a number of fluorescent protein fusions to motor components were generated and their order of assembly was monitored (Li & Sourjik, 2011). FliF-YFP oligomerization was seen to be promoted by the T3S protein FlhA, whose self-assembly was more robust compared to FliF. The data were interpreted as suggesting that assembly of the basal body is initiated by oligomerization of FlhA, which then promotes MS ring assembly.

The MS ring serves as a mounting platform for the C ring, which constitutes the rotor/switch complex (composed of proteins FliG, FliM, and FliN) (Kubori et al, 1997; Li & Sourjik, 2011). After assembly of the C ring, the rest of the flagellar T3S apparatus is

thought to assemble within the central pore of the MS ring. The T3S system then exports the remaining flagellar components in an ordered manner to self-polymerize into the rod, hook and filament structures (Minamino et al, 2008). This system, which also uses PMF to drive secretion (Chevance & Hughes, 2008), will be described in more detail in Chapter 1.4.2.

The proximal rod (FliE, FlgB, FlgC, and FlgF) and the distal rod (FlgG) components are exported sequentially and assembled accordingly. FlgJ, the rod cap, has both binding affinity for the rod proteins in its N-termnal domain as well as muramidase activity in its C-terminal domain (Nambu et al, 1999; Hirano et al, 2001). The cap activity is essential for rod polymerization whereas the muramidase activity digests the peptidoglycan layer locally, allowing passage of the rod structure through the periplasm.

After completion of the rod and its associated L and P rings, the rod cap is discarded and replaced with the hook cap (FlgD), with the hook subunits (FlgE) added beneath the cap (Ohnishi et al, 1994). Hook development is completed when the hook reaches an approximate length of 55 nm. For hook length control, FliK and FlhB are intimately involved (Hirano et al, 1994). This mechanism will be described in Chapter 1.4.3. Completion of the hook signals the secretion of late substrates, which includes the anti-sigma factor FlgM. This releases σ^{28} (FliA) to transcribe the P_{class3} promoter genes. The hook cap is now discarded and replaced sequentially by three hook-associated proteins: the first hook-associated protein (FlgK), the second hook-associated protein (FlgL), and the filament cap protein (FliD) (Ikeda et al, 1987). FliD forms a filament cap beneath which flagellin subunits (FliC or FljB) polymerize to form the filament

(Yonekura et al, 2000). The stators are incorporated into the cytoplasmic membrane surrounding the MS ring (Hughes et al, 1993).

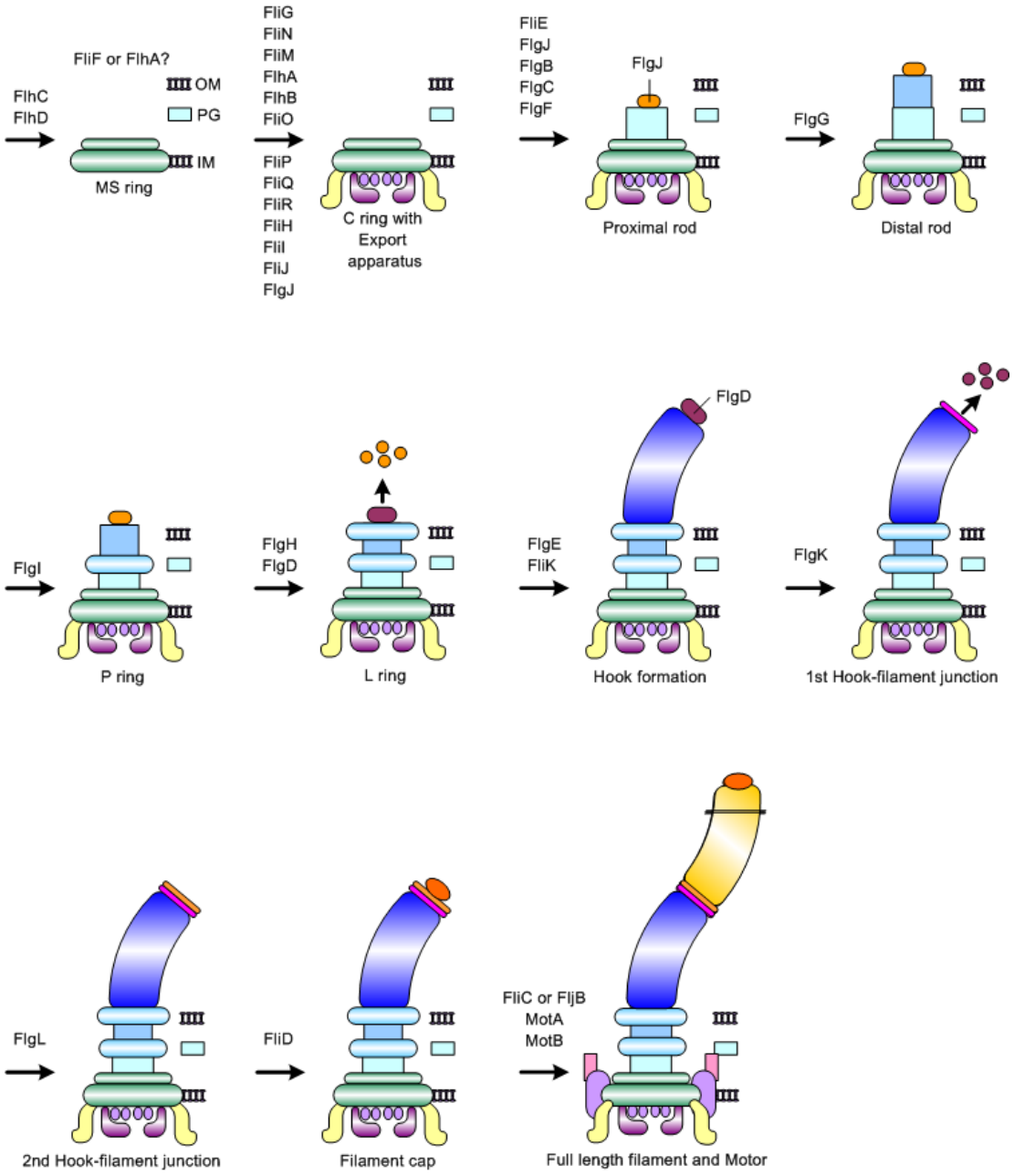

Fig. 1.3. Morphogenetic flagellar assembly pathway of *Salmonella*. See text for description. Adapted from Macnab, 2003.

Table 1.1. Flagellar proteins arranged by cellular location. Adapted from Macnab, 2003.

Protein	Common name and function	Cellular location
FliI	ATPase; facilitates the release and disassembly of the FliH-FliI complex from the flagellar T3S gate	Cytoplasm
FliH	Negative regulator of FliI	Cytoplasm
FliJ	General chaperone	Cytoplasm
FlgN	FlgK-, FlgL-specific chaperone	Cytoplasm
FliS	FliC-specific chaperone	Cytoplasm
FliT	FliD-specific chaperone	Cytoplasm
FliG	C ring; rotor/switch protein; torque generation; strong interaction with MS ring	Peripheral
FliM	C ring; rotor/switch protein; target for CheY-P binding	Peripheral
FliN	C ring; rotor/switch protein	Peripheral
FliF	MS ring protein; mounting flange for rotor/switch and rod; housing for T3S apparatus	Cytoplasmic membrane
MotA	Stator protein; exerts torque against rotor/switch	Cytoplasmic membrane
MotB	Stator protein; converts proton energy into torque	Cytoplasmic membrane
FlhA	T3S component; target for soluble export complex	Center of MS ring
FlhB	T3S component; substrate specificity switch; target for soluble export complex	Center of MS ring
FliO	T3S component	Center of MS ring
FliP	T3S component	Center of MS ring
FliQ	T3S component	Center of MS ring
FliR	T3S component	Center of MS ring
FliE	MS ring rod junction protein; T3S gate	Periplasmic space
FlgB	Rod protein; transmission shaft	Periplasmic space
FlgC	Rod protein; transmission shaft	Periplasmic space
FlgF	Rod protein; transmission shaft	Periplasmic space
FlgG	Distal rod protein; transmission shaft	Periplasmic space
FlgJ	Rod capping protein; muramidase	Periplasmic space
FlgI	P ring protein; part of bushing; internal disulfide bridge	Periplasmic space
FlgA	Chaperone for P ring protein	Periplasmic space
FlgH	L ring protein; part of bushing; lipoprotein	Outer membrane
FlgD	Hook-capping protein	Cell exterior
FlgE	Hook protein	Cell exterior
FliK	Hook-length-control protein	Cell exterior
FlgK	HAP1; first hook-filament junction protein	Cell exterior
FlgL	HAP2; second hook-filament junction protein	Cell exterior
FliD	Filament-capping protein; flagellin folding chaperone	Cell exterior
FliC	Filament protein; flagellin	Cell exterior

1.4.2 Type III secretion apparatus

Bacteria have many distinct pathways to translocate proteins across the inner and outer membranes. The T3S export apparatus dedicated to flagellar protein transport faces the cytoplasmic side of the basal body, and translocates proteins through a narrow rod/filament channel about 2.5 nm in diameter (Brumell & Grinstein, 2004). Thus, the flagellar proteins to be exported must be largely unfolded for entry into and translocation through the channel. A homologous T3S system is used as an injectisome in many Gram-negative bacteria to secrete virulence factors into host cells (Winfield & Groisman, 2003). All T3SSs share the following common features: (1) the secretion signal is usually a structurally disordered N-terminal peptide (Namba, 2001), (2) specific secretion chaperones associated with the substrates stabilize or target their cognate substrates (Parsot et al, 2003), and (3) secretion across the inner membrane is PMF-dependent and coupled with ATP hydrolysis (Minamino & Namba, 2008).

As illustrated in Fig. 1.4, the flagellar T3S apparatus consists of six integral membrane proteins (FlhA, FlhB, FliO, FliP, FliQ, FiR), and three soluble components (FliH, FliI, FliJ) (Minamino & Macnab, 1999). Four other cytoplasmic proteins act as substrate-specific chaperones (FlgN, FliA, FliS, FliT; shown in Fig. 1.2). FliH/I/J form the ATPase complex, which plays an important role in substrate recognition and escort of the chaperone-substrate complex to the export gate (Hosking et al, 2006). FliI is an ATPase, whose catalytic domain shows extensive similarity to the catalytic α and β subunits of F_0F_1-ATPase synthase (Hamilton-Miller, 1966; Kojima et al, 2009). In the cytoplasm, FliI forms a stable hetero-trimeric complex with FliH ($FliH_2$-FliI). FliH is a

negative regulator of FliI (Shaner et al, 2005) and plays an important role in effective docking of FliI to FlhA and FlhB (Minamino & Namba, 2008). FliI forms a stable homo-hexameric ring in the presence of ATP and phospholipids to fully exert its ATPase activity (Lin et al, 1995; Wilks & Slonczewski, 2007). FliJ is a general chaperone of flagellar secretion substrates and interacts with FliH, FliI, and the cytoplasmic regions of FlhA and FlhB (Minamino & MacNab, 2000; Merdanovic et al, 2011; Gonzalez-Pedrajo et al, 2002; Fraser et al, 2003a). Export of flagellar substrates is facilitated by PMF itself, and does not require FliI (Minamino & Namba, 2008; Paul et al, 2008). When the catalytic site of FliI was mutated to have no ATPase activity, the binding of $FliH_2FliI$ complex to the export gate totally inhibited the export process, suggesting that the energy of ATP hydrolysis energy is required to promote the release of the complex from the export gate (Minamino & Namba, 2008).

FlhA and FlhB have substantial cytoplasmic domains, which play an important role in docking the ATPase complex (Erhardt & Hughes, 2010; Konishi et al, 2009). The C ring proteins (FliG, FliM, FliN) responsible for torque generation and switching motor direction are also important for flagellar assembly; FliN interacts with FliH, and FliM interacts with FliJ (Gonzalez-Pedrajo et al, 2006). The proposed general mechanism for the export is showed in Fig. 1.4. First, the ATPase complex binds to substrate proteins ($FliH_2FliI$-FliJ-substrate complex) in the cytoplasm and this complex binds to FliN in the C ring, increasing the local concentration of the complex to promote substrate delivery to the cytoplasmic regions of FlhA and FlhB. Interactin of FliJ with FliM promotes release of the $FliH_2FliI$-substrate complex from the C ring. This complex now docks to the FlhA-

FlhB platform where FliI subunits form the hexamer ring. The substrates are then translocated through the export channel by PMF. Later, the complex is released from the export gate by the energy from ATP hydrolysis (Minamino et al, 2008; Harshey, 2011). FlhA is implicated in harboring the proton channel for PMF-driven secretion (Hara et al, 2011). FlhB is important for the late stage of secretion, where a change in its conformation acts as a switch to allow export of late substrates (Ferris & Minamino, 2006) (see below). The roles of the other T3S components - FliO, FliP, FliQ, FliR - are not yet understood.

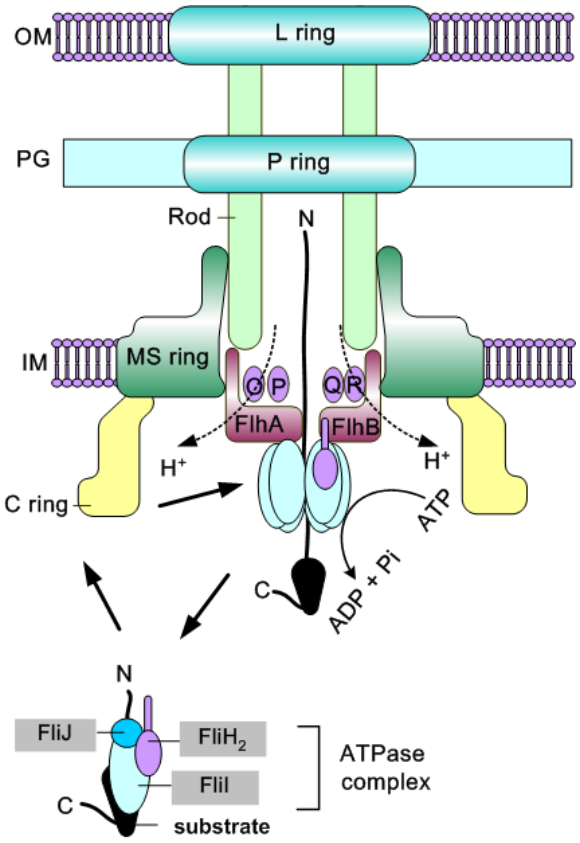

Fig. 1.4. Flagellar Type III secretion. See text for details.

1.4.3 Late secretion switch

During flagellar assembly, there is a morphological checkpoint between rod-hook formation and filament formation. Prior to hook completion, rod and hook proteins are exported most efficiently, but after the hook reaches its optimal length of 55 nm (or the rod-hook reach a combined length of 75 nm), late flagellar substrates are more efficiently exported (Minamino & Macnab, 1999; Wollmann & Zeth, 2006). Two key players – FliK and FlhB – determine the rod-hook length and the switch to late secretion, respectively (Fig. 1.5).

FlhB and the switch to late secretion. During HBB assembly, FliK is secreted through the flagellar export apparatus (Boggon & Shapiro, 2000). FliK binds strongly to the hook cap protein FlgD and weakly to the hook protein FlgE (Moriya et al, 2006). Absence of FliK affects hook-length control, resulting in abnormally long 'polyhooks' (Hirano et al, 1994). These mutants are unable to secrete the late substrates and are non-motile (Patterson-Delafield et al, 1973). Motile revertants of the *fliK* mutants were mapped to the *flhB* locus (Hirano et al, 1994), but these revertants in *flhB* still lost the control of the hook length. It was suggested that FlhB is involved primarily in switching but that FliK is involved in both switching and hook length determination. The study of suppressors suggested that the interaction between C-terminal region of FliK and FlhB is required for the substrate-specificity switching. FlhB has a large C-terminal cytoplasmic domain (Minamino et al, 1994), which is specifically cleaved between Asn-269 and Pro-270 during the switching event (Otwinowski & Minor, 1997). An *in vitro* assay for FlhB cleavage showed it to be an autocatalytic process (Ferris et al, 2005). A non-cleavable

mutant of FlhB does not flip the secretion specificity, suggesting that the cleavage event is essential for the switch (Fraser et al, 2003b).

Rod-hook length control. A ruler model for rod-hook length control has posited that FliK serves as a molecular ruler by being secreted intermittently (Ferris & Minamino, 2006; Shibata et al, 2007; Erhardt et al, 2011). When the rod-hook reaches its mature length of 75 nm, interaction of the FliK N-terminus ($FliK_N$) with the assembled hook cap (FlgD) is proposed to elicit a pause in FliK secretion. If the C-terminus of FliK ($FliK_C$) is near the C-terminus of FlhB ($FlhB_C$) when the pause occurs, which happens only when the hook has reached its specific length, their interaction causes auto-cleavage of FlhB, flipping the switch to a late secretion mode. A second non-flagellar regulatory protein (RflH/Flk) also controls the substrate specificity switch in an unknown manner (Aldridge et al, 2006a). Proteolytic cleavage of FlhB first promotes FlgM secretion, relieving the repression of σ^{28} and allowing late gene expression. Efficient secretion of all late protein substrates requires dedicated chaperones.

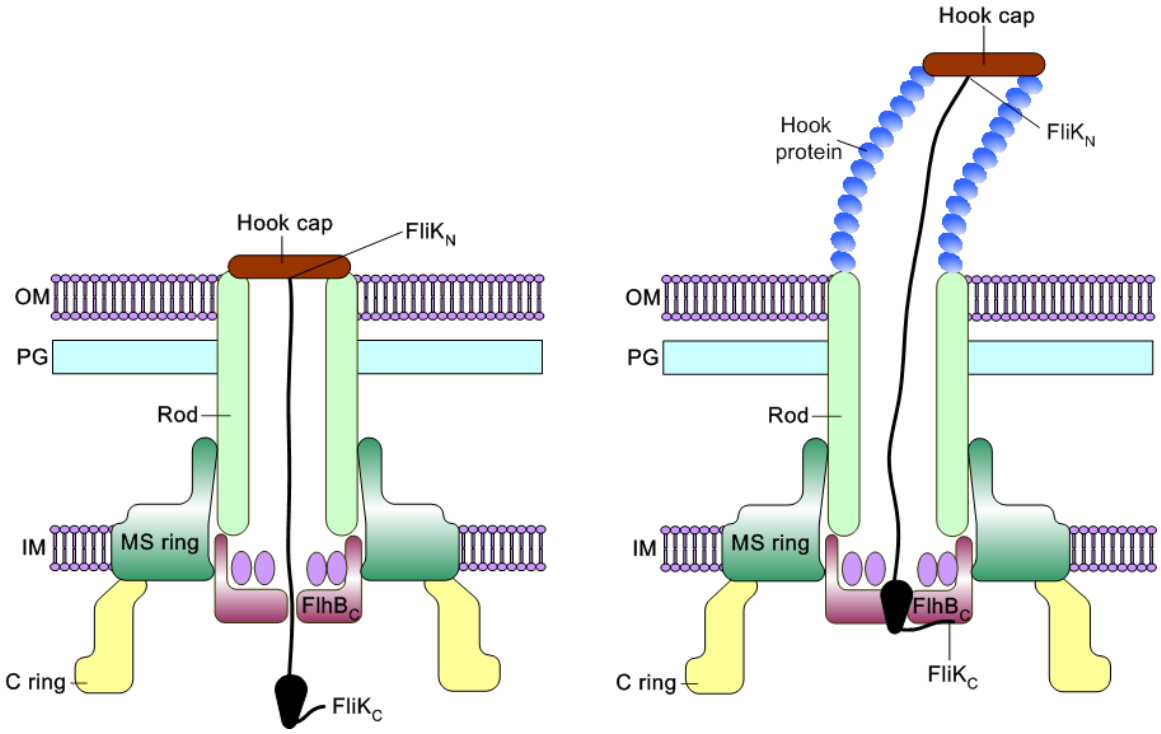

Fig. 1.5. Hook length control by the molecular ruler FliK, adapted from Harshey, 2011. See text for details. Subscripts C and N refer to the C- and N-termini of the indicated proteins.

1.5 SWIMMING AND SWARMING MOTILITY

Salmonella and *E. coli* have two types of flagella-dependent motilities, swimming and swarming (Fig. 1.6). Swimming is an individual-cell based motility in liquid medium (cells can also swim through 0.3% semisolid agar medium). In an isotropic medium, swimming cells display a 'random walk', in which periods of smooth swimming (or runs) are interrupted by short re-orientations (or tumbles), corresponding to counter-clockwise (CCW) and clockwise (CW) rotation of the flagellar motors, respectively (Harms et al, 2001). CCW rotation results in bundling of all the helical flagella, which exerts a pushing motion on the cell; CW rotation disrupts the bundle. The chemotaxis system enables bacteria to bias their random walk towards higher concentrations of attractants and away from repellents by sensing temporal changes in chemoeffector concentrations, transmitting the signal to the motor to modulate the CW/CCW bias (Sourjik & Armitage, 2010; Porter et al, 2011). The direction of swimming is still chosen randomly, but movement in a favorable direction suppresses tumbles, resulting in longer runs. In the swim plate assay shown in Fig. 1.6A, an attractant gradient is created by depletion of nutrients at the center where the bacteria are inoculated; the bacteria migrate outwards to higher attractant concentrations, responding individually to the chemotactic gradient (Fig. 1.6B, left).

Swarming is defined as flagella-dependent group movement on the surface of solid media (Harshey, 2003). The nutrient composition (rich media, glucose) and viscosity (agar percentage) of the media are important for swarming. *Salmonella and E. coli* swarm only on low percentage agar media (0.5 - 0.8%) and there is no morphological

differentiation of the bacteria during swarming (Wang et al, 2004; Harshey, 2011). On the other hand, bacteria such as *Proteus mirabilis* can swarm on higher percentage agar (1.5 - 3.0%), and show an elongated cell morphology with increased flagella numbers (Harshey, 2003). Moving on a surface presents bacteria with several challenges not encountered in the swimming mode, the most critical being the availability of water (Toguchi et al, 2000; Wang et al, 2005). Some bacteria secrete dedicated polysaccharides, which aid in drawing water to the surface colony (Gygi et al, 1995). If the flagella do not detect a sufficient amount of water in their environment, the expression of flagella is repressed (Wang et al, 2005). Other challenges include surface tension and friction. Some bacteria secrete specific surfactants such as lipopeptides or glycolipids that lower surface tension and allow for rapid colony expansion (Matsuyama et al, 1992; Kearns & Losick, 2003; Caiazza et al, 2005). *Salmonella* and *E. coli* do not produce such surfactants (Korndorfer et al, 2004); the lipopolysaccharide layer in the outer membrane has been suggested to serve a surfactant function in these bacteria (Toguchi et al, 2000). Surface friction can be overcome by increasing motor torque. Some bacteria achieve this by their increased flagella numbers. *Salmonella* and *E. coli* increase torque by employing a swarming-specific protein FliL (Rychlik & Barrow, 2005), which likely increases stator occupancy as well as proton flow to the motor (Partridge & Harshey, unpublished data). The initiation of swarming movement is dependent upon building-up a high cell density (Rauprich et al, 1996; Fraser & Hughes, 1999). Cell density-dependence is related to surfactant-production in bacteria where its synthesis is regulated by quorum-sensing. In *Salmonella* and *E. coli*, the cell-density-dependence has been proposed to assist in

accumulation of secreted osmotic agents which attract water to the colony (Toguchi et al, 2000). *Salmonella* and *E. coli* mutants defective in the chemotaxis pathway are defective in swarming (Burkart et al, 1998). Chemotaxis is not required for swarming, but the ability to switch motor direction is somehow important for maintaining surface humidity (Chevance & Hughes, 2008).

Bacteria at the advancing edge of a swarm are generally mono-layered, while those following behind are multi-layered (Fig. 1.6B, right). Edge-cells are less motile, whereas the interior shows large-scale swirling and streaming motion of billions of cells (Dauter et al, 2000; Harshey, 2011). A recent study tracking the motion of fluorescently labeled flagella in an *E. coli* swarm showed that cells often stall at the advancing edge of the swarm, where their flagella are mostly pointing outward (Turner et al, 2010). The authors suggest that flagellar rotation of the stalled cells pumps fluid outward, wetting the virgin agar ahead of the swarm and aiding swarm expansion. Based on polymorphic shape transitions observed within the flagellar filaments, the motor was deduced to have the same CCW/CW bias in swarming bacteria as observed in swimming ones; however, in swarming bacteria these directional motor changes resulted in run-reverse instead of run-tumble cell movements. Thus, in confined, densely packed environments, CW motion allows cells to change directions by backing up.

The study of bacterial swarming is not only uncovering the pathways bacteria employ for overcoming the navigational challenges presented by a surface habitat, but is also shedding light on the function of flagellar genes that are not required in the swimming mode. Bacterial swarming is an excellent example of collective motion in

nature, and is also revealing how bacteria hunt for food and survive harsh environments (Butler et al, 2010; Dauter et al, 2000; Chevance & Hughes, 2008).

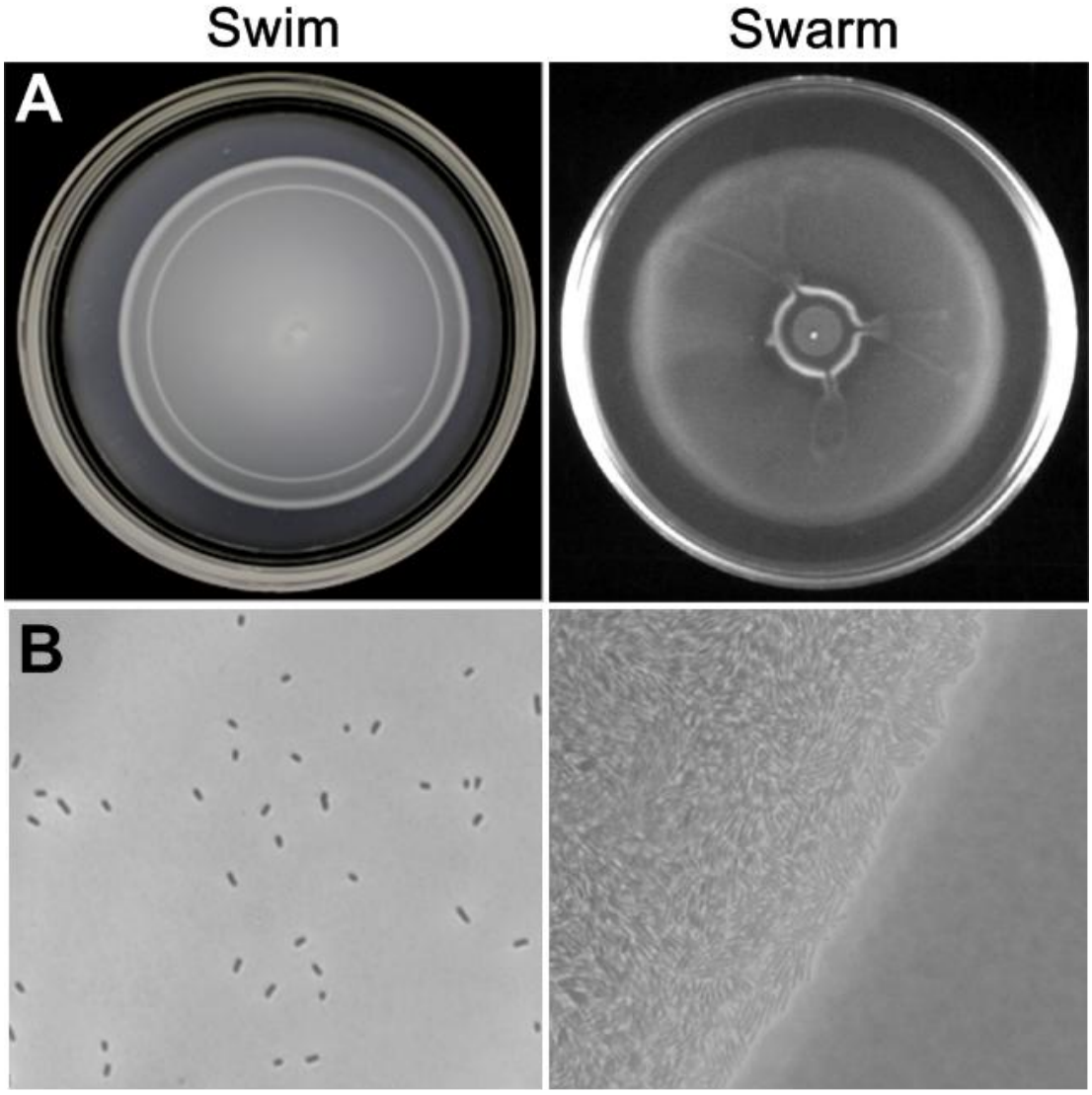

Fig. 1.6. Swimming and swarming assays. **A**. Swim and swarm plates differ mainly in their agar composition. Swim media are solidified with 0.3% agar and swarm media with 0.6% agar. Both media contain LB, with swarm media supplemented with 0.5% glucose in addition, Wild-type *S. enterica* cells have been inoculated at the center of the plate and incubated at 37^{o}C for 6 hr. Taken from Lee & Harshey, 2012. **B**. Phase contrast images showing individually dispersed cells in the swimming mode (left), and group of cells near the edge of the colony in the swarming mode (right). The swarm colony image was taken from Harshey, 2011.

CHAPTER 2: Materials and methods

BACTERIAL GROWTH CONDITIONS, STRAIN CONSTRUCTION AND REAGENTS

Strains and plasmids are listed in Table 2.1. Bacteria were grown in 2% L-broth (LB) base unless otherwise stated. Swim plates were made with 0.3% Bacto agar, and swarm plates with 0.6% (*S. enterica*) or 0.5% (*E. coli*) Eiken agar (Eiken Chemical, Tokyo, Japan) supplemented with 0.5% glucose (Wang et al, 2004; Wang et al, 2005; Wang et al, 2006a). Both swim and swarm plates were inoculated in the centre of the plate with 8 µl of an overnight. All experiments were at 37℃ for *S. enterica* and 30℃ for *E. coli* (Parkinson, 1978). Green plates were prepared with 2% LB supplemented with 0.86% glucose, aniline blue (0.67 g l^{-1}), alizarin yellow (0.065 g l^{-1}), and either 1.5% Bacto agar (hard agar) or 0.5% Eiken agar (swarm agar; glucose concentration was 0.5% in these plates). Photographs of colonies growing on green plates were taken by Canon PowerShot SD1000. Antibiotics used in this study were ampicillin (100 µg l^{-1}), chloramphenicol (30 µg l^{-1}), kanamycin (50 µg l^{-1}), and tetracycline (12.5 µg l^{-1}).

Deletion of *S. enterica* and *E. coli* genes was achieved by the one-step mutagenesis procedure previously described (Datsenko & Wanner, 2000; Wang et al, 2005). All primers used are listed in Table 2.2. Initial deletions involved selection with a kanamycin (*kan*) or tetracycline (*tetRA*) cassette. In *S. enterica*, the region replaced in *flhE* covers 330 bp, starting from nucleotide (nt) 61 (1 refers to A of the start codon), in *flgL*, 896 bp from nt 51, in *fliD*, 1404 bp from nt 1, in *fliS*, 248 bp from nt 100, and in

flgHI, 1670 bp from nt 61 in *flgH* to nt 70 in *flgI*. In *E. coli*, for *flhE*, the region replaced covers 330 bp from nt 61, for *flgL* 876 bp from nt 40, and for *fliK* 1028 from nt 61. Verification of deletions was achieved by DNA sequencing. Mutant combinations in *S. enterica* were constructed by P22 transduction. Curing the *kan* cassette was achieved by expression of the FLP recombinase encoded on pCP20 (Datsenko & Wanner, 2000).

PLASMIDS

Plasmids obtained from other laboratories are indicated in Table 2.1. Flagellar genes from *S. enterica* were amplified with PCR from the chromosomal DNA and ligated into pTrc99a or pBAD33 (Amann et al, 1988; Guzman et al, 1995). Epitope tags (FLAG, Myc, His) were conjugated to the C-terminus of FlhE respectively by PCR with different sets of primers containing restriction sites EcoRI and HindIII for cloning in pTrc99a. Primers are listed in Table 2.2. For GFPmut3b expression, gene sequences were amplified with XbaI and HindII recognition sites by PCR from the plasmid pMMB1311 and moved to pTrc99a. For genes expressed from pBAD33, a Shine-Dalgano sequence (AGGAGGAATTCACC) was added by PCR. Both *fliA* and *fliF* genes were amplified with SacI and HindIII recognition sites for cloning in pBAD33. To express fluorescent fusion proteins, mCherry and YFP fusion vectors were made; mCherry and YFP were amplified by PCR from p*mCherry* and pVS respectively with a GSGGG linker on the N-terminal region of the fluorescent proteins and cloned with restriction sites BamHI and HindIII in pTrc99a. FlhE was linked to the N-terminus of mCherry with EcoRI and BamHI recognition sites and FlhA to YFP with NcoI and BamHI recognition sites. For

co-localization experiments, the FlhA-YFP fusion was amplified with SacI and HindIII recognition sites and moved to pBAD33.

Table 2.1. Strains and plasmids used.

Strain	Genotype[a]	Source (ref.)
Salmonella		
14028	Wild-type ATCC strain	(Chevance & Hughes, 2008)
ST005	*flhE*::*kan*	This study
ST004	Δ*flhE*	This study
ST084	*flhE-FLAG*	This study
QW215	*flhDC*::*tetRA*	(Wang et al, 2007)
ST496	*flhDC*::*tetRA flhE*::*kan*	This study
RH2153	SJW/ *fliA*::*kan*	Joe Mireles
ST649	*fliA*::*kan*	This study
ST214	*fliA*::*kan* Δ*flhE*	This study
RH2217	Δ*fljB* Δ*fliC*	Adam Toguchi
ST212	Δ*fljB* Δ*fliC flhE*::*kan*	This study
ST155	Δ*fliD*	This study
ST146	Δ*fliD flhE*::*kan*	This study
TH2955	LT2/ *fliK77*::Tn*10*	Kelly Hughes
ST120	*fliK77*::Tn*10*	This study
ST121	*fliK77*::Tn*10* Δ*flhE*	This study
ST209	Δ*flgL*	This study
ST210	Δ*flgL* Δ*flhE*	This study
TH2929	LT2/ *flgK563*::Tn*10*	Kelly Hughes
ST136	*flgK563*::Tn*10*	This study
ST137	*flgK563*::Tn*10* Δ*flhE*	This study
ST450	*flgHI*::*kan*	This study
ST453	Δ*flgHI*	This study
ST454	Δ*flgHI* Δ*flhE*	This study
ST478	*flgHI*::*kan* Δ*flhE flgK563*::Tn*10*	This study
ST482	*flgHI*::*kan* Δ*flhE* Δ*flgL*	This study

Table 2.1, cont.

QW178	Δ*motA*	(Wang et al, 2005)
ST157	Δ*motA flhE*::*kan*	This study
ST441	*fliS*::*kan*	This study
ST442	*fliS*::*kan* Δ*flhE*	This study
RH2858	Δ*tsr*	Susana Mariconda
ST557	Δ*tsr flhE*::*kan*	This study
RH2202	Δ*hin* (flagellar phase variation locked for fljB expression)	Adam Toguchi
RH2204	Δ*hin* (flagellar phase variation locked for fliC expression)	Adam Toguchi
ST149	Δ*hin* (RH2202) *flhE*::*kan*	This study
ST150	Δ*hin* (RH2204) *flhE*::*kan*	This study
TH341	F::Tn*10d*Cm	Kelly Hughes
E. coli		
RP437	Wild-type	(Parkinson, 1978)
ST839	*flhE*::*kan*	This study
ST893	*fliK*::*kan*	This study
ST903	Δ*fliK*	This study
ST907	Δ*fliK flhE*::*kan*	This study
ST963	*flgL*::*tetRA*	This study
ST964	*flgL*::*tetRA flhE*::*kan*	This study
DH5α	Δ(*lacIZYA-argF*) ϕ80d*lac* Δ(*lacZ*)M15	New England Biolabs
Phage		
P22	HT12/4*int*103	(Chevance & Hughes, 2008)

Plasmid	**Expressed protein**	**Resistance**	**Replication Origin**	**Induction**	**Source (ref.)**
pNK972	Tn*10* transposase in pBR322	Ampicillin	ColE1	Constitutively active	Kelly Hughes
pAmCyan	Expression vector used for Tn*10d*Cm insertion mapping	Ampicillin	pUC	IPTG	CLONTECH
pKD4	Source for Kan cassette	Kanamycin	oriR6K gamma	N.A	(Datsenko & Wanner, 2000)
pKD46	Lamda Red recombinase	Ampicillin	repA101ts & oriR101	Arabinose	(Datsenko & Wanner, 2000)

Table 2.1, cont.

pCP20	FLP recombinase	Ampicillin & Chloramphenicol	repA101ts	Constitutively active	(Datsenko & Wanner, 2000)
pMMB1311	Source for GFPmut3b	Ampicillin	oriC	Constitutively active	(Kitko et al, 2010)
pmCherry	Source for mCherry	Ampicillin	pBR	IPTG	Qingfeng Wang
pVS	Source for YFP	Amplicillin	pBR	IPTG	Victor Sourjik
pTrc99a	Expression vector	Ampicillin	pBR	IPTG	(Amann et al, 1988)
pBAD33	Expression vector	Chloramphenicol	pACYC	Arabinose	(Guzman et al, 1995)
pJM01	FlhE-FLAG	Ampicillin	pBR	IPTG	This study
pJM02	FlhE-Myc	Ampicillin	pBR	IPTG	This study
pJM68	FlhE-His	Ampicillin	pBR	IPTG	This study
pJM37	GFPmut3b	Ampicillin	pBR	IPTG	This study
pJM40	YFP with GSGGG linker for C-terminal fusions; pTrc99a derivative	Ampicillin	pBR	IPTG	This study
pJM41	FlhA-YFP	Ampicillin	pBR	IPTG	This study
pJM46	FlhA-YFP	Chloramphenicol	pACYC	Arabinose	This study
pJM48	FlhA	Chloramphenicol	pACYC	Arabinose	This study
pJM57	mCherry with GSGGG linker for C-terminal fusions; pTrc99a derivative	Ampicillin	pBR	IPTG	This study
pJM59	FlhE-mCherry	Ampicillin	pBR	IPTG	This study

Table 2.1, cont.

pJM65	FliF	Chloramphenicol	pACYC	Arabinose	This study
p*flhDC*	FlhDC	Chloramphenicol	pACYC	Arabinose	Asaka Suzuki

a. Unless otherwise indicated (e.g. SJW/LT2), all *S. enterica* strains are derivatives of 14028, and all *E. coli* strains constructed in this study are derivatives of RP437. D and :: refer to deletion of, or insertion/substitution within, respectively, the indicated gene. Note that deletions created by the Datsenko and Wanner (2000) method leave behind a 'scar' sequence of ~ 80 base pairs.

Table 2.2. Primers used.

Primer	Sequence (5' -> 3')
Substituting *S. enterica flhE* gene with *kan*	
flhE(F)	gttgctctttcccctgacggttcaggccgcaggcgaaggcgtgtaggctggagctgcttcg
flhE(R)	gattgctccgcacttttaacgccgggataagtcggccgcccatatgaatatcctccttagt
Addition of *FLAG*::*kan* at the C-terminal region of *S. enterica flhE* gene	
JL0042(F)	gttaaaagtgcggagcaatcaggtgattgtgaactaccgcgactacaaagatgacgacgataaataagtgtaggctggagctgcttc
JL0043(R)	aaagagagtcaggtctgctacctggcaaagaaaggggcggatgaatatcctccttagt
Substituting *S. enterica fliD* gene with *kan*	
JL0070(F)	tgccgataacgcgcttaactactgtttgcaatcaaaaaggaagaaggcgtgtaggctggagctgcttc
JL0071(R)	tgacttgcgcataagctttgataccgctcgcggtgtacatatgaatatcctccttagttcct
Substituting *S. enterica flgL* gene with *kan*	
JL0093(F)	gtacccagatgatgtacgaacaaaatatgagcggcatcacgtgtaggctggagctgcttc
JL0094(R)	tccagtttcgtgatatgtttcaaaaagaggtgttaccggtatgaatatcctccttagt
Substituting *S. enterica fliS* gene with *kan*	
JL0224(F)	caaagcttatgcgcaagtcagcgtggaaagcgccgtgatggtgtaggctggagctgcttc
JL0225(R)	tgctttcggtgaaatctgcttccaggcttctgcaatattgatgaatatcctccttagttc
Substituting *S. enterica flgHI* genes with *kan*	
JL0232(F)	ttacccagttatggccctgatggtcgcgacgctgacagtgtaggctggagctgcttc
JL0233(R)	agcccgcgctctgcatggactgcaaaatcgacatcagatcatgaatatcctccttagttc
Substituting *E. coli flhE* gene with *kan*	
JL0327(F)	attattgtttccgctgctggtgcaagccgccggggaggggtgtaggctggagctgcttc
JL0328(R)	attaaacatactcgcgagcgcgtaatttttttgtccttcacatatgaatatcctccttag

Table 2.2, cont.

Substituting *E. coli fliK* gene with *kan*	
JL0337(F)	gattaccgccgacgttgacaccaccacattgcctggcggcgtgtaggctggagctgcttc
JL0338(R)	ttaggcgaaaatatcaacgccgctgttgcctgttacacgccatatgaatatcctccttag
Substituting *E. coli flgL* gene with *tetRA*	
JL0358(F)	atgcgtttcagtacacagatgatgtaccagcaaaacatgttaagacccactttcacatt
JL0359(R)	ttatttgctgagctggaagagcgacaatccctgcatatcctaagcacttgtctcctg
Sequencing *kan* substitution of *S. enterica flhE*	
Evl(F)	atgcgtaaatggctggcg
Ev2(R)	gcggtagttcacaatcac
Sequencing *FLAG*::*kan* insertion at the C-terminal region of *S. enterica flhE*	
JL0073(F)	accttgagctttccgataaccgt
Sequencing *tetRA* substitution of *S. enterica flhDC*	
flhDC(F)	ccatgctggttttatcg
flhDC(R)	gacatccttccgctgtt
Sequencing *kan* substitution of *S. enterica fliA*	
fliA(F)	gagccttataggcgcatctg
fliA(R)	gtaatgcggtcgagcagttt
Sequencing deletion of *S. enterica fljB*	
JL0068(F)	tcgcttttctcatggaggattgct
JL0069(R)	gtgaattcggggctttttcatttagca
Sequencing deletion of *S. enterica fliC*	
fliC(F)	attcaggtgccgatacaagg
fliC(R)	cacaggctccggaattaaaa
Sequencing deletion of *S. enterica motA*	
motA(F)	acactccagcagcggtaagt
motA(R)	tctttagggctggagatgga
Sequencing deletion of *S. enterica tsr*	
JL0366(F)	aaatgggacgatccttgttg
JL0367(R)	gtatgaatcacgctgcacca
Sequencing Tn*10* insertion of *S. enterica fliK*	
JL0052(F)	agatggatgaatttgctcagcgt
lS10L(R)	gacaagatgtgtatctaccttaac
Sequencing Tn*10* insertion of *S. enterica flgK*	
JL0058(F)	tgccgataacaacgagtattgaagga
JL0059(R)	tgacatgcgtatcagtacccaga
Sequencing *kan* substitution of *S. enterica fliD*	

Table 2.2, cont.

JL0165(F)	ttattccgcgcattatttttg
JL0072(R)	ctcatcacggcgctttcca
Sequencing *kan* substitution of *S. enterica flgL*	
JL0098(F)	gtattatctggcgaatgcgca
JL0099(R)	gaaatacgtacggatggcgtc
Sequencing *kan* substitution of *S. enterica fliS*	
JL0228(F)	tttgacccagcaatttacagc
JL0229(R)	ttgactgagcagcgcaatac
Sequencing *kan* substitution of *S. enterica flgHI*	
JL0234(F)	accggctccctgattttg
JL0235(R)	tcgctttcagttcgttcaga
Sequencing deletion of *S. enterica hin*	
JL0081(F)	aggagaaaatcatggctactattgggt
JL0082(R)	gtttttttatgcggcttgccgga
Sequencing *kan* substitution of *E.coli flhE*	
JL0329(F)	taaccgacatatccgcatga
JL0330(R)	catcgagccttttcactgag
Sequencing *kan* substitution of *E.coli fliK*	
JL0339(F)	cgcctcgatcagaaaaagat
JL0340(R)	cggctaattatcctgcgtct
Sequencing *tetRA* substitution of *E.coli flgL*	
JL0355(F)	gatgcgctgattaacattcg
JL0356(R)	cagagcaggcagacaaaaca
Sequencing pAmCyan for Tn*10d*Cm insertion site	
JL0023(F)	tgtgtggaattgtgagcgga
JL0108(R)	acggtaaagtaatgcccattgaca
Sequencing pTrc99a	
JL0197(F)	taatgtgtggaattgtgagcgga
JL0135(R)	ctgatttaatctgtatcaggctga
Sequencing pBAD33	
JD0094(F)	gcatcagacattgccgtcactg
JD0095(R)	cagttccctactctcgcatgg
Sequencing pJM41, pJM46, and pJM48	
JL0284(F)	gctacaccctgctgaccatt
JL0304(F)	tgatgccatctggattgaaa
Sequencing pJM65	

Table 2.2, cont.

JL0345(F)	tctgctcacgcaatccaata
Cloning *flhE-FLAG* in pTrc99a	
JL0013(F)	gagagagaattcatgcgtaaatggctggcgttgt
JL0015(R)	gagagaaagcttctatttatcgtcgtcatctttgtagtcgcggtagttcacaatcacct
Cloning *flhE-Myc* in pTrc99a	
JL0016(R)	gagagaaagcttctacagatcttcttcagaaataagtttttgttcgcggtagttcacaatcacct
Cloning *flhE-His* in pTrc99a	
JL0035(R)	gagagaaagcttttaatgatgatgatgatgatggcggtagttcacaatcacct
Cloning *gfpmut3b* in pTrc99a	
JL0188(F)	gagagatctagaatgagtaaaggagaagaacttttcactggagttgtc
JL0018(R)	gagagaaagcttttatttgtatagttcatccatgcca
Cloning *mCherry* in pTrc99a	
JL0278(F)	gagagaggatccggaggaggagtgagcaagggcgaggagga
JL0187(R)	gagagaaagcttctacttgtacagctcgtccatgccgccggt
Cloning *flhE* in pJM57	
JL0038(F)	gagagagaattcatgcgtaaatggctggcgttgttg
JL0316(R)	gagagaggatccgcggtagttcacaatcacct
Cloning *yfp* in pTrc99a	
JL0302(F)	gagagaggatccggaggtggagtgagcaagggcgaggagctgtt
JL0303(R)	gagagaaagcttttacttgtacagctcgtccatgccga
Cloning *flhA* in pJM40	
JL0300(F)	gagagaccatggctaatctggtcgcgatgc
JL0301(R)	gagagaggatccttttcctccaatggtcgccgtc
Cloning *flhA* in pBAD33	
JL0309(F)	gagagagagctcaggaggaattcaccatggctaatctggtcgcgatg
JL0275(R)	gagagaaagcttttattttcctccaatggtcgccg
Cloning *flhA-yfp* in pBAD33	
JL0309(F)	gagagagagctcaggaggaattcaccatggctaatctggtcgcgatg
JL0303(R)	gagagaaagcttttacttgtacagctcgtccatgccga
Cloning *fliF* in pBAD33	
JL0341(F)	gagagagagctcaggaggaattcaccatgagtgcgactgcatcgact
JL0342(R)	gagagaaagcttttactcatgatcgttactcatccac

GROWTH CURVES, CELL COUNTS AND AGAROSE GEL ELECTROPHORESIS

The growth profiles of strains were measured as colony forming units (cfu). Overnight cultures were diluted 1:100 in fresh LB (50ml) and 100 µl of the cultures were collected every 1 h for up to 6 h. Serial dilutions were made with 1X PBS and plated to determine cfus. To measure cfus on green swarm plates, overnight cultures were diluted 1:100 in fresh LB and grown at 37^{o}C for 2 h until OD_{600} reached 0.6. Ten milliliters of the culture was poured on the surface of green swarm agar plates and allowed to sit for 1 min. The culture was then poured out and the excess of liquid was drained with Kim wipes. The plates were allowed to dry for 10 min without a lid on the bench, after which the lid was put back on and the plates incubated at 37^{o}C for 6 h. Cells were collected with 5ml of 1X PBS, normalized to OD_{600} = 0.3, and cfus was determined after serial dilution. Anaerobic green swarm assays were conducted in a 2.5 L Oxoid AnaeroJar system AG0025 as described (Lazova et al, 2012). The inoculated green swarm plates as described above were placed in the Oxoid AnaeroJar. After AnaeroGen sachet (Oxoid Ltd) was placed in the jar and immediately the jar was sealed and incubated at 37^{o}C for 6 h. AnaeroGen sachet placed in the sealed jar rapidly absorbs the atmospheric oxygen with the simultaneous generation of carbon dioxide, resulting in the oxygen and carbon dioxide levels to below 1% and between 9 - 13% respectively.

To detect chromosomal DNA released from cells growing on green swarm agar, cells were harvested from plates after 6 h and adjusted to similar OD_{600} readings for all strains. The whole cell (WC) suspension was centrifuged at 3000 *g* for 5 min to separate the cell pellet and supernatant. Fifteen microliters of supernatant were mixed with 3 µl of

loading dye, electrophoresed on a 0.8% agarose gel with a 1 kbp DNA size marker ladder (NEW ENGLAND BioLabs) and visualized by a BioRad Gel Doc. The position and identity of genomic DNA were confirmed independently by monitoring the migration position of isolated genomic DNA under the same conditions, as well as testing the DNA band for chromosomal markers by PCR.

THIN LAYER CHROMATOGRAPHY (TLC)

Overnight cultures were diluted 1:100 in fresh LB and grown at 37^{o}C for 2 h until OD_{600} reached 0.6. Ten milliliter of the culture was poured on the surface of swarm agar plates, allowed to sit for 1 min and then poured out, and the excess of liquid was drained with Kim wipes. The plates were allowed to dry for 10 min without a lid on the bench, the lid was put back and the plates incubated at 37^{o}C for 6 h. Cells were harvested with 5 ml of dH_2O and centrifuged at 5500 g for 15 min after OD_{600} was normalized to 1.2. The supernatant was filtered by 0.45 µl syringe filters (VWR) and concentrated by the centrifuge vacuum dryer (Eppendrof) at 30^{o}C overnight.

Thin layer chromatography (TLC) was performed as previously described in order to separate amino acid-related compounds (Hadley et al, 1998) and sugars (Muller & Sinn, 1977). Whatman 250-µm thick silica gel glass plates (Whatman®) were purchased and immediately before use, they were marked and activated as follows. For marking, a straight line was lightly drawn by a pencil parallel to about 1 cm from the one bottom of the plate and two small marks were made on this line, on which the samples for analysis were spotted. For activation, the marked plates were placed in an oven at 55^{o}C

for 20 min. Activation refers to drying out water molecules that bond to the polar sites on the plate. Two micro-liters of each sample were spotted on the marks made on the plates and separated for 1 h by the following solvent systems: 1-butanol: acetic acid: dH_2O (6:2:2 v/v) and 0.5% boric acid: 1-butanol: 2-propanol (2:3:5 v/v). The plates were dried at 55^oC for 30 min. To develop the plates, different reagent solutions were sprayed in a hood for each plate as follows. To detect amino acid-related compounds, ninhydrine reagent (FisherScience) was used and to detect sugars, 4% methanolic solution (2,3,5 Triphenyltetrazolium chloride, 1N NaOH 1:1 v/v), 25% lead (II) acetate basic solution, and Urea-HCl solution (Urea, HCl, enthanol 1:4:20 v/v) were used. The plates were dried for 1 h and photographed using Canon PowerShot SD1000.

CELL FRACTIONATION TO IDENTIFY FLHE LOCATION

S. enterica wild-type cells containing pTrc99a-*flhE-Myc* were grown at 37°C with shaking in LB supplemented with 10 µM IPTG and ampicillin until OD_{600} reached 0.6, and cell fractionation was performed as described (Aldridge et al, 2006a). The periplasmic fraction was prepared by the osmotic shock protocol. Three milliliters of cells were centrifuged and resuspended in 300 µl of cold periplast buffer (20% sucrose, 100 mM Tris-His (pH 8.0), 1 mM EDTA, 20 µg ml^{-1} PMSF), and 100 µl of the cells were saved for the WC fraction. Lysozyme was added to the remaining suspension at the final concentration of 0.1 mg ml^{-1} and incubated on ice for 5 min. After addition of the same volume of cold water, the mixture was kept on ice for 5 min and centrifuged (12000 g, 3 min), and the supernatant was saved for the periplasmic fraction. The pellet was

resuspended in 600 µl of spheroplast buffer (10 mM Tris-HCl (pH 7.5), 50 mM KCl, 1mM EDTA, 0.1% deoxycholate), sonicated, and centrifuged (12000 g, 3 min). The supernatant was saved for the cytoplasmic fraction. The pellet was rinsed with 10 mM Tri-HCl (pH 8.0) buffer, centrifuged (16000 g, 30 min), resuspended with 50 µl of the same buffer, and saved for the membrane fraction. All fractions were analyzed by SDS-PAGE gel electrophoresis, followed by transfer to Western blots.

ISOLATION OF INTACT FLAGELLA (WITH HBB) FROM CELLS

Bacterial flagella were isolated as previously described (Francis et al, 1994) with some modifications. A liter of wild-type *S. enterica* cells containing pTrc99a-*flhE-FLAG* were grown at 37°C with shaking in LB supplemented with 10 µM IPTG and ampicillin. They were collected in late log phase (4 h time point) by centrifugation at 4000 *g* for 20 min, and resuspended with 100 ml of ice-cold sucrose solution (0.5 M sucrose, 0.1 M Tris-HCl, pH 8.0). The bacterial suspension was diluted to an OD_{600} = 0.6, after which lysozyme and EDTA were added at a final concentration of 0.1 mg ml^{-1} and 0.01 M respectively, and the mixture was incubated on ice for 40 min with gentle stirring. The spheroplasts were lysed by adding 10 ml of 10% Triton X-100. When the lysis was completed, 10 ml of 0.1 M $MgSO_4$ was added and the lysate was incubated at 30^{o}C for 30 min. Unlysed cells and cell debris were removed by centrifugation at 4000 g for 10 min. The pH of the supernatant was raised with 1 M NaOH to pH 10 - 12. The lysate was ultra-centrifuged at 60000 g for 1 h and the pellets containing whole flagella were

resuspended in 10 ml of alkaline solution and used for SDS-PAGE gel electrophoresis followed by transfer to Western blots.

SDS-PAGE, SILVER STAINING, LIPOPOLYSACCHARIDE STAINING AND WESTERN BLOTS

All samples for SDS-PAGE gel electrophoresis were suspended in 6X SDS-PAGE sample buffer before electrophoresis. To examine proteins from the supernatants of swarm cultures, cells were harvested from swarm agar plates with 1X PBS after 6 h, and OD_{600} was normalized to 0.8. Cells were centrifuged at 3000 g for 5 min and the supernatant was electrophoresed in 18% polyacrylamide gels. The gels were stained by Pierce® Color Silver Stain Kit (Thermo SCIENTIFIC) according to the manufacturer's instructions as follows: the gels (10 cm X 13 cm) were fixed in a fixative buffer (50% ethanol, 5% acetic acid v/v) for 2 h, washed 4 times with dH_2O for 30 min, and stained in a Silver working solution (20 ml of Silver reagent with 280 ml of dH_2O) for 30 min. The gels were rinsed with dH_2O for 10 sec, incubated in a Reducer working solution (20 ml of Reducer Aldehyde Reagent with 130 ml of dH_2O) for 30 min, transferred to a Stabilizer working solution (20 ml of Stabilizer Base Reagent with 880 ml of dH_2O), and incubated for 30 min until protein bands appeared.

To detect lipopolysaccharides (LPS), cells were harvested from swarm agar plates with dH_2O. Supernatants were prepared from the cells (OD_{600} = 1.2) as described above and successively ultra-centrifuged at 200000 g for 2 h. The pellets were resuspended by dH_2O. For WC, 0.5 ml of the cells (OD_{600} = 0.6) were prepared. The samples mixed with the sample buffer were heated at 100^{o}C for 30 min, 2.5 μl of protease K (20mg ml^{-1}) was

added, incubated at 55^{o}C for 3h, and separated by 12% SDS-PAGE gels. LPS was stained by Pro-Q® Emerald 300 LPS Gel Stain Kit (Molecular PROBES), using the following the procedures: the gels were fixed in a solution (50% methanol, 5% acetic acid v/v) at room temperature for 45 min and washed twice in 3% glacial acetic acid for 20 min. Because the Pro-Q® Emerald 300 dye reacts with periodate-oxidized carbohydrate, the carbohydrates were oxidized by incubating gels in Oxidizing solution (Molecular PROBES) for 30 min and washed 3 times described above. The gels were stained in Pro-Q® Emerald 300 Staining solution in the dark with gentle agitation for 2 h, washed twice and visualized using a BioRad Gel Doc under UV illumination (~300 nm).

To detect secreted flagellin, cells were harvested from green swarm agar plates with 1X PBS after 6 h and normalized to OD_{600} = 0.3. They were centrifuged at 3000 *g* for 5 min and the supernatant was electrophoresed in 10% polyacrylamide gels. The gels were washed twice with deionized water and stained for 1 h with SimpleBlue™ SafeStain (Invitrogen). Purified FlhE-His protein was similarly detected by staining.

Samples for western blot analysis were electrophoresed in 12% polyacrylamide gels, followed by transfer to Immobilion-P membrane (Millipore), performed according to standard protocols (Sambrook *et al*., 1989) and developed using the Enhanced chemiluminescence (ECL) kit from Amersham. Antibodies against *E. coli* FliG and MotB were provided by David Blair, *S. enterica* anti-FlgG antibody by May Macnab and *E. coli* anti-TonB antibody by Kathleen Postle. Anti-MBP antibody was purchased from New England Biolabs, anti-MYC antibody from Invitrogen, anti-FLAG antibody from Sigma, and anti-His antibody from Abgent.

MEASUREMENT OF PROTEIN CONTENT

Protein concentration was measured using the NanoDrop (ND-1000 Spectrophotometer, NanoDrop Technologies) according to the manufacturer's instructions. By the A280 method, the absorbance of the purified FlhE-His (2 µl) was measured at 280 nm and the protein concentration was calculated by the extinction coefficient (EC) equation ($A = \varepsilon bc$, where A is absorbance, ε is the protein EC ($M^{-1} cm^{-1}$), b is the path length that the light has travelled (1cm in A280), and c is concentration (M)). The EC of FlhE-His was calculated by the protein EC calculator provided from BioMol.net. Protein bands obtained from the SDS-PAGE and Western blots were quantified by Bio-Rad Gel Doc and Quantity One 4.4.0 software.

LIVE/DEAD STAINING

The stain was purchased from Invitrogen, and cells were stained according to the manufacturer's specifications. The kit includes two nucleic acid stains: green-fluorescent STYO 9 and red-fluorescent propidium iodide (PI). STYO 9 labels both live and dead bacteria alike, whereas PI reduces STYO 9 stain intensity only after crossing damaged cellular membranes. Staining was performed as described (Butler et al, 2010) with the following modifications. Cells were grown on swarm agar plates for 6 h, harvested with 1X PBS and diluted $OD_{600} = 0.6$. To determine red/green cell numbers, at least 200 cells were counted from *S. enterica* wild-type and *flhE* samples analyzed.

pH MEASUREMENT OF BACTERIAL CULTURES

S. enterica cultures were grown overnight in LB (pH 7.0), diluted 1:100 in fresh LB broth (100 ml) with and without the addition of 0.5% glucose, and incubated up to 6 h. Five milliliters of culture were collected every 30 min and pH of the culture was measured by a UB-10 UltraBasic pH/mV Meter (Denver Instruments).

TRANSPOSON MUTAGENESIS TO ISOLATE EXTRAGENIC SUPPRESSORS OF THE *flhE* GREEN PHENOTYPE

Phage P22 was grown on donor stain (TH341) carrying Tn*10d*Cm (defective Tn*10*, lacking the transposase), and used to generate a random pool of Tn*10d*Cm by infection of a wild-type *S. enterica* strain harboring pNK972 (plasmid expressing the functional transposase gene of Tn*10*). The Cm^R transductants were pooled together, P22 lysates were prepared from the pool, and the Tn*10d*Cm insertions transduced into the *S. enterica flhE::kan* strain ST005, selecting on green plates supplemented with chloroamphenicol and kanamycin. Out of 26,827 colonies screened, 915 were yellow. 84% (771/915) of yellow mutants were non-motile. The remaining 144 motile mutants were re-tested by moving the Tn*10d*Cm into clean *flhE::kan* strain by P22 transduction to confirm the yellow phenotype. Although all the transductants were still motile, only 37 were truly yellow. These yellow motile mutants could be categorized into three classes based on their swimming speed: compared to the parent strain, the motilities of class I - class III mutants were > 80%, 40 - 80% and < 40% respectively. The Tn*10d*Cm insertion sites of the class I and II mutant subtypes were mapped as follows: Chromosomal DNA

from the mutants was purified by Wizard® Genomic DNA purification kit (Promega), partially fragmented by Sau3AI, and then ligated to a BamHI site in the high-copy number plasmid pAmCyan (Clontech) containing Amp^R. Ligation mixtures were electroporated into *E. coli* DH5α. Plasmid DNA from Cm^R/Amp^R transformants was purified using Qiagen mini-prep kit and sequenced using vector primers from both sides of the insert (Table 2.2). The data are shown in Table 4.2, with gene descriptions from (McClelland et al, 2001).

RNA PREPARATION AND MICROARRAY EXPERIMENTS

Transcription profiles of *S. enterica* wild-type and *flhE* mutant strains propagated on swarm plates for 3 h were obtained by microarray experiments performed as described (Wang et al, 2004).

Total RNA was isolated from ~ 1X 10^{10} cells for each strain using an AquaPure RNA isolation kit (Bio-Rad) and treated with DNA-free™ DNase (Ambion) to remove DNA. The RNA was labeled by reverse transcription as follows (all reagents were from Invitrogen unless otherwise indicated): 50 µg of RNA with 1.2 µl of random hexamer (2 µg μl^{-1}) in 30.8 µl of dH_2O was denatured at 65°C for 10 min and transferred to ice. This was mixed with the master mix (6 µl of 0.1 M dithiothreitol (DTT), 12 µl of 5X buffer, 1.2 µl of dNTP (25 mM dATP, 25 mM dGTP, 25 mM dCTP, 10 mM dTTP), 4 µl of Superscript II, 3 µl of RNasIn (Ambion) and 4 µl of either Cy3 (wild-type)- or Cy5 (*flhE* mutant)-labeled dUTP (Amersham Biosciences). This mixture was incubated at 42°C for 2 h, supplemented with 2 µl of Superscript II at the end of the first hour, followed by

denaturation with 3 µl of 1 M NaOH and renaturation with 3 µl of 1 M HCl. Cy3 and Cy5 labeled reactions were combined, purified with a PCR purification kit (Quagen), and concentrated to 32 µl with Micron YM-30 (Millpore). The probe was mixed with 45 µl of 2X hybridization buffer (50% formamide, 10X SSC, 0.2% SDS) and 3 µl of sonicated salmon sperm DNA (10 mg ml^{-1}, Sigma) and denatured by boiling at 95^{o}C for 5 min.

The microarray chip provided by Sidney Kimmel Cancer Center covers 96.6% of the 4600 *S. enterica* LT2 open reading frames (ORFs). Each slide had 3 repeats of the entire array. Immediately before use, the slide was pre-hybridized with 40 ml of pre-hybridization buffer (25% formamide, 5X SSC, 10 mg ml^{-1} BSA, 0.1% SDS) at 42^{o}C for 1 h, rinsed with dH_2O, dried by centrifugation (500 r.p.m, 7 min). Denatured probe was applied to the slide for hybridization. Successively, the slide was covered by a LifterSlip coverslip (Erie Scientific), sealed in a hybridization chamber, and incubated at 42^{o}C water bath overnight. The slide was washed successively with 3 solutions: wash I (2X SSC, 0.1% SDS), wash II (0.1X SSC, 0.1% SDS), wash III (0.1X SSC). The slide was dried by centrifugation at 400 g for 5 min and scanned on a GenePix 4000A scanner (Axon Instruments). Each fluorescence data of the 3 repeats on the slide was collected separately by GENEPIX PRO 4.1 software. The 3 sets of data were normalized so that the mean of the ratio of medians of all the features was equal to one. The GenePix data file (.gpr) was converted to an EXCEL file. Background was subtracted by filtering out individual genes flagged as -75 (empty spots) and -50 (spots defined as not found by GENEPIX PRO because of signal levels similar to background). Also, a set of 100 genes which do not have cross-hybridization with *S. enterica*, were used as negative controls.

For each gene spot, the median of the ratio from 3 repeats on one chip was used as the expression level of that particular gene relative to the reference.

REPELLENT RESPONSE MEASURED BY MONITORING TRAJECTORIES OF SWIMMING CELLS

S. enterica wild-type, *flhE*, *tsr*, and *tsr flhE* mutant strains containing pBAD33-*flhDC* were used. Overnight cultures were diluted 1:100 in LB and shaken at 37°C until the cultures reached an OD_{600} of 0.6. A 10 µl aliquot (pre-induction) was sampled before arabinose was added (0.2% v/v) to induce *flhDC* expression and a second sample was taken after 30 min. Cells were observed by phase-contrast microscopy and recorded up to 10 min on an external Sony video recording device with Windows Movie Maker software. Three biological replicates were prepared for swim-motility analysis, and 90 to 200 cells were observed under each condition. To measure reversal frequencies, the straight-swimming distance was defined as 10 times the length of a bacterial cell (25 µm). Cells that swam straight without a tumble in this distance were categorized as having a wild-type or 'normal' bias. The swimming distance of each cell was measured manually on the computer screen.

MEASUREMENT OF CYTOPLASMIC pH WITH GFP REPORTER PLASMID

Cytoplasmic pH was measured using GFPmut3b, a pH-sensitive green fluorescent protein, as described (Wilks & Slonczewski, 2007; Kitko et al, 2009). A standard pH curve was generated using a wild-type strain containing pTrc99a-*gfpmut3b*. An overnight culture grown at 37°C was diluted 1:100 in fresh potassium-modified LB (LBK [pH7.5]),

which was buffered with 20 mM homopiperazine-*N*, *N'*-bis-2-(ethanesulfonic acid) (HOMOPIPES) and supplemented with 40 µM IPTG and ampicillin. Cells were grown to OD_{600} = 0.6 and pelleted at 4800 *g* for 4 min. They were resuspended to an OD_{600} of 0.4 in M63 minimal-medium (1.5% casein hydrolysate, 0.8% glycerol, and 50 mM HOMOPIPES). The pH of M63 medium was adjusted with KOH to pH 5.5 to 7.5. To equilibrate cytoplasmic pH with external pH, 30 mM sodium benzoate was added to the cultures.

Measurement of cytoplasmic pH of experimental samples was performed as described above, except that cultures were grown LBK buffered with 20 mM HOMOPIPES pH 5.5, the external pH attained by cultures growing in the presence of glucose, and sodium benzoate was omitted. Cultures were kept on ice prior to recording the GFPmut3b excitation spectra.

FLUORESCENCE MEASUREMENT OF PH REPORTER PLASMIDS

The excitation spectra of GFPmut3b were recorded using a PTI Quanta Master Model C scanning spectrofluorometer. Three milliliters of cell suspension were placed into a Bio-Rad VersaFluor cuvette with a path length of 10 mm. Excitation was measured from 480 to 510 nm (slit width of 2 nm), using an emission wavelength of 545 nm (slit width of 20 nm) (Wilks & Slonczewski, 2007). Three biological replicates were measured. To determine the standard curve correlating internal pH with fluorescence intensity, GFPmut3b intensities at pH 5.5, 6.0, 6.5, 7.0, and 7.5 were obtained. The intensities at pH5.5 and 7.5 were fitted to a linear equation (y = mx + b, where y is the

GFPmut3b intensity, x is pH value, m is slope, and b is y-intercept) to obtain the slope (m = 4.75 x 10^4) and y-intercept (b = - 1.9 x 10^5). The equation (GFPmut3b signal intensity = 4.75 x 10^4 x pH - 1.9 x 10^5) was used to convert the signal intensities (sum of 480 nm to 510 nm) obtained from experimental samples to pH units.

FLAGELLA STAINING AND MICROSCOPY

To observe swarm colonies, swarm cultures were prepared as described in TLC. Cells on swarm plates were viewed with an Olympus BH2 microscope and photographed using an attached DP-12 digital camera (Olympus).

Flagellar filaments were stained as described (Attmannspacher et al, 2008) and cells were observed as reported previously (Paul et al, 2010). For the localization assay of FlhE-mCherry fusion protein in *S. enterica* wild-type and *flhDC* cells, the cultures were grown overnight at 37^{o}C, diluted 1:100 in LB supplemented with ampicillin, and subsequently grown at 26^{o}C for 3 h to OD_{600} of 0.4-0.6. For the co-localization assays of FlhE-mCherry with FlhA-YFP, FlhA, or FliF in *flhDC* cells, overnight cultures were diluted 1:100 in fresh LB supplemented with 0.02% arabinose, ampicillin, and chloroamphenicol. Cells were placed in a slide glass with a poly-lysine treated coverslip for 10 min, washed once with 100 µl of 1X PBS and observed through a Nikon Eclipse 50i upright microscope using a B-2E/C filter for YFP and G-2A filter for mCherry, and photographed as described (Paul et al, 2010).

PROTEIN EXPRESSION AND PURIFICATION

6His-tagged FlhE protein was purified for crystallization by an osmotic shock procedure that released the periplasmic protein into the medium (Chen et al, 2004), with the following modifications. An overnight culture of *S. enterica flhE* mutant (ST004) cells containing pTrc99a-*flhE-6His* was diluted 1:100 in a 2 L flask with a working volume of 1 L LB supplemented with ampicillin and grown at 37℃ for 2 h. To induce FlhE-6His, IPTG was added at a final concentration of 50 μM. After 3.5 h, cells were centrifuged at 4000 g and 4℃ for 20 min. All procedures for FlhE-6His purification and concentration were performed at 4℃. Cells (3.5 g of wet weight) were resuspended in 100 ml solution containing 30 % sucrose and 30 mM Tris-HCl (pH8.0), and 500 mM EDTA was added dropwise to 1 mM final concentration. The cells were incubated for 15 min in a rotation carousel and centrifuged at 8000 g for 25 min. The supernatant was saved in a 200 ml flask and the pellet was resuspended in 100 ml of cold 5 mM $MgSO_4$ solution. The suspension was incubated and centrifuged as described above. Supernatants (total 200 ml) from the sucrose and the $MgSO_4$ solutions were transferred to a Spectra/Por® 3 Dialysis Membrane (SPECTRUM® LABORATORIES) and dialyzed twice against 2 L of buffer *A* (50 mM NaH_2PO_4, 300 mM NaCl, 10 mM imidazole, pH 8.0) for 2 h before continuing with the purification. Five milliliters of 50% Ni-NTA matrix (Ni-NTA Fastflow, Qiagen) equilibrated in buffer *A* were added to a column (Flex-Column, Kontes). The supernatant was applied to the column 3 times and the matrix was extensively washed with four 15 ml buffer *A* containing 50 mM imidazole. FlhE-6His was eluted with six 5 ml of buffer *A* containing 250 mM imidazole. The FlhE-

6His-containing eluate was dialyzed against 1 L of buffer *B* (20 mM Tris-HCl (pH 7.0), 10 % (v/v) glycerol) twice and concentrated to 7 mg ml^{-1} for crystallization by a centrifugal filter unit (Amicon® Ultra-15, MILLPORE) and a centrifugal filter device (Microcon, MILLPORE).

To produce seleno-methionine labeled FlhE-6His, cells were prepared as described (Van Duyne et al, 1993) with the following modifications. An overnight culture of ST004 containing pTrc99a-*flhE-6His* in LB was diluted 1:25 in 100 ml of M9 mininal-medium supplemented with ampicillin and grown overnight again at 37°C. M9 medium was prepared as follows: 5X M9 minimal salts were prepared using 33.9 g Na_2HPO_4, 15 g KH_2PO_4, 5 g NH_4Cl, and 2.5 g NaCl in 1L dH_2O. After being autoclaved, 200 ml of 5X M9 salts were diluted to 800 ml with autoclaved dH_2O and supplemented with $MgSO_4$ (2 mg ml^{-1}), $CaCl_2$ (0.1 mg ml^{-1}), and 0.4% glucose. The M9 culture was diluted to 1:100 in a 2 L flask with a working volume of fresh M9 medium (1 L) supplemented with ampicillin and grown at 37℃ for 6 h until OD_{600} reached 0.6. Before FlhE-6His induction, an amino acid mix (100 mg of lysine, phenylalanine, and thereonine, 50 mg of isoleucine, leucine, and valine, and 60 mg of seleno-methionine) was added to the culture and incubated for an additional 15 min. The addition of the amino acid mix inhibits the methionine synthesis pathway by targeting aspartokinase, and promotes incorporation of the supplemented seleno-methionine into proteins. The induction and purification of FlhE-6His were performed as described above.

PROTEIN CRYSTALLIZATION AND DATA COLLECTION

The crystallization of FlhE-6His was started by the sitting-drop vapor diffusion method using a commercially available 96-screen kit (Crystal Screen HT, Hampton Research). Crystallization drops were set up automatically by the Phoenix crystallization robot (Art Robbins Instruments) with two 96-well protein crystallization plates (Intelli-Plate^{TM} 96-3 LVR, Hampton Research). Each protein sample drop was prepared by mixing 0.1 µl reservoir solution with either 0.1 µl or 0.2 µl protein solution. Drops were equilibrated against 50 µl reservoir solutions. The plates were stored at 4^{o}C and at room temperature, respectively, for two weeks. Photographs of each drop were taken by the Art Robbins CrysCam and scored by the crystal score schemes: 0 clear, 1+ phase separation, 2+ precipitate, 3+ grainy precipitate/ microcrystals, 4+ precipitate web, 5+ sherulites, 6+ dusco balls, 7+ needles, 8+ plates, 9+ 3D crystals. From the initial screen, 11 conditions were chosen for crystal optimization, and the hanging-drop method was performed with 24-well plates (VDX Plate with sealant, Hampton Research). Each drop was set up on a cover-slide (Siliconized Glass Circle Cover Slide, Hampton research) with 1 µl reservoir solution and 1 µl protein solution, equilibrating against 500 µl reservoir. The plates were sealed with the cover slides and subsequently stored at 4°C. Micro-crystals were only observed in 2 out of 11 screen conditions: E8 (1.5 M NaCl, 10% ethanol) and E9 (2M NaCl, 0.1 M $CH_3COONa \cdot 3H_2O$ (pH 4.6)). To increase the size of crystals, a streak-seeding method was performed. Protein and reservoir solution were mixed 1:1 to the final drop volume of 2 µl on a slide. By using a micro-needle (CrystalProbe, Hampton Research), several micro-crystals were streaked on the drop, and the plate filled with 500

µl of the precipitant solution was sealed with the slide. After 24 h, crystals large enough (~ 0.1 mm in one dimensional size) to be used for data collection were observed in E8. Prior to data collection, a FlhE-6His crystal was transferred briefly to a drop of the E8 solution containing 20% glycerol for cryoprotection. The crystal mounted in a cryoloop (Hampton Research, Laguna Niguel, CA) was flash frozen in liquid nitrogen and mounted in the cold stream on the goniostat. X-ray diffraction data were collected from the crystal at 100 K on a Rigaku R-AXIS IV++ image plate detector (Rigaku, The Woodlands, TX) with X-rays generated by a Rigaku MicroMax-007 HF rotating anode generator operated at 40 kV, 30 mA. Diffraction images were processed and data reduced using HKL2000 (Otwinowski & Minor, 1997).

CHAPTER 3: Phenotypes of *flhE* deletion mutants in *S. enterica*

3.1 INTRODUCTION

Bacterial flagella enable individual swimming motility through liquid or group swarming motility over a surface as described in Chapter 1 (Harshey, 2003; Chevance & Hughes, 2008; Kearns, 2010). Flagellar biogenesis has been best studied in *Salmonella* (Macnab, 2003; Chevance & Hughes, 2008; Harshey, 2011). The function of most genes involved in this process is now largely understood. I have focused on the function of *flhE*, one of the few flagellar genes with an unassigned role. This gene is found mainly in Enterobacteria (Liu & Ochman, 2007), where it is co-expressed with *flhBA* genes, which encode two major components of the T3S system. Absence of FlhE does not affect swimming motility in *S. enterica* (Minamino et al, 1994). My initial experiments showed that a *flhE* mutant reduces swarming motility. Around this time a paper was published reporting that absence of FlhE eliminates swarming motility (Stafford & Hughes, 2007). This study concluded that the *flhE* mutant was not defective in flagella biosynthesis, but that it was affected in biofilm formation.

FlhE contains an N-terminal signal sequence for export into the periplasm via the Sec pathway, suggesting that it is a periplasmic protein (Minamino et al, 1994; Stafford & Hughes, 2007). This sequence was shown to be essential for its swarming phenotype (Stafford & Hughes, 2007). In this chapter, I present results that confirm the periplasmic

location of the protein. I observed that *flhE* mutant cells were lysing on swarm plates. I discovered a new 'green colony' phenotype associated with this mutation, which confirmed the lysis phenotype seen on swarm plates. In *Salmonella*, lysis was dependent on the presence of glucose. I then used the green phenotype to carry out an extensive Tn*10d*Cm suppressor analysis, as well as microarray analysis to understand the basis of the *flhE* phenotype. These analyses showed that cell lysis is associated with the assembly of flagellar filaments, and that cells induce stress-related pathways under these conditions.

3.2 RESULTS

3.2.1 Absence of FlhE affects swarming, but not swimming, motility in *S. enterica.*

The swimming and swarming phenotypes of a *flhE* mutant compared to wild-type *S. enterica*, were shown in Fig. 3.1. As noted earlier (Minamino et al, 1994; Stafford & Hughes, 2007), there was no effect of the *flhE* mutation on swimming; however, there was ~50% inhibition of swarming. This result was different from the Stafford & Hughes finding of complete inhibition of swarming in a *flhE* mutant (Stafford & Hughes, 2007). The difference in the extent of swarming inhibition could be due to differences in the parental strains used or the growth conditions; swarming is also sensitive to parameters such as humidity or commercial source of the agar (Harshey, 2003). Consistent with the earlier report (Stafford & Hughes, 2007), however, the swarming bacteria were not defective in flagella synthesis.

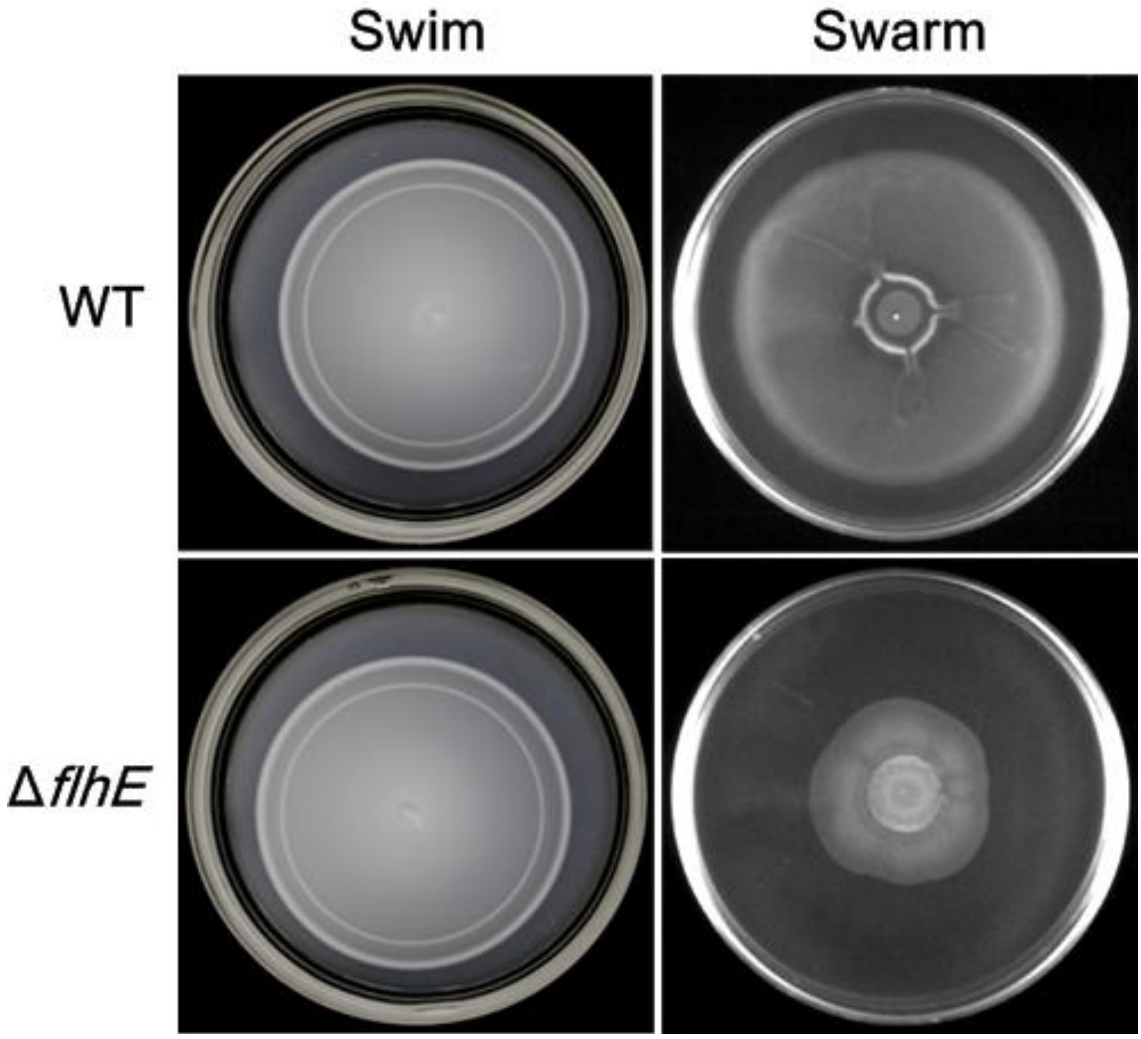

Fig. 3.1. Motility phenotype of a *flhE* mutant. Swimming and swarming motility of wild-type and a *flhE* mutant of *S. enterica*. Cultures were inoculated at the center of 0.3% agar plates for swimming and 0.6% agar plates for swarming motility. Plates were incubated at 37^{o}C for 6 h.

3.2.2 Swarm colony morphology is different between wild-type and *flhE* mutant cells in *S. enterica.*

When the *flhE* swarm colony was examined by phase-contrast microscopy, material floating with/around the cells was observed, producing a cobweb-like structure not seen in the wild-type colony (Fig. 3.2A). To determine the composition of this floating material, swarm colony supernatants were collected and examined by thin-layer chromatography (TLC), SDS-PAGE with silver-staining, and lipopolysaccharide (LPS) staining (see Methods in Chapter 2 for details). For TLC, ninhydrine reagent was used for the detection of amino acid-related compounds and 2,3,5-triphenyltetrazolium chloride/ lead(II) acetate basic/ Urea-HCl reagent for detection of sugars. All spots detected by TLC were the same between wild-type and the *flhE* mutant (only data with the ninhydrin reagent are shown in Fig.3.2B). No differences in LPS were observed between wild-type and the *flhE* mutant (Fig. 3.2C); this was also reported previously (Stafford & Hughes, 2007). However, the silver staining analysis showed more protein bands from the supernatant of the *flhE* mutant compared to wild-type (Fig. 3.2D). It appears from these data that the cob-web structure observed in the *flhE* swarm colony might be due to cell debris generated by lysis of the cells.

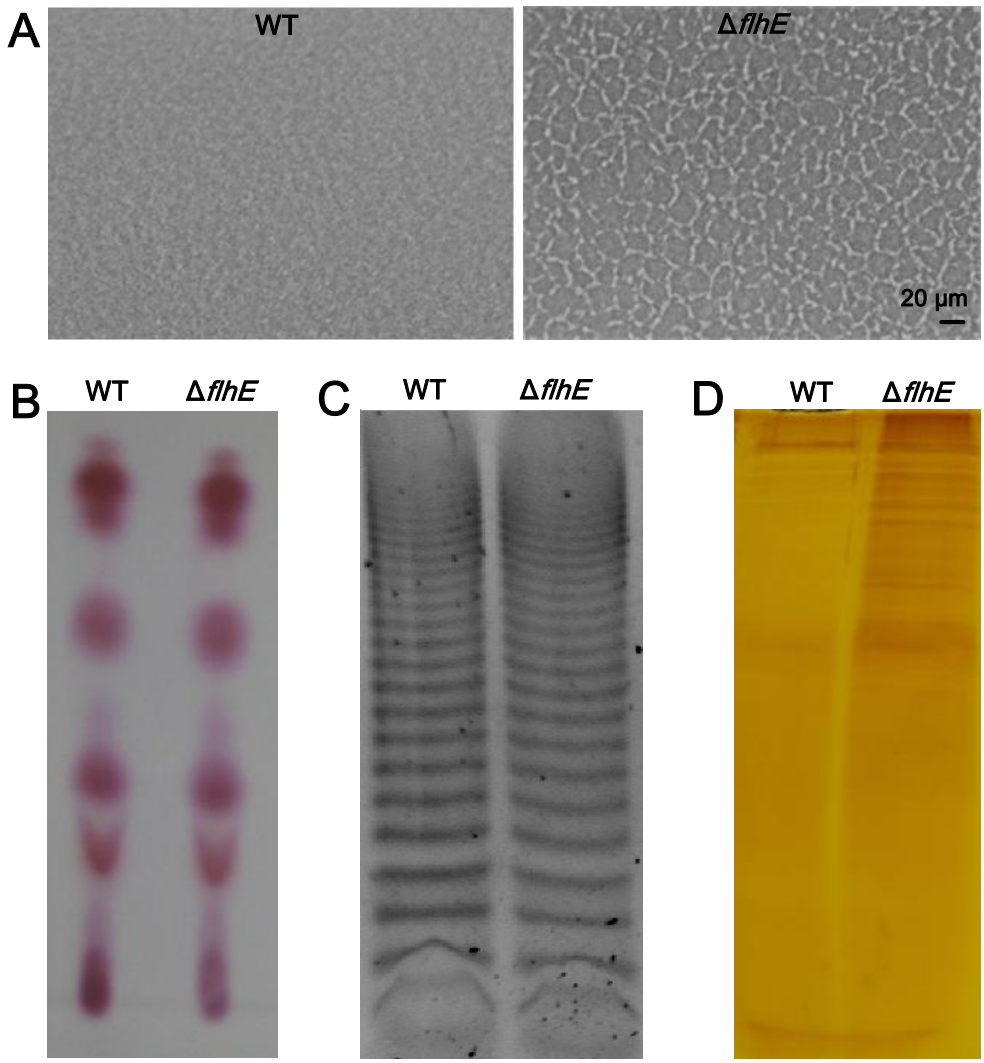

Fig. 3.2. Microscopic observations of swarming colonies of *S. enterica* wild-type and *flhE* mutant, and studies of their culture supernatants. **A**. Phase-contrast images showing wild-type and *flhE*::*kan* (ST005) swarming cells on swarm plates at 3 h after inoculation, when cells were actively moving. The supernatants collected from these colonies were analyzed by thin-layer chromatography (TLC) in B, LPS staining in C, and silver staining to detect proteins in D. In B, TLC was performed by the solvent (0.5% boric acid: 1-butanol: 2-propanol = 2:3:5 v/v) and visualized with a ninhydrin reagent. See Chapter 2 for details of all procedures.

3.2.3 *flhE* mutants are green on pH indicator plates, a phenotype associated with cell lysis.

Salmonella geneticists routinely use 'green' plates in transduction experiments to distinguish phage P22-carrying or P22-free transductants as green versus yellow colonies respectively. Green plates contain LB media with ~0.8% glucose and the pH indicator dyes aniline blue and alizarin yellow. In the case of P22 lysogens, lysis is required to observe the green color (Smith & Levine, 1967). Other mutants that show a green phenotype, for example *recA* strains, are also associated with cell death and lysis (data not shown). Although the molecular basis of the color-lysis association is not known, it is generally believed that anything that weakens the membrane integrity to cause solute leakage and cell lysis, gives green colonies.

Even in the absence of exposure to P22, *flhE* mutant colonies were observed to be green on these plates (Fig. 3.3A). When propagated on green swarm plates, the whole cell (WC) suspension of the *flhE* mutant was clearly green compared to wild-type (Fig. 3.3B). When centrifuged (3000 *g*, 5 min), the green material formed a top layer on the cell pellet. The yellow and green layers in the *flhE* mutant pellet were both seen to consist of cells under the microscope. Aniline blue is known to bind to different macromolecules: nucleic acids, glucans as well as hydrophobic proteins (Shennawy et al, 1984; Hough et al, 1985; Kippert & Lloyd, 1995). The green color appears to be the result of binding of the dyes to some cellular fraction either released from lysed cells or bound by dye that can permeate the dead cells (likely peptidoglycan, since spotting this macromolecule on the plates gave rise to green spots; data not shown). Several tests for cell lysis were

conducted and are shown in Fig. 3.3C-E. First, there was a 10% reduction in colony forming units (cfu) in the *flhE* mutant compared to wild-type (Fig. 3.3C). Second, live-dead staining, where live cells are stained green and dead cells red, revealed a similar proportion (10%) of dead cells in the *flhE* mutant (Fig. 3.3D). Finally, agarose gel electrophoresis of supernatants of cultures, prepared as in Fig. 3.3B, showed the presence of released genomic DNA only in the *flhE* mutant (Fig. 3.3E). It is concluded that the green color on the dye-containing plates arises from cell lysis within the *flhE* mutant colony. Cells in the green layer in Fig. 3.3B seem to be lighter because of loss of their cytoplasmic content.

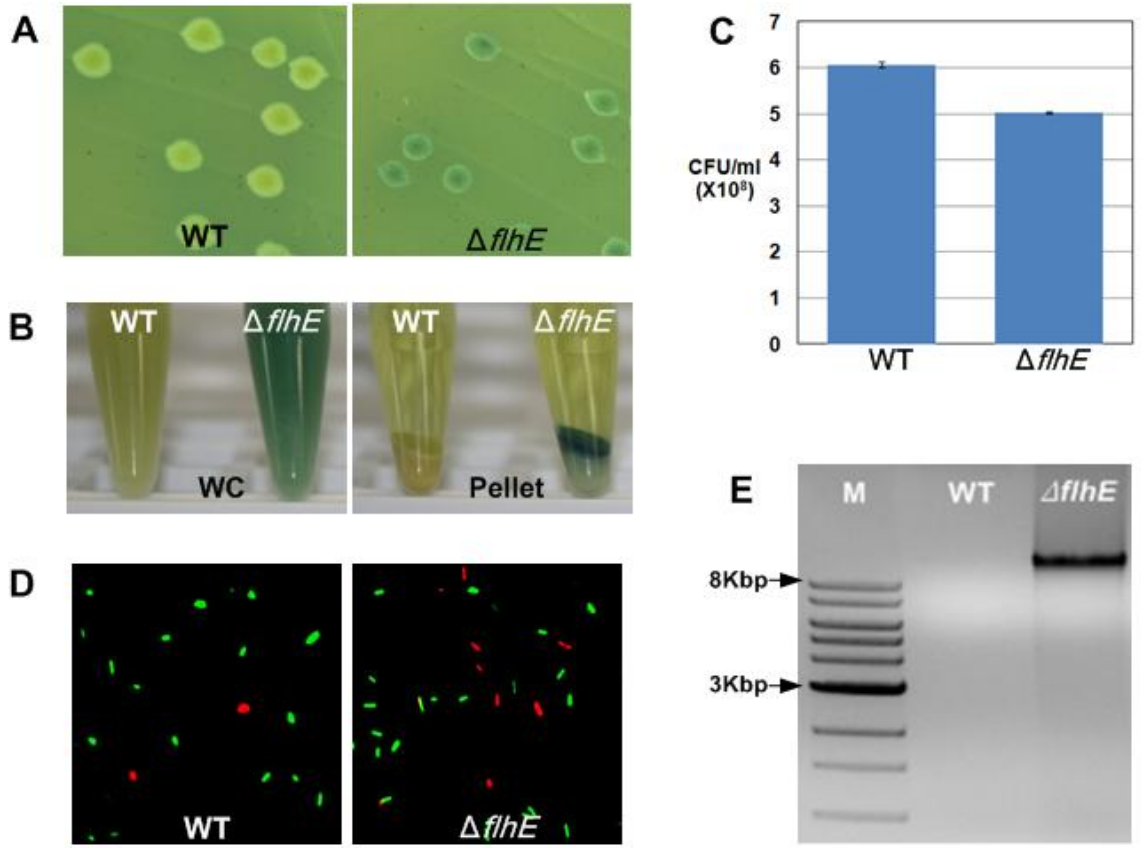

Fig. 3.3. *S. enterica flhE* mutant colonies are green on pH indicator plates and show cell lysis. **A**. Color phenotype of wild-type and *flhE* (ST004) colonies on green plates. **B**. Color of cell suspensions of the strains in A, isolated from green swarm plates after 6 h of growth. WC, whole cell suspension; Pellet, low-speed centrifugation of WC showing a clear supernatant and yellow/green pellets. **C**. Colony-forming units (cfu) of strains isolated as in B. **D**. Live–dead stain used to visualize cell death in strains isolated as in B. **E**. Genomic DNA in the supernatants from B, electrophoresed on 0.8% agarose gels and stained with ethidium bromide. DNA size markers are indicated. See methods in Chapter 2 for details.

3.2.4 Cell lysis in *S. enterica flhE* mutants requires glucose.

Glucose is a common component of both green plates and swarm plates. To test if glucose is needed for the cell lysis phenotype, *S. enterica* wild-type and *flhE* mutant strains were grown on green swarm plates with and without glucose. The genomic DNA release-assay showed cell lysis only in the presence of glucose in the *flhE* mutant (Fig. 3.4A). Similar results were observed when arabinose was substituted for glucose.

Sugar metabolism in bacteria generates acids (Stokes, 1956), which lowers the pH of the growth medium, as seen in a broth culture in Fig. 3.4B. To test if it is the lowered pH that is responsible for cell lysis, the medium was initially buffered with HEPES to prevent pH changes. Increasing buffer concentration resulted in decreasing cell lysis (Fig. 3.4C), supporting this notion (HEPES concentrations higher than 100 mM were toxic in that they induced lysis in wild-type cells). These results indicate that FlhE provides a protective function against acidic pH in *S. enterica*. In experiments described below, the green colony phenotype and/or genomic DNA release assay have been used to dissect the timing and requirements for FlhE fuction.

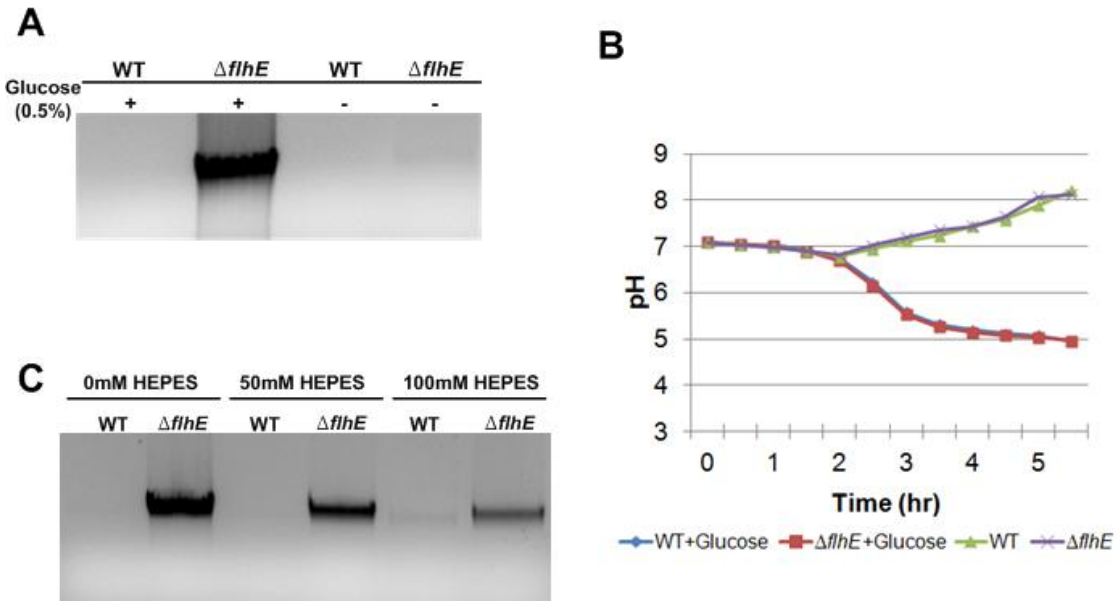

Fig. 3.4. Cell lysis in a *S. enterica flhE* mutant depends on added glucose, whose metabolism lowers external pH. **A**. Agarose gel assay for lysis as in Fig. 3.3. **B**. External pH of indicated strains grown in LB medium with and without the addition of glucose, measured as described in Chapter 2. **C**. Effect of increasing HEPES buffer on cell lysis, measured as in A. The buffer was added to green swarm plates, and cells were harvested at 6 h. HEPES buffered well only at concentration over 200 mM. However, at these higher concentrations it was not well-tolerated by wild-type cells, which began to lyse. At 100 mM, the pH of the culture was ~0.5 units higher than the unbuffered culture.

3.2.5 Filament assembly is essential for cell lysis and increased filament numbers exacerbate cell lysis in *flhE* mutants.

The green colony phenotype of the *S. enterica flhE* mutant provides a convenient handle for isolating second-site color suppressor mutants. A large-scale Tn*10d*Cm transposon mutagenesis of the *flhE* strain yielded 3.4% yellow suppressors (i.e. wild-type colony color; see Methods in Chapter 2). A majority of these suppressors were non-motile, suggesting that the flagellar system was important for the green phenotype. Of those that were motile, none had wild-type levels of motility. Suppressor mutants displaying > 40-80% of parent motility were sequenced (Table 3.1). Of these, 15 suppressors mapped between *lrhA* and *yfbQ* genes, 3 in *mdo* genes, and 2 in *rcs* genes. Mutations were also recovered in *fliC, ptsI, bcfB, ilvG, mrcA, serB,* and *yddG* genes.

LrhA is a positive regulator of *flhDC* in *E. coli* (Lehnen et al, 2002). Given that the mutants had diminished motility, it is fair to assume that the insertion diminished *lrhA* expression. *mdo* and *rcs* mutations are known to down-regulate flagellar gene expression in *S. enterica* (Toguchi et al, 2000; Wang et al, 2007). FliC is one of two types of flagellins in *S. enterica*, expressed alternatively as described in Chapter 1 (Bonifield & Hughes, 2003). PtsI is the enzyme I of the phosphoenolpyruvate-protein phosphotransferase, known to be required for swarming in *E. coli* (Inoue et al, 2007). BcfB is a periplasmic fimbrial chaperone, showing 96% amino acid homology to FimC by T-COFFEE Multiple Sequence Alignment (data not shown). A *fimC* mutant was reported to down-regulate flagellar gene expression during swarming in *E. coli* (Inoue et al, 2007). The remaining four genes (*ilvG, mrcA, serB, yddG*) are unrelated to flagella

function. It appears therefore that the majority of the suppressors had flagella-related defects. All of these mutants regained full motility and turned green when complemented with *flhDC* on a plasmid (p*flhDC*) (data not shown). A consensus emerged that the green color depended on increased numbers of flagella.

To determine whether FlhE function is associated with a particular step of flagellar biogenesis, mutations in key flagellar genes in the *flhE* mutant background were systematically examined, only a subset of which was shown in Fig. 3.5. *flhDC, fliK, fliA, flgK/L, fliC-fljB,* and *fliD* mutants were yellow (Fig. 3.5A), and showed no lysis (genomic DNA release) on agarose gels (Fig. 3.5B), whereas the *motA* mutant was green and showed lysis. *fliK* and *fliA* mutants are defective in P_{class3} gene expression (see Fig. 1.2), while *flgK/L, fliC-fljB and fliD* mutants are proficient in both P_{class3} transcription and protein export but cannot assemble an intact filament. The *motA* mutant can assemble flagella but cannot power their rotation. These results show that filament assembly, but not rotation, is essential for cell lysis.

Salmonella has two types of flagellin proteins FljB and FliC, but only one is expressed due to flagellar phase variation as described in Chapter 1 (Bonifield & Hughes, 2003). To examine whether the cell lysis of a *flhE* mutant is dependent on the specific filament type - FljB or FliC - *hin* recombinase mutants expressing either *fljB* or *fliC* genes were tested. Hin controls alternate expression of these two genes. No differences in either green colony morphology or amount of DNA released (i.e. cell lysis) were observed between strains expression one or the other filament genes (Fig. 3.6C and D). Thus, cell lysis is independent of the filament subunit types.

As described above, when p*flhDC* was introduced into yellow suppressor mutants shown in Table 3.1, they not only regained higher levels of motility, but their colonies became darker green compared to the *flhE* mutant parent. Also, the green color of the *flhE* mutant (but not the wild-type parent) turned darker green in the presence of p*flhDC* (Fig. 3.5A, compare last two panels on row 2). This darkening of the green color was accompanied by dramatically increased cell lysis as measured by both the genomic DNA release assay (Fig. 3.5B and 3.6A) as well as the cfu measurement (Fig. 3.5C). Under the inducing conditions used, p*flhDC* increases flagella numbers two- to three-fold (Fig. 3.6B). However, lysis depended on filament assembly under these conditions as well i.e. all of the yellow mutants shown in Fig. 3.5A remained yellow and no genomic DNA detected in the presence of p*flhDC* (Only data for the *flgL* mutant were shown in Fig. 3.6A and B). These results show that not only were filaments important for cell lysis, but also higher numbers caused more lysis.

Table 3.1. Motile yellow suppressors of *flhE*.

Strain	Genotype[a]	Swimming[b]
AS006	*flhE*::*kan ptsI*409::Tn*10d*Cm	I
STS14	*flhE*::*kan lrhA*::Tn*10d*Cm::*yfbQ* (ig.2441432)	I
STS15	*flhE*::*kan rcsC*126::Tn*10d*Cm	I
STS16	*flhE*::*kan lrhA*::Tn*10d*Cm::*yfbQ* (ig.2441441)	I
STS19	*flhE*::*kan lrhA*::Tn*10d*Cm::*yfbQ* (ig.2441432)	I
STS20	*flhE*::*kan lrhA*::Tn*10d*Cm::*yfbQ* (ig.2441441)	I
STS21	*flhE*::*kan rcsD*203::Tn*10d*Cm	I
STS22	*flhE*::*kan lrhA*::Tn*10d*Cm::*yfbQ* (ig.2441432)	I
STS25	*flhE*::*kan bcfB*466::Tn*10d*Cm	I
STS34	*flhE*::*kan lrhA*::Tn*10d*Cm::*yfbQ* (ig.2441441)	I
STS35	*flhE*::*kan lrhA*::Tn*10d*Cm::*yfbQ* (ig.2441441)	I
STS36	*flhE*::*kan lrhA*::Tn*10d*Cm::*yfbQ* (ig.2441432)	I
AS002	*flhE*::*kan mdoG*1428::Tn*10d*Cm	II
AS005	*flhE*::*kan fliC*83::Tn*10d*Cm	II
AS011	*flhE*::*kan mdoH*1154::Tn*10d*Cm	II
STS02	*flhE*::*kan lrhA*::Tn*10d*Cm::*yfbQ* (ig.2441432)	II
STS05	*flhE*::*kan ilvG*26::Tn*10d*Cm	II
STS06	*flhE*::*kan lrhA*::Tn*10d*Cm::*yfbQ* (ig.2441115)	II
STS17	*flhE*::*kan mdoH*110::Tn*10d*Cm	II
STS23	*flhE*::*kan lrhA*::Tn*10d*Cm::*yfbQ* (ig.2441432)	II
STS24	*flhE*::*kan lrhA*::Tn*10d*Cm::*yfbQ* (ig.2441432)	II
STS26	*flhE*::*kan lrhA*::Tn*10d*Cm::*yfbQ* (ig.2441441)	II
STS27	*flhE*::*kan mrcA*1373::Tn*10d*Cm	II
STS28	*flhE*::*kan serB*734::Tn*10d*Cm	II
STS29	*flhE*::*kan lrhA*::Tn*10d*Cm::*yfbQ* (ig.2441441)	II
STS30	*flhE*::*kan yddG*630::Tn*10d*Cm	II
STS32	*flhE*::*kan lrhA*::Tn*10d*Cm::*yfbQ* (ig.2441432)	II

[a] The number after the gene is the nt position before the Tn*10* insertion. For insertions within intergenic (ig) regions, both flanking genes are listed; all insertions were independent, yet only 3 insertion positions were repeatedly recovered in the ig region. Gene descriptions are below (McClelland et al, 2001).

[b] Category I: > 80% of *flhE*::*kan* (ST005) parent motility; category II: 40% - 80% of *flhE*::*kan* motility.

- *bcfB*: periplasmic, fimbrial chaperone
- *fliC*: flagellin, filament structural protein
-*ilvG*: inner membrane, acetolactate synthase II, large subunit, fragment 1, a cryptic
- *lrhA*: inner membrane, NADH dehydrogenase transcriptional repressor (LysR family)
- *mdoG*: periplasmic, glucans biosynthesis protein
- *mdoH*: inner membrane, membrane glycosyltransferase; synthesis of membrane-derived oligosaccharide (MDO)/synthesis of OPGs (osmoregulated periplasmic glucans)
- *mrcA*: inner membrane, transpeptidase of penicillin-binding protein 1a (peptidoglycan synthetase)
- *ptsI*: inner membrane, general PTS family (Enzyme I) PEP-protein phosphotransferase
- *rcsC*: inner membrane, sensory histidine kinase in two-component regulatory system with RcsB, regulates colanic capsule biosynthesis
- *rcsD*: inner membrane, putative sensor/kinase in regulatory system
- *serB* : cytoplasm, 3-phosphoserine phosphatase
- *yddG* : inner membrane, putative permeasetic amino acids
- *yfbQ*: cytoplasm, putative aminotransferase (ortho), paral putative regulator

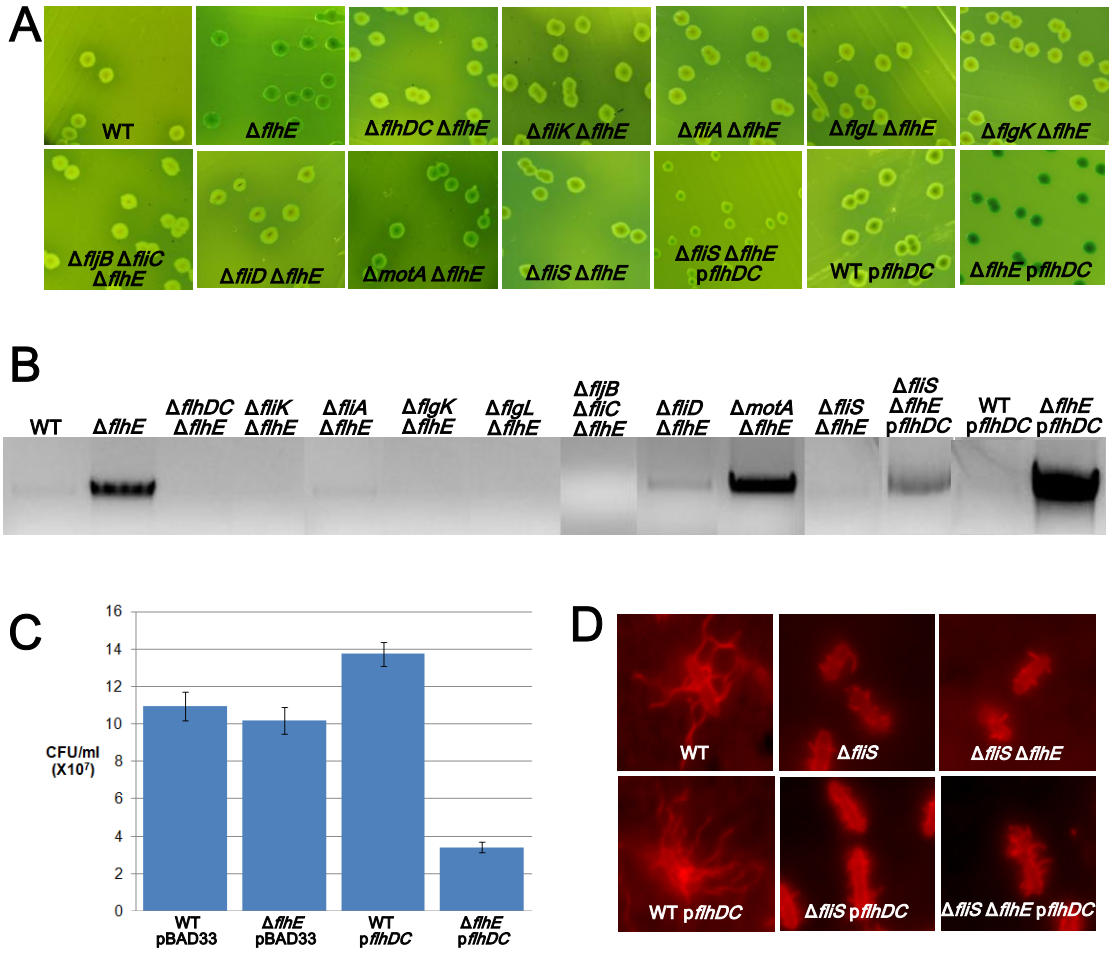

Fig. 3.5. Filament assembly, number and length, but not rotation, are essential for cell lysis in a *S. enterica flhE* mutant. **A**. Color phenotype on green plates of mutants defective in various steps of flagellar assembly. In strains with p*flhDC*, arabinose (0.8%) was substituted for glucose in the medium to induce gene expression. Strains used from left to right (not including those with plasmids): WT 14028, ST004, ST496, ST121, ST214, ST210, ST137, ST212, ST146, ST157, ST442. **B**. Agarose gel electrophoresis of *flhE* mutants shown in A, propagated on green swarm plates, in which arabinose was substituted for glucose in strains with p*flhDC*. **C**. Cell viability of wild-type and *flhE* mutant strains complemented with p*flhDC*; 0.2% arabinose added as inducer. **D**. Flagellar staining of indicated strains with Texas Red coupled anti-IG antibody to FljB antibody.

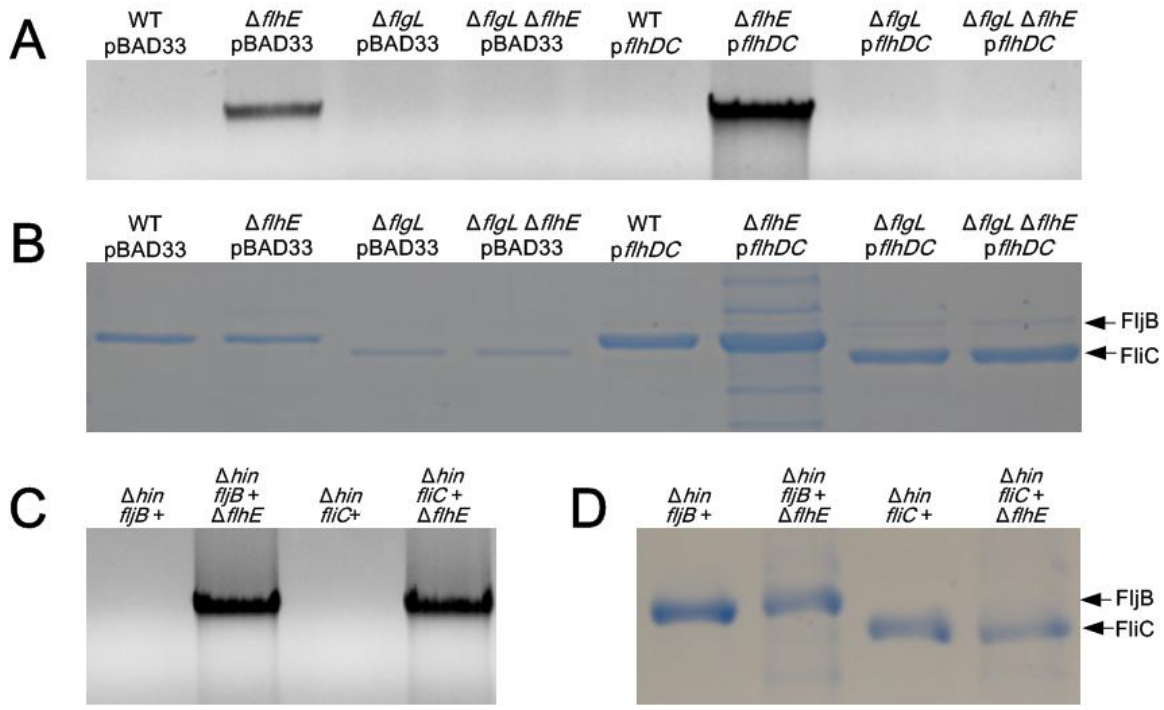

Fig. 3.6. Filament subunit (flagellin) secretion and filament types are not sufficient for cell lysis in *S. enterica flhE* mutants. **A**. Agarose gel electrophoresis assay for cell lysis of wild-type and *flgL* mutants defective in *flhE* propagated on green swarm plates. Strains used (not including plasmids): WT 14028, ST004, ST209, ST210. **B**. SDS-PAGE gel electrophoresis of cell culture supernatants isolated from mutants shown in A, stained with SimpleBlue as described in Chapter 2. The filament subunit protein flagellin is the predominant extracellular protein. It phase-varies alternately between FljB and FliC subunit type (see Fig. 1.1). **C**. Agarose gel electrophoresis of *hin* mutants expressing either *fljB* or *fliC* genes. Strains used from left to right: RH2202, ST149, RH2204, ST150. **D**. SDS-PAGE gel electrophoresis of cell culture supernatants of mutants shown in C, as described in B.

3.2.6 Flagellar filament length is important for cell lysis of a *flhE* mutant.

As shown above, the filament assembly and the number of flagella are important for the cell lysis of *flhE* mutants. To explore these results further, a mutation in the filament-protein chaperone gene *fliS* was introduced into the *flhE* strain. This mutant is reported to make short filaments (Yokoseki et al, 1995; Auvray et al, 2001) (Fig. 3.5). The *flhE fliS* double mutant was yellow (Fig. 3.5A), and showed no lysis (Fig. 3.5B), unless the strain also had p*flhDC*, in which case the number of short filaments doubled (Fig. 3.5D). Under those conditions, lysis increased modestly compared to the *flhE* strain with p*flhDC* (Fig. 3.5B). These data show that filament length is important for lysis.

3.2.7 Absence of FlhE shows filament assembly-dependent cell lysis even when flagella grow in the periplasm.

In order to gain insight into FlhE function by a different method, differences in gene expression profiles between wild-type and *flhE* mutant strains were monitored by microarray experiments. The data showed a slight upregulation of colanic acid biosynthesis genes in the *S. enterica flhE* mutant compared to wild-type (yellow-labeled rows in Table 3.2). Upregulation of these genes can be indicative of stress on the cell envelope activating, via the outer membrane protein RcsF, the Rcs signaling pathway (Laubacher & Ades, 2008). In gram-negative bacteria, stress sensors monitor permeability of the outer membrane, folding of envelope proteins, and energization of the inner membrane (Raivio, 2005; Rowley et al, 2006).

To test whether the filament-dependent cell lysis was due to stress on the outer membrane from the point of exit of the filament, the experiments described above were repeated in a *S. enterica* PL-ring mutant (*flgHI*) background. Flagella do not exit the outer membrane in this situation, and they grow inside the periplasm when combined with a *flhE* mutation (Chevance et al, 2007) (Fig. 3.7A). Here too, the green color and lysis depended on absence of FlhE and the presence of an intact filament (Fig. 3.7B and C). *flgK* and *flgL* (HAP) mutants, which lack the hook-filament junction proteins, secrete flagellin subunits but fail to assemble a flagellum (see Fig. 3.6A). The *flhE flgHI* mutant was observed to be more susceptible to lysis compared to the *flhE* mutant alone (Fig. 3.7C); indeed, induction of p*flhDC* in the *flhE flgHI* background was lethal. These data indicate that filament-dependent lysis is independent of either external or periplasmic location of the flagella.

Table 3.2. *S. typhimurium* 14028: Microarray Experiment of WT vs *flhE*.

mRNA from 3.0h sample on 0.6% swarming agar plates

Regulation	UNIQID	NAME	Transcription ratio	Gene Function
Positve	STM0462	-	**2.4**	hypothetical protein
	STM0463	amtB	**3.5**	putative Amt family, ammonium transport protein
	STM2355	argT	**2.8**	ABC superfamily (bind_prot), lysine/arginine/ornithine transport protein
	STM2104	cpsG	**2.2**	phosphomannomutase in colanic acid gene cluster
	STM3280.S	deaD	**2.2**	cysteine sulfinate desulfinase
	STM3629	dppB	**2.0**	ABC superfamily (membrane), dipeptide transport protein 1
	STM4007	glnA	**2.3**	glutamine synthetase
	STM4005	glnG	**2.1**	response regulator in two-component regulatory system with GlnL (EBP family)
	STM0830	glnH	**2.0**	ABC superfamily (bind_prot), glutamine high-affinity transporter
	STM4006	glnL	**2.3**	sensory kinase (phosphatase) in two-component regulatory system with GlnG (nitrogen regulator II, NRII)
	STM0665	gltI	**2.0**	ABC superfamily (bind_prot), glutamate/aspartate transporter
	STM0664	gltJ	**2.4**	ABC superfamily (membrane), glutamate/aspartate transporter
	STM0663	gltK	**2.1**	ABC superfamily (membrane), glutamate/aspartate transporter
	STM2109	gmd	**3.6**	GDP-D-mannose dehydratase in colanic acid gene cluster
	STM2352	hisM	**2.6**	ABC superfamily (membrane),histidine and lysine/arginine/ornithine transport protein
	STM2351	hisP	**2.6**	ABC superfamily (atp_bind), histidine and lysine/arginine/ornithine transport protein
	STM2353	hisQ	**2.6**	ABC superfamily (membrane),histidine and lysine/arginine/ornithine transport system
	STM2898	invG	**2.0**	invasion protein; outer membrane
	STM2892	invJ	**2.0**	surface presentation of antigens; secretory proteins
	STM2105.S	manC	**2.1**	mannose-1-phosphate guanylyltransferase
	STM2086	rfbU	**2.1**	LPS side chain defect: mannosyl transferase

Table 3.2, cont.

	STM2087	rfbV	**2.0**	LPS side chain defect: abequosyltransferase
	STM1308	spy	**2.0**	periplasmic protein related to spheroblast formation
	STM1911	STM1911	**3.2**	putative cytoplasmic protein
	STM3031	STM3031	**2.6**	ail and ompX homologue
	STM4262	STM4262	**2.1**	putative ABC-type bacteriocin/lantibiotic exporter, contain an N-terminal double-glycine peptidase domain
	STM1714	topA	**2.0**	DNA topoisomerase type I, omega protein
	STM2115	wcaA	**2.4**	putative glycosyl transferase in colanic acid biosynthesis
	STM2112	wcaD	**2.9**	putative colanic acid polymerase
	STM2111	wcaE	**2.6**	putative transferase in colanic acid biosynthesis
	STM2110	wcaF	**3.3**	putative acyltransferase in colanic acid biosynthesis
	STM2108	wcaG	**3.1**	bifunctional GDP fucose synthetase in colanic acid biosyntheis
	STM2107	wcaH	**2.1**	GDP-mannose mannosyl hydrolase in colanic acid biosynthesis
	STM2106	wcaI	**2.3**	putative glycosyl transferase in colanic acid biosynthesis
	STM2118	wza	**3.3**	putative polysaccharide export protein, outer membrane
	STM2117	wzb	**2.6**	putative protein-tyrosine-phosphatase in colanic acid export
	STM2116	wzc	**3.3**	putative tyrosine-protein kinase in colanic acid export
Negative	STM2444	cysP	2.2	ABC superfamily (bind_prot), thiosulfate transport protein
	STM0831	dps	2.1	stress response DNA-binding protein; starvation induced resistance to H2O2
	STM2141	fbaB	2.9	3-oxoacyl-[acyl-carrier-protein] synthase I
	STM0543	fimA	2.1	major type 1 subunit fimbrin (pilin)
	STM1764	narG	2.4	nitrate reductase 1, alpha subunit
	STM1563	osmC	2.1	putative resistance protein, osmotically inducible
	STM1505	rspA	2.3	putative dehydratase, starvation sensing protein
	STM3028	stdB	2.2	putative outer membrane usher protein
	STM0520	STM0520	2.4	putative permease
	STM0721	STM0721	2.3	putative glycosyl transferase
	STM0898A	STM0898A	2.0	putative protein
	STM1485	STM1485	2.4	acid shock protein

Table 3.2, cont.

	STM1637	STM1637	2.3	putative inner membrane protein
	STM2607	STM2607	10.0	Gifsy-1 prophage: similar to head to tail joining protein
	STM2722	STM2722	2.0	Fels-2 prophage: similar to gpP, ATP charging, in phage P2
	STM2724	STM2724	2.4	Fels-2 prophage: hypothetical protein
	STM2750	STM2750	2.0	putative PTS system, glucitol/sorbitol-specific enzyme II
	STM3132	STM3132	2.0	putative xylanase/chitin deacetylase
	STM3254	STM3254	2.5	putative fructose-1-phosphate kinase
	STM3260	STM3260	2.1	PTS family galactitol-specific enzyme IIC
	STM1361	ydiM	2.0	putative MFS family transport protein
	STM2646	yfiD	2.0	putative formate acetyltransferase
	STM2802	ygaM	2.0	putative inner membrane protein

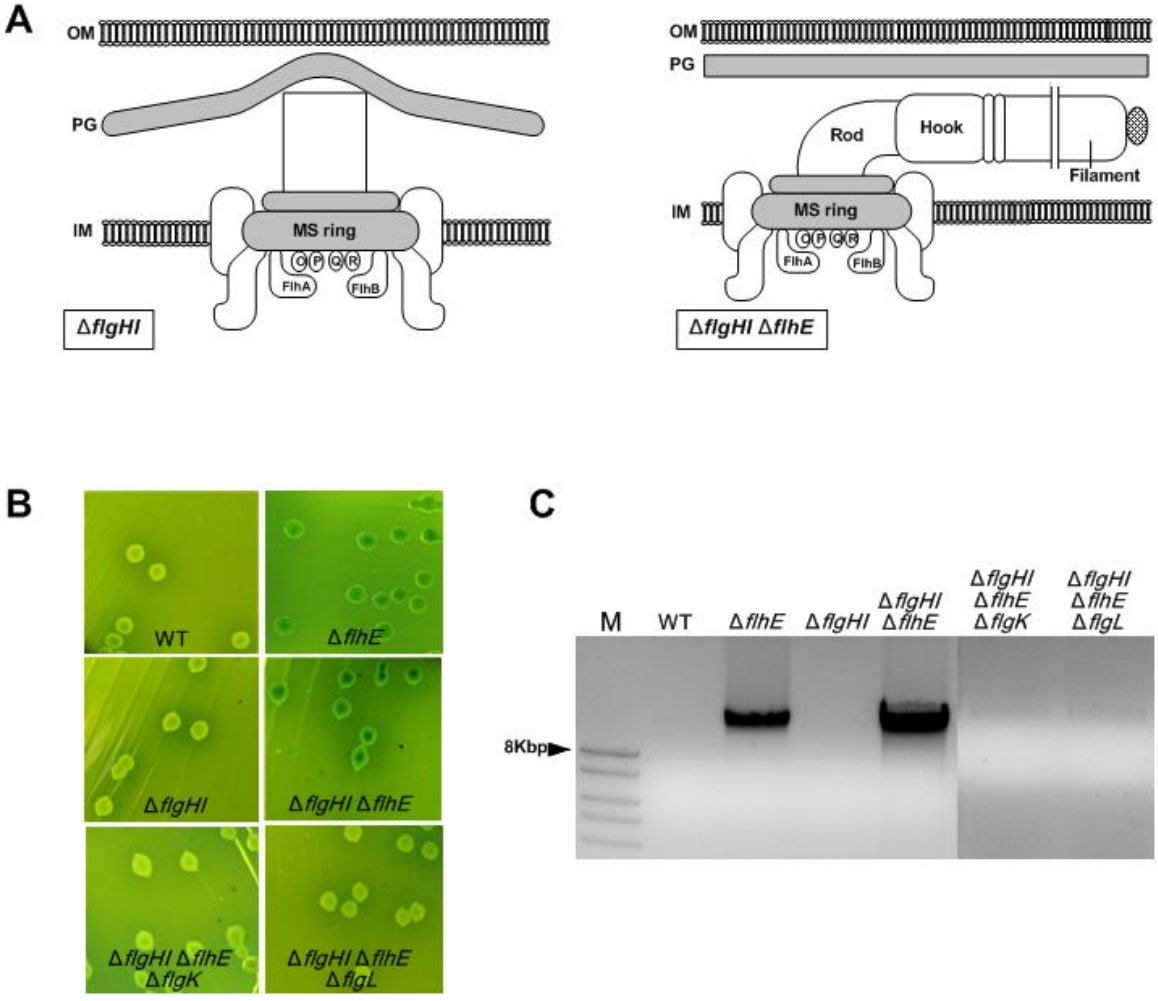

Fig. 3.7. Cell lysis of *flhE* mutants in a *S. enterica* PL-ring mutant background. **A**. Cartoon showing impairment of rod growth in a *flgHI* mutant (lacking P and L rings); deletion of *flhE* relieves this defect, allowing filaments to assemble in the periplasm (Hirano et al, 2009). **B**. Color phenotype of wild-type and *flgHI* mutants defective in *flhE* and/or *flgK*, *flgL* on green plates. Strains used from left to right: WT 14028, ST004, ST453, ST454, ST478, ST482. **C**. Agarose gel electrophoresis of mutants shown in B.

3.2.8 Increased cell lysis in aerobic vs anaerobic growth of *flhE* mutatns.

The swarming environment is more aerobic than when swimming under the agar (Wang et al, 2004). To test whether oxygen levels affect cell lysis of *flhE* mutants, the following two experiments were conducted. First, the difference in lysis of *flhE* mutants growing on swarm agar plates versus in liquid medium was tested. More DNA was detected on swarm agar plates by genomic DNA release assay (data not shown). Next, the effect of oxygen on cell lysis was tested on green swarm plates under aerobic versus anaerobic growth conditions as described in Chapter 2. The *flhE* cells grown under the aerobic conditions showed more DNA release as assyed by agarose gels (Fig. 3.8). These results suggest that oxygen availability contributes to the swarming-specific defect observed for *flhE* mutants.

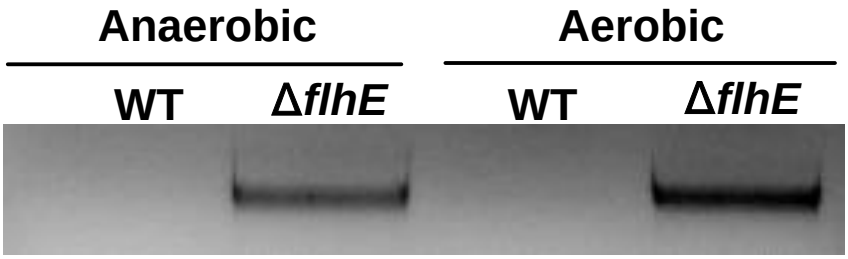

Fig. 3.8. Cell lysis in *S. enterica flhE* mutant in aerobic and anaerobic growth conditions. Agarose gel assay for cell lysis of wild-type and *flhE* mutant (ST004) cells grown on green swarm plates under aerobic and anaerobic conditions (see Chapter 2 for detail).

3.2.9 FlhE is a periplasmic protein detectable in flagellar basal body preparations.

The *flhE* gene encodes a 130-amino-acid protein. The N-terminal 16 amino acids of FlhE display features typical of a cleavable signal sequence. Full-length and cleaved forms of the protein were identified in maxicell labeling experiments in *S. enterica*, consistent with secretion of FlhE into the periplasm by the general secretory pathway (Minamino et al, 1994). To determine the cellular localization of FlhE, both Myc and FLAG epitope tags were respectively fused to the C-terminus of FlhE. Myc- and FLAG-tagged FlhE were used for cell fractionation and flagellar basal body preparation, respectively. When the tagged proteins were expressed from their chromosomal locations, the *flhE* defect was fully complemented but the Myc and FLAG signals were weak (data not shown), as expected due to the low mRNA levels of the *flhBAE* operon (Wang et al, 2004). When FlhE-Myc was expressed from a plasmid, cell fractionation experiments showed that FlhE using Myc antibodies was present in the cytoplasmic and periplasmic fractions, but not in the membrane fraction (Fig 3.9A). As a control, periplasmic maltose-binding protein (MBP) and inner membrane protein (MotB) showed appropriate locations in these cell fractions. Isolated basal body preparations showed the presence of FlhE using FLAG antibodies when the plasmid expressed FlhE-FLAG, but not in the vector control (Fig. 3.9B). The recovery of intact basal bodies was confirmed by detection of two proteins integral to it - the cytoplasmic C-ring protein FliG and the rod protein FlgG (see Fig. 3.9C). Cross-contamination of the flagellar preparation from membrane or periplasmic fractions was assessed by probing for the presence of the cytoplasmic membrane protein TonB and the periplasmic MBP in these preparations.

These proteins were not detected. In summary, these data show that the periplasmic protein FlhE is also included within the basal body.

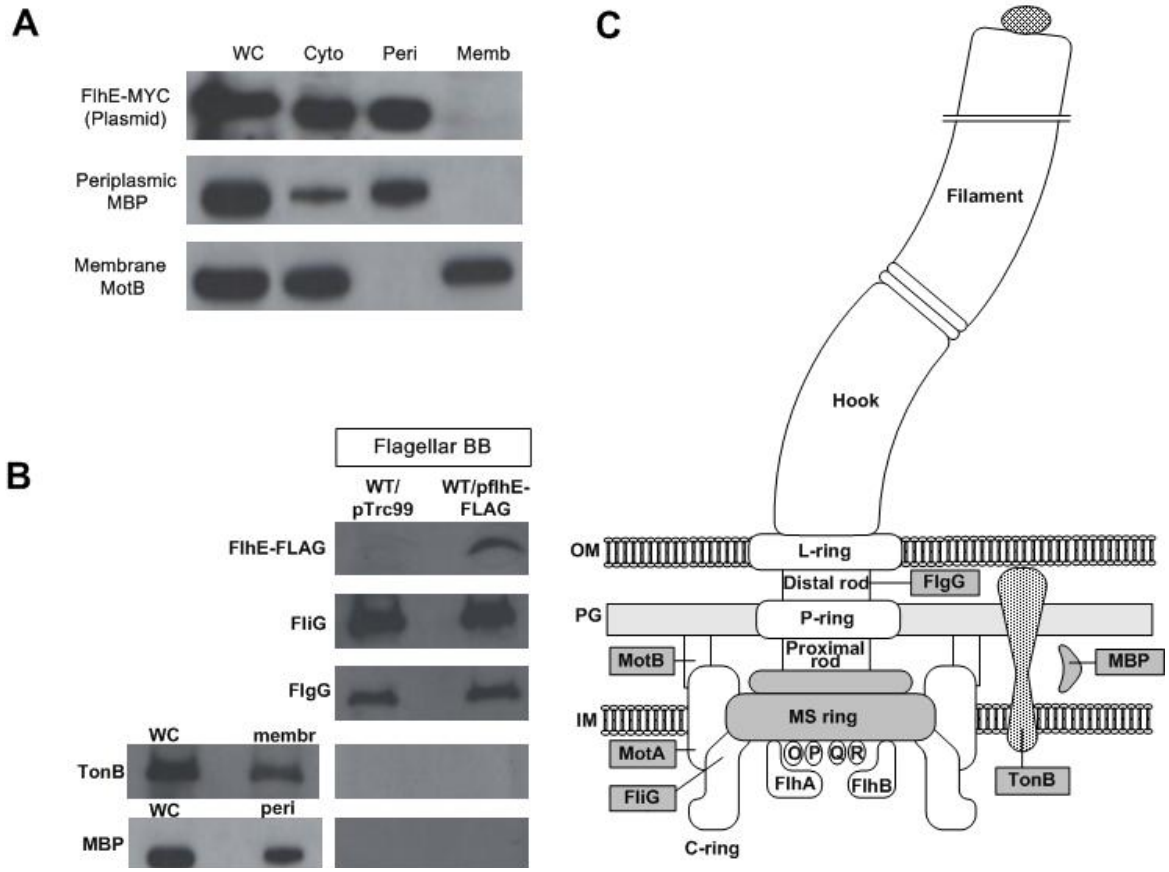

Fig. 3.9. Localization of FlhE in *S. enterica.* **A**. Western blots detecting the presence of FlhE-Myc in different cellular localization in the top panel. Wild-type cells expressing FlhE-MYC from a plasmid pTrc99a were fractionated into cytoplasmic (cyto), periplasmic (peri), and membrane (memb) fractions. WC, whole cells. The bottom two panels are controls that follow the location of the membrane protein MotB and periplasmic maltose-binding protein (MBP), using antibodies to these proteins. **B**. Western blots detecting the presence of FlhE-FLAG in isolated flagellar basal bodies. C-ring protein FliG and rod protein FlgG were detected with antibodies specific to these proteins. In the bottom two panels, the membrane protein TonB and periplasmic MBP in either WC, membr, peri or basal body (BB) preparations were used as controls. All lanes contained ~3 mg of protein. **C**. Schematic showing location of the flagellar and membrane proteins shown in B.

3.3 DISCUSSION

Flagellar biogenesis has been extensively characterized in *S. enterica*, yet the function of FlhE is unknown. A plausible role of FlhE might be related to the secretory functions of T3SS proteins FlhA and/or FlhB, because *flhE* is co-transcribed with these two genes (Stafford & Hughes, 2007). However, absence of swimming phenotype in a *flhE* mutant precluded understanding its function. The first breakthrough in the problem came with the report of a swarming-related phenotype associated with a *flhE* mutation (Stafford & Hughes, 2007), which I had also observed around the same time (Fig. 3.1). A second important breakthrough was my observation of a green colony phenotype for *flhE* mutants on green pH indicator plates (Fig. 3.3). Investigation of this phenomenon led to two important findings. First, both swarming and the green phenotype are closely associated with cell-lysis created by an acidic environment in the presence of added glucose (Fig. 3.4). Second, using the green color as a handle to isolate non-green suppressors, I found that cell lysis is also dependent on assembly of the filament (Figs. 3.5, 3.6, and 3.7), which most likely generates membrane stress. I also observed FlhE localized to the periplasm and within the basal body (Fig. 3.9).

***Glucose-dependence of cell lysis*.** The cells lysis phenotype was observed not only in the presence of glucose, but also other sugars such as arabinose. Sugar metabolism lowers the pH of the growth medium in bacteria as demonstrated in Fig. 3.4B. That it was the lowered external pH that was causing lysis was confirmed when lysis was reduced in

response to added buffer (Fig. 3.4C). It can be inferred from these data that FlhE acts in a manner that buffers or protects the bacteria from acidic pH.

***Filament assembly-dependence of cell lysis*.** It is puzzling why deletion of *flhE* did not cause cell lysis when the only the basal body and hook were assembled (Figs. 3.5, 3.6, and 3.7), but rather only when a full-length filament was added (Figs 3.5, 3.6, and 3.7). Not only was a fully assembled flagellum necessary, but over-expression of *flhDC*, which produces more flagella, exacerbated the lysis (Figs. 3.5 and 3.6). When flagella grow in the periplasm, where they are not anchored firmly in the peptidoglycan layer, the lysis phenotype was even greater (Fig. 3.7). The latter observation suggests that the assembled filament might cause stress on the inner membrane. In cells already stressed by the inability to protect against acidic pH, the added stress of a long filament may lead to solute leakage and lysis. Results in the next chapter will address the former issue. I cannot attribute filament-induced lysis to the viscous load known to be exerted on rotating external filaments, because neither rotation nor an external location of the filaments was required (Figs. 3.5 and 3.7).

Why does a flhE mutation affect swarming and not swimming? An obvious explanation for this differential effect of *flhE* is that swarm media contain glucose, whereas swim media do not. However, even if glucose was added to swim media, cell lysis was not as pronounced as on swarm plates (not shown). I offer two explanations for this result. First, the swarming environment is more aerobic compared to broth grown conditions (Wang *et*

al., 2004); lysis was more pronounced in aerobic compared to anaerobic swarm cultures (Fig. 3.8). Second, in a swarm colony, the fraction of cells with more flagella tends to lead the swarming pack. Because higher flagella number increase cell lysis, the leading edge of the swarm is disproportionally affected, interfering with movement of cells that follow.

CHAPTER 4: Acidification of the cytoplasm in *flhE* mutants

4.1 INTRODUCTION

Flagellar rotation in *E. coli* and *S. enterica* is powered by the PMF across the cytoplasmic membrane. The stator proteins MotA and MotB form the trans-membrane proton channel as described in Chapter 1 (Hosking et al, 2006). A 20-amino acid periplasmic segment of *E. coli* MotB has been suggested to function as a proton plug because an in-frame deletion of this segment causes considerable proton influx, inhibiting cell growth (Hosking et al, 2006). PMF is also required for secretion of flagellar substrates during flagellar assembly (Minamino & Namba, 2008; Paul et al, 2008). The assembly begins inside the cell and all flagellar components located beyond the cytoplasmic membrane are exported by the flagellar T3S system as described in Chapter 1 (Macnab, 2003; Harshey, 2011). Among the six integral membrane proteins of the T3S apparatus, a recent mutagenesis study of *flhA*, which is co-expressed with *flhE*, has assigned FlhA a PMF-driven export function (Hara et al, 2011).

In Chapter 3, the experiments in Fig. 3.4 showed that the cell lysis phenotype of the *flhE* mutant depends on a lower external pH. In this Chapter, I show that the *motB* plug-region deletion mutant ($MotB_{\Delta 51\text{-}60}$), which has been demonstrated to leak protons into the cells (Hosking et al, 2006), has a cell lysis phenotype similar to that of the *flhE* mutants in its dependence on filament assembly and numbers of flagella. These results

suggested that absence of FlhE might cause a proton leak as well. This idea was tested and confirmed by two different assays: a Tsr-dependent repellent response to low pH, and changes in the fluoresce intensity of a GFP pH reporter. Co-localization of fluorescent fusion proteins suggests a plausible interaction between FlhA and FlhE.

4.2 RESULTS

4.2.1 Cell lysis in an *S. enterica motB* proton plug mutant is dependent on filament assembly and increased flagella numbers.

S. enterica flhE mutants showed cell lysis in an acidic environment (Chapter 3). To test whether one of the known MotB plug deletion mutants (amino acid residues from 51 to 60), which causes cytoplasmic acidification and cell growth arrest in *E. coli* (Hosking et al, 2006) also causes cell lysis in *Salmonella*, $MotB_{\Delta 51\text{-}60}$ was overexpressed from a plasmid in a *S. enterica motB* deletion mutant and green swarm assay was performed as described in Chapter 2. Cell lysis was observed in this mutant by the genomic DNA release assay (Fig. 4.1A). When a *fliA* mutation, which prevents late gene expression and flagellar filament assembly, was introduced into the *motB* mutant background, cell lysis was suppressed (Fig. 4.1A), similar to the suppression observed for the *flhE* mutant (Fig. 3.5B). Ovexpression of FlhDC increased cell lysis dramatically in the $MotB_{\Delta 51\text{-}60}$-expressing strain (Fig. 4.1B), as seen in the *flhE* mutant strain (Fig. 3.5B and 3.6A). These results suggest that cytoplasmic acidification likely causes cell lysis in the *flhE* mutants.

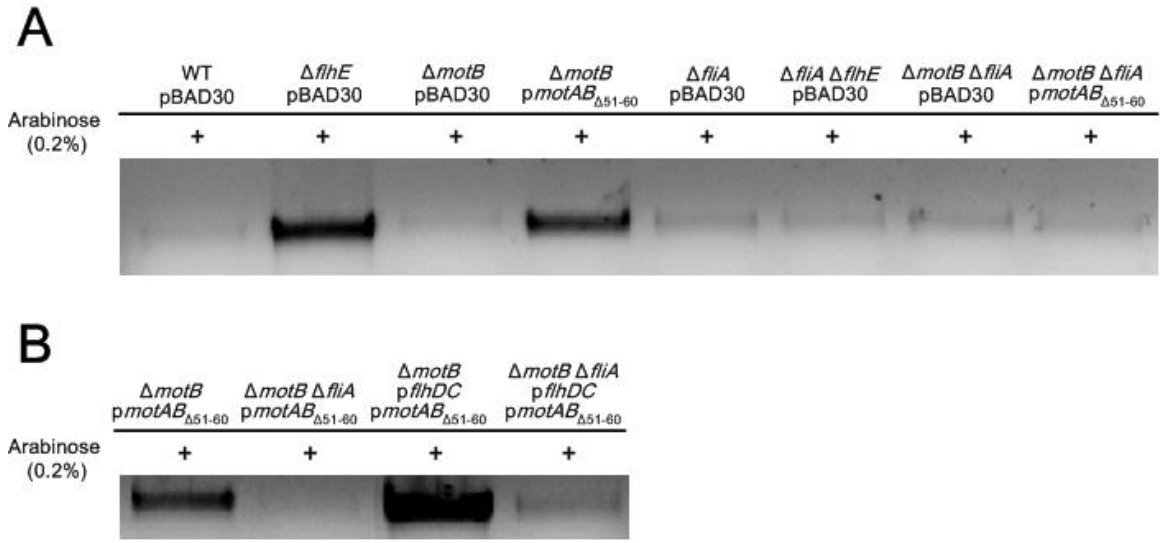

Fig. 4.1. A Mot B 'plug' mutant shows filament-dependent cell lysis in *S. enterica*. A plasmid carrying deletion of residues 51-60 in the MotB plug region (pBAD30-*motAB*$_{\Delta 51\text{-}60}$) was introduced in a *motB* mutant strain and assayed for cell lysis using the DNA-release assay in agarose gels as described in Chapter 2. **A**. Strains used from left to right (not including those with plasmids): WT 14028, ST004, QW180, ST649, ST214, ST580. **B**. Increase of flagella numbers by co-expressing p*flhDC* increases cell lysis in the *motB* mutant, also similar to that observed in the *flhE* mutant (Figs 3.5B and 3.6A). Arabinose concentration for induction was 0.2%.

4.2.2 Tsr-dependent tumbling response indicates lowered cytoplasmic pH in *S. enterica flhE* mutant.

Acidification of the cytoplasm is perceived as a repellent (tumble-inducing or CW rotation-producing) signal by the Tsr chemoreceptor (Kihara & Macnab, 1981; Repaske & Adler, 1981). Therefore, this assay was used to assess whether the cytoplasm was acidified in the *flhE* mutant when the external pH was lowered. Because cells adapt rapidly to attractants and repellents, the experimental design incorporated the previous observation that upregulation of *flhDC* increases cell lysis (Fig. 3.5). p*flhDC* is under P_{BAD} promoter control, and is thus induced by arabinose. Addition of arabinose has the dual effect of lowering the external pH and increasing flagella. Wild-type and *tsr* strains with and without the *flhE* mutation and harboring p*flhDC* were videotaped and their run-tumble bias monitored at 0 min (no inducer) and 30 min after arabinose addition as described in Chapter 2. The data are shown in Fig. 4.2. In the *flhE* mutant, tumble frequency increased in the tsr^+ (compare Fig. 4.2A and B) but not in the *tsr* strain (compare Fig. 4.2C and D). Based on this assay, it is concluded that absence of FlhE leads to acidification of the cytoplasm.

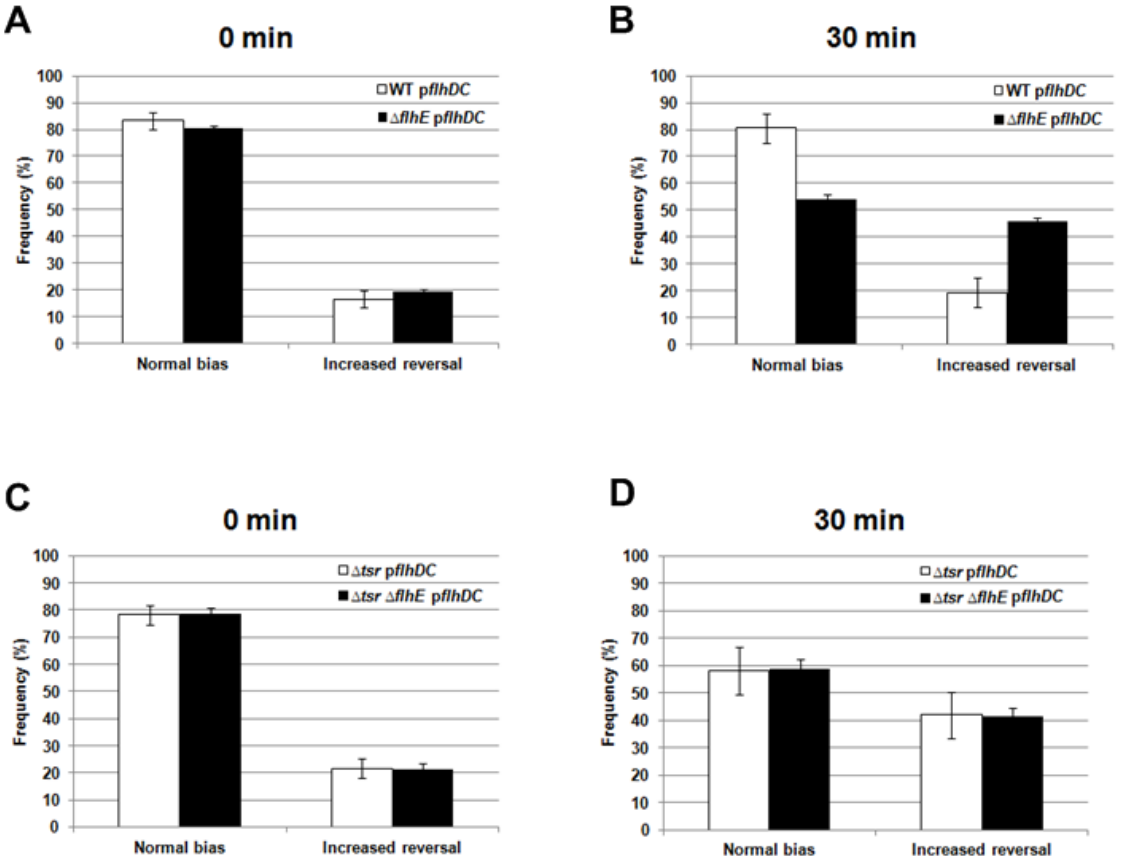

Fig. 4.2. Swimming behaviour of *flhE* mutants with and without chemoreceptor Tsr. *S. enterica* wild-type, *flhE* (ST004), *tsr* (RH2858) and *tsr flhE* (ST557) strains containing p*flhDC*, were induced for *flhDC* expression with addition of arabinose, and their swimming trajectories were observed and recorded at 0 min and 30 min after induction, as described in Chapter 2. 'Normal bias' refers to cells that swam straight for a distance of 25 µm without a tumble, which is the wild-type bias of cells in an isotropic medium.

4.2.3 Intracellular pH monitored by GFP reporter plasmids in *S. enterica*.

The chemoreceptor-based assay described above can only be performed after the switch to late or P_{class3} flagellar gene expression has taken place, because both the filament and the chemoreceptors are P_{class3} gene products (see Fig. 1.2). To test cytoplasm acidification by a second method, as well as to determine if the acidification is seen prior to the P_{class3} switch, a GFP reporter plasmid (GFPmut3b) that reports effectively on pH changes in the cytoplasm was used (Kitko et al, 2009). The data are shown in Fig. 4.3. The fluorescence emission spectra at various intracellular pHs, when equilibrated to the external pH using sodium benzoate, responded to changes in pH, as previously reported (Fig. 4.3A). These data were used to generate a standard curve correlating internal pH with fluorescence intensity (Fig. 4.3B). To test whether the internal pH of the *flhE* mutant was lower than that of its wild-type parent, the cultures were suspended in LB buffered to pH 5.5, similar to the pH measured during growth in glucose (Fig. 3.4B). Under these conditions, the cytoplasmic pH of the *flhE* mutant was seen to be lower than wild-type (Fig. 4.3C), supporting the results from the chemoreceptor/repellent assay shown in Fig. 4.2. However, attempts to measure pH differences in mutants stalled at various steps in the flagellar biogenesis pathway, gave variable results (showing differences between the mutants on some days and not on others), and were inconclusive.

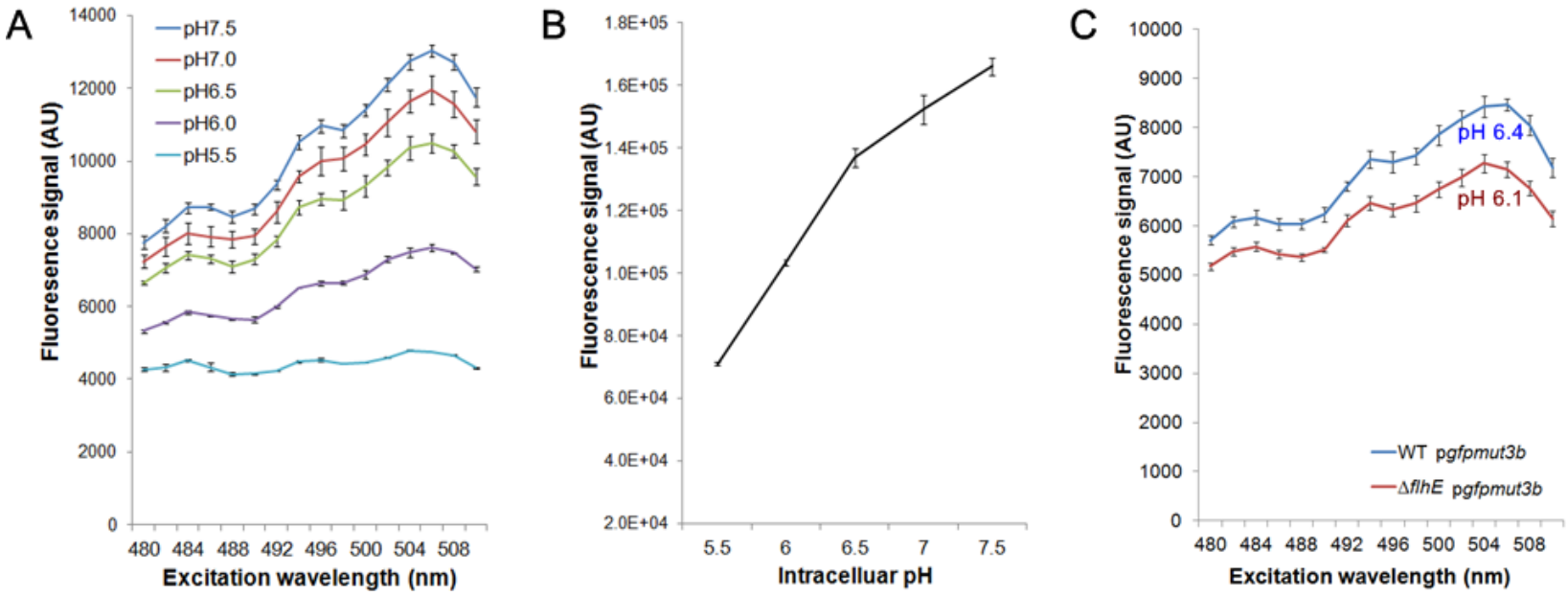

Fig. 4.3. Measurement of cytoplasmic pH in *S. enterica* by Green Fluorescent Protein Fluorimetry. **A**. Excitation spectra of cytoplasmic GFPmut3b as a function of pH. Wild-type *S. enterica* cells containing the GFP plasmid were suspended in M63 minimal-media adjusted to pH values varying from 5.5 to 7.5. Internal pH was equilibrated with external pH by addition of 30 mM sodium benzoate. **B**. Standard curve of cytoplasmic pH as a function of fluorescence signal (sum of 480 nm to 510 nm). See Chapter 2 for details. The error bars represent standard deviation of the mean (n = 3). **C**. Wild-type and *flhE* (ST004) *S. enterica* strains were resuspended in media adjusted to pH 5.5, and GFP excitation spectra were recorded without addition of benzoate. Fluorescence measurements were converted to pH units using the standard curve (B) as described in Chapter 2. AU, arbitrary units.

4.2.4 Intracellular pH monitored by GFP reporter plasmids in *E. coli.*

Salmonella and *E. coli* have somewhat different acid resistance mechanisms (Foster, 2004). Therefore, *E. coli* was chosen both to verify the *S. enterica* results and to test if the GFP pH reporter gives more reliable data in *E. coli*. In contrast to *S. enterica*, the *E. coli flhE* mutant grew poorly (Fig. 4.5A), and formed tiny colonies on LB plates. This mutant also showed a smaller swim-colony diameter and was completely defective in swarming (Fig. 4.4A). The growth defect is sufficient to explain the poor swim/swarm phenotypes of this mutant. Faster-growing variants, all of which were non-motile, accumulated readily, indicating that the growth defect of *E. coli flhE* strain is also related to the flagellar system. The *E. coli flhE* mutant behaved similarly to the *S. enterica flhE* mutant on green plates and in agarose-gel assays for cell lysis, except that these phenotypes were independent of added glucose (Fig. 4.4B and C). As in *S. enterica*, the phenotypes depended on filament assembly. For example, in *fliK* and *flgL* mutant backgrounds which cannot assemble filaments, the *flhE* mutant failed to show growth defects (Fig. 4.5A; only *fliK* mutant shown) or release of genomic DNA (data not shown). GFPmut3b reporter assays were more reproducible in *E. coli* (Fig. 4.5B), although here too day-to-day variations were experienced in the absolute pH values. However, the difference in pH between the strains measured on the same day is statistically significant (p-value < 0.005 for pH difference between wild-type and *flhE* mutant). As with *S. enterica*, the *flhE* mutation lowered the cytoplasmic pH in *E. coli*. The lower pH was associated with the *flhE* mutation in both the *fliK* and *flgL* mutant backgrounds. These data indicate that the cytoplasm is acidified prior to the switch to late

secretion (*fliK flhE*), is still seen after the switch (*flgL flhE*), and gets worse upon filament addition (*flhE*). Because the former two mutants neither lyse nor show growth defects (Fig. 4.5A), acidification, in and of itself, is not responsible for lysis.

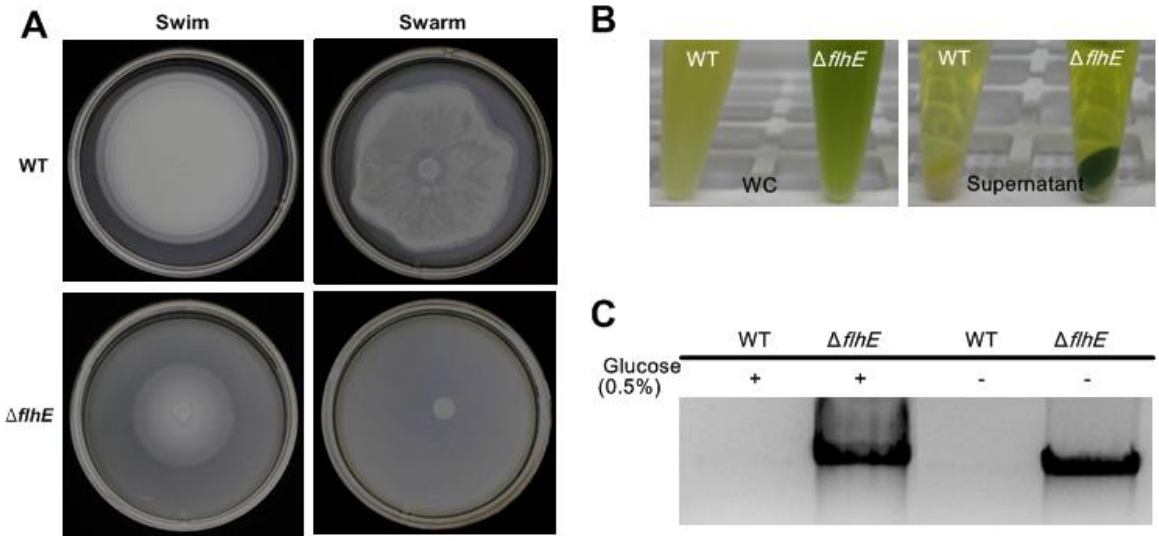

Fig. 4.4. Comparison of wild-type *E. coli* (RP437) and its *flhE* mutant (ST839) in **A**. motility, **B**. green swarm plates, and **C**. agarose-gel assays. Swarm plates were set with Eiken agar as described in Chapter 2. Other descriptions as in legends to Figs. 3.1 and 3.3.

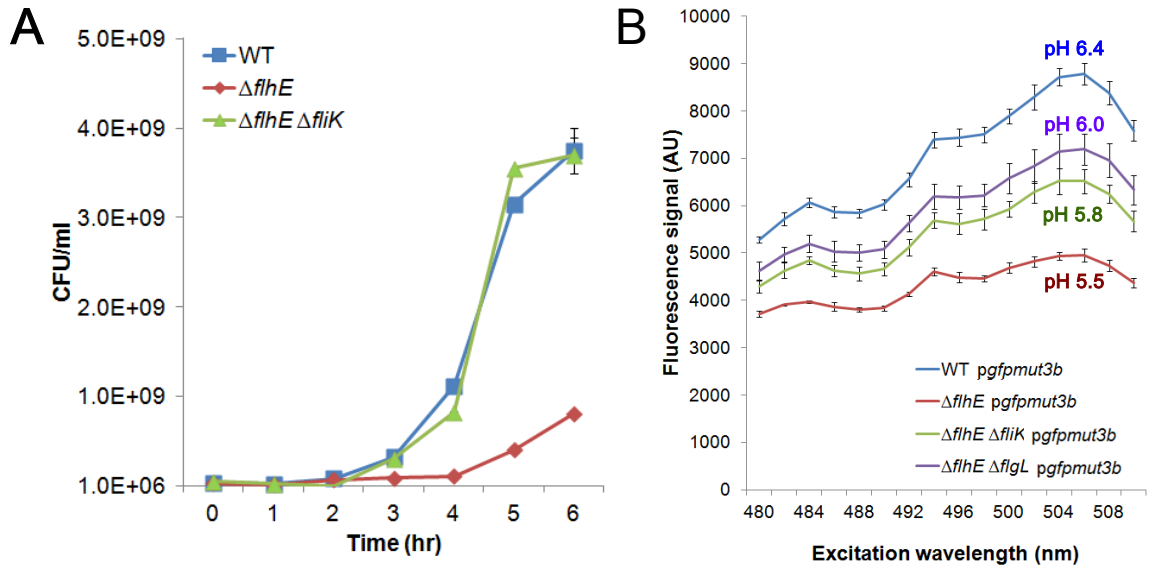

Fig. 4.5. Measurement of growth rates and cytoplasmic pH of *E. coli flhE* mutants. **A**. Growth curves in LB broth of the indicated *E. coli* strains, expressed as colony-forming units (cfu). Strains used: wild-type RP437, ST839, ST907. **B**. GFPmut3b excitation spectra in wild-type *E. coli* and its *flhE* mutant derivatives measured and converted to pH units as described in Fig. 4.3C. Strains as in A with the addition of ST964.

4.2.5 FlhE-mCherry co-localizes with FlhA-YFP.

In a recent study, a number of fluorescent proteins fusions to motor components were generated and their order of assembly monitored (Li & Sourjik, 2011). Among the T3S components, a FlhA-YFP fusion was stable, functional, and formed fluorescent puncta even when expressed by itself, while fusions to FlhB, FliP and FliR were unstable. Based on this, and on the observation that FliF-YFP oligomerization is promoted by FlhA, the study suggested that self-assembly of the basal body is initiated by oligomerization of FlhA, followed by the recruitment of the MS ring component FliF, and then the ordered association of other proteins as described in Chapter 1. FlhE localizes at periplasm within the basal body. Whether FlhE co-localizes with FlhA or FliF was tested by construction a FlhE-mCherry fusion. This fusion protein complemented *Salmonella flhE* moderately and *E. coli flhE* fully for motility (data not shown). However, it is uncertain whether the complementation was from small amounts of native protein that might be generated from proteolysis of the fusion protein in the periplasm.

As reported earlier (Li & Sourjik, 2011), a FlhA-YFP fusion showed fluorescent puncta in both *flhDC* and wild-type strains (Fig. 4.6A; the yellow signal is artificially colored green). A FlhE-mCherry fusion whose basal level expression from pTrc99a was sufficient to observe red fluorescence, showed a prominent red ring along the cell border, consistent with its periplasmic location (Fig. 4.6A). Curiously, while all *flhDC* cells showed red fluorescence, only 20-22% of wild-type cells did (Fig. 4.6B), even though the selection for the plasmid was maintained and there was no apparent loss of the *flhE*-mCherry construct as determined by PCR testing (data not shown). Of the wild-type cells

that showed red fluorescence, ~4% also showed red puncta (Fig. 4.6A). In a *flhDC* strain expressing both FlhA-YFP and FlhE-mCherry fusions, most cells appeared to have bleached the YFP fluorescence, while ~10% showed mCherry fluorescence. Of the latter, ~17% showed red puncta. The YFP fluorescence was difficult to see, but 30-40% of the cells showing red puncta had several which co-localized with weakly fluorescent YFP puncta (Fig. 4.6A).

To ascertain the specificity of interaction of FlhE with FlhA, its association with the MS ring protein FliF was tested, which, like FlhA, shows punctate localization by itself (Li & Sourjik, 2011). The FliF-YFP fusion was weakly fluorescent by itself. Since the YFP signal of FlhA was also weak in the presence of FlhE-mCherry, a *flhDC* strain expressing native FlhA or FliF (i.e. not fused to YFP) was used for co-localization assay with FlhE-mCherry. These native proteins were functional in complementation of *flhA* and *fliF* mutants, respectively (data not shown). Similar to the results seen with co-expression of FlhE-mCherry and FlhA-YFP, co-expression of FlhE-mCherry and FlhA in a *flhDC* strain showed the mCherry signal in only 13-20% of the cells, in contrast to expression of FlhE-mCherry alone in this background, when 100% of the cells were fluorescent (Fig. 4.6B). Many cells that were not fluorescent appeared to misshapen (Fig. 4.7). In contrast, 100% of *flhDC* cells retained the mCherry signal in cells co-expressing FlhE-mCherry and FliF (Fig. 4.6B). While it is uncertain why wild-type or *flhDC*/FlhA strains lose the mCherry signal in a majority of cells, absence of this phenomenon in *flhDC*/FlhE-mCherry or *flhDC*/FliF might be indicative of FlhE interaction with FlhA not observed with FliF.

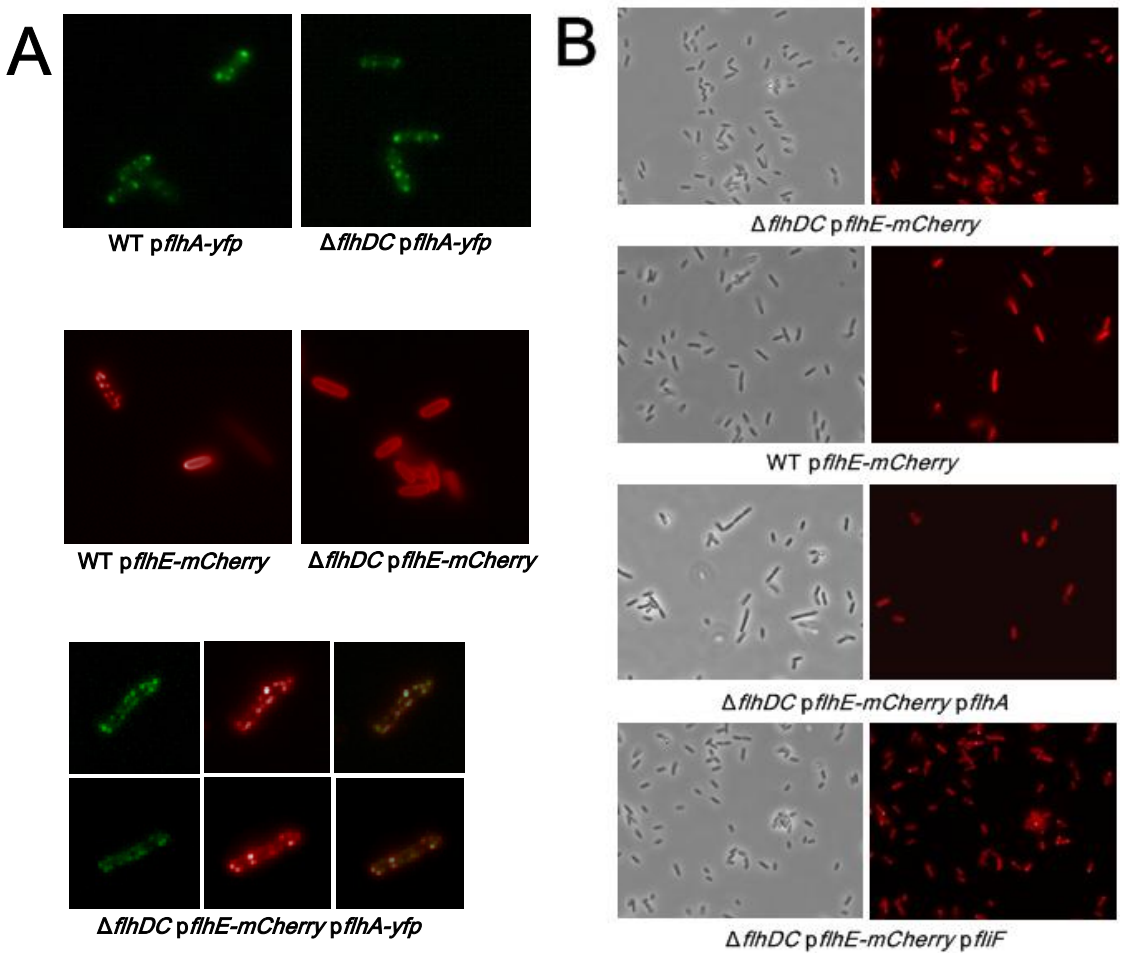

Fig. 4.6. Localization of FlhA-YFP and FlhE-mCherry in wild-type and *flhDC* *Salmonella* strains. **A**. The yellow YFP signal was artificially colored green in order to generate a yellow signal to observe co-localization with the red mCherry signal shown in the bottom panel. See Chapter 2 for details. **B**. Phase contrast and fluorescence images demonstrating loss of the mCherry signal in WT or p*flhA*-containing strains, but not in p*fliF*-containing strains.

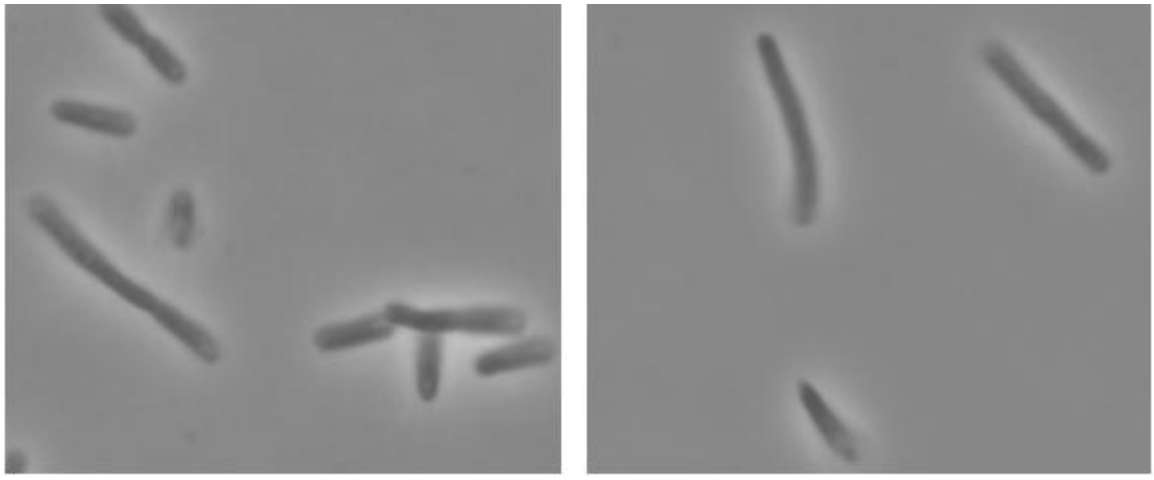

Δ*flhDC*/ p*flhE-mCherry* p*flhA*

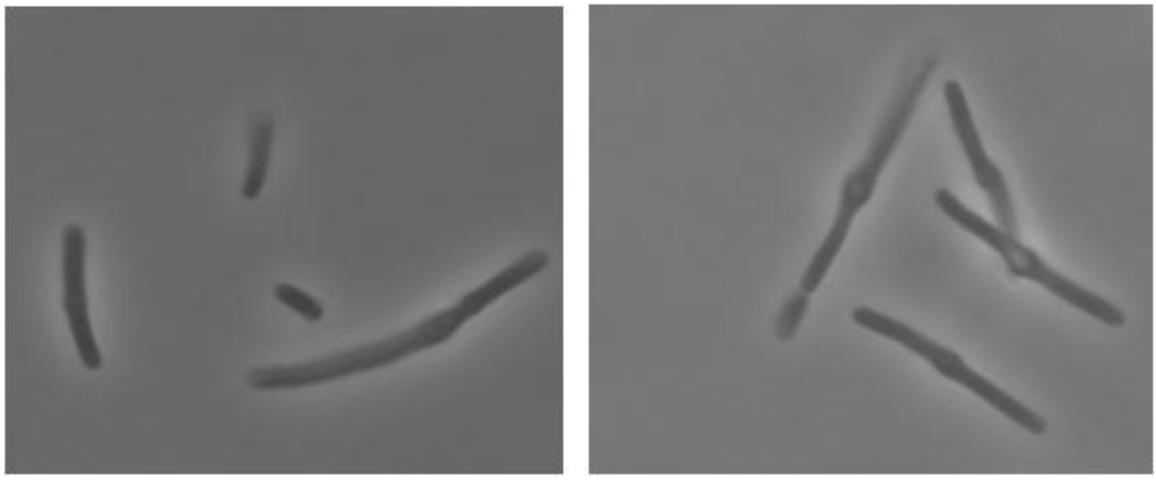

Δ*flhDC*/ p*flhE-mCherry* p*flhA-yfp*

Fig. 4.7. Phase contrast images of misshapen and elongated cells in *Salmonella* strains co-expressing FlhE-mCherry with FlhA or FlhA-YFP. These cells had lost the mCherry signal.

4.3 DISCUSSION

PMF is the major power source not only for the export of flagellar components through the T3S, but also for driving flagellar rotation through the MotAB stators in *E. coli* and *S. enterica.* A possible role for FlhE in regulating proton flow through T3S system was suggested by the observation of acidic pH-dependent cell lysis in a *flhE* mutant (Fig. 3.4). The co-expression of FlhE with FlhA, a protein implicated in PMF-driven export function (Hara et al, 2011), makes this a reasonable role for FlhE. Moreover, the plug region-deleted *motB* mutant, demonstrated to leak proton through the stators, showed the same cell lysis phenotypes as the *flhE* mutant (Fig. 4.1). In this Chapter therefore, I tested whether absence of FlhE lowers cytoplasmic pH. Two different assays - Tsr receptor-dependent tumble frequency (Fig. 4.2), as well as direct cytoplasmic pH measurement - indeed showed a lower pH in a *flhE* mutant compared to wild-type in both *Salmonella* and *E. coli* (Figs 4.3 and 4.5). I interpret these data to indicate proton leakage in the absence of FlhE. Also, I found that the leakage must be through the flagellar T3S channels, because it depends on the flagellar system (Fig. 4.5); however, the *flhE* mutant phenotype is independent of Mot proteins (Fig. 3.5).

***flhE deletion phenotypes are similar in* E. coli *and* S. enterica.** The gram-negative *E. coli and S. enterica* are members of *Enterobacteria* and FlhE from *S. enterica* fully complemented the *E. coli flhE* mutant (data not shown). Overall, the *flhE* phenotypes were similar in *S. enterica* and *E. coli*. For example, *flhE* mutants in both bacteria were

impaired for swarming (Figs 3.1 and 4.4), were green on pH indicator plates (Figs 3.3 and 4.4), showed filament-dependent cell lysis (Figs 3.5, 3.6, 3.7, 4.1, and 4.5), and had lower cytoplasmic pH (Figs 4.3 and 4.5). However, there were important differences. For example, these phenotypes were glucose-dependent in *S. enterica* (Fig. 3.4), but were not glucose-dependent in *E. coli* (Fig. 4.4). The *E. coli flhE* mutant grew poorly in LB media (Fig. 4.5) in contrast to the *S. enterica* mutant (Fig. 3.4). Thus, *E. coli* is more sensitive to the loss of FlhE. This could be due to subtle differences in the T3S systems of the two bacteria, or to better tolerance of acid stress in *Salmonella*.

Cytoplasmic acidification vs filament assembly for cell lysis. GFP reporter assays in *E. coli* indicate that the proton leak is present before the switch to late secretion and gets worse after the switch and upon filament addition (Fig. 4.5). However, cells do not lyse until filaments are added in both *S. enterica* (Figs 3.5, 3.6 and 3.7) and *E. coli* (Figs 4.4 and 4.5). Thus, cell-lysis is a filament-dependent, post-acidification event. Perhaps the added stress of long filaments pulling on the inner membrane weakens the membrane further, and exacerbates the proton leak to cause solute efflux and lysis.

Fluorescence signal bleaching, and misshapen and elongated cells. In the co-localization assay, FlhA-YFP fusion was fully functional in complementing a *flhA* mutant and showed a punctate appearance in both wild-type and *flhDC* mutant backgrounds (Fig. 4.6A). However, co-expression of both FlhA-YFP and FlhE-mCherry resulted in bleaching of the YFP signal and loss of the mCherry signal. It has been reported that the

mCherry signal is acid-stable (Shaner et al, 2005), whereas acidic pH quenches the YFP signal (Wilks & Slonczewski, 2007). The observed bleaching of the GFPmut3B signal (Figs 4.3 and 4.5) is therefore consistent with cytoplasm acidification. Based on the data presented here, I offer the following speculative explanation for the FlhA (or flagellar system)-specific loss of the FlhE-mCherry signal. I suggest that while FlhE normally interacts with FlhA to prevent proton leaks through the T3S system, interaction of the FlhE-mCherry fusion protein with FlhA (and possibly other flagellar components) is somewhat different, triggering inappropriate proton leakage. Acidification of the cytoplasm may activate antiporters that quench the mCherry signal in the periplasm and cause solute leakage, which also affects cell shape.

FlhE function. Acidification of the cytoplasm in the absence of FlhE may imply a 'proton plug' or 'lid' function for FlhE as a periplasmic segment of the stator protein MotB, which together with MotA forms a transmembrane proton channel (Hosking *et al*., 2006). The deletion of this plug-region in MotB caused a massive influx of protons, acidifying the cytoplasm without significantly depleting the PMF. The growth inhibition associated with the plug mutation was surmised to be a result of the acidification itself or some following consequence, such as potassium or water efflux from the cells. Under those conditions, cell lysis also depends on filament assembly (Fig. 4.1).

An alternative function for FlhE is that of a chaperone. Dedicated cytoplasmic chaperones are common in T3S systems, where they help maintain their substrates in a secretion-competent state, delivering them to the secretion machinery in a manner

designed to facilitate travel through the T3S apparatus in an unfolded or partially folded form (Galan & Wolf-Watz, 2006; Chevance & Hughes, 2008; Minamino & Namba, 2008). Periplasmic chaperones have been identified in assembly of the structural elements of flagella (Nambu & Kutsukake, 2000), needle complexes (Schuch & Maurelli, 2001) and pili (Sauer et al, 2000), where they are thought to bind, stabilize and cap interactive surfaces of subunits until they are assembled. The MS ring scaffold has to accommodate six different T3S transport proteins, all correctly juxtaposed to regulate timely export. It is possible that FlhE assists in optimizing their packing arrangement, ensuring a tight seal.

A plug/lid role for FlhE fits in with the observation that the phenotype in *Salmonella* is manifest when the external pH is low. Such a role would tie in nicely with acquisition of the *flhE* gene mainly by the enterics, as these bacteria experience low pH during transit through the stomach. However, in *E. coli*, the *flhE* mutant phenotype does not depend on lowering of the external pH. Also, the highly conserved proton plug-region of MotB was not detected in FlhE by T-COFFEE Multiple Sequence Alignment (data not shown). Furthermore, the presence of *flhE* in some non-enterics such as *Azotobacter*, *Chromobacter* and *Ralstonia*, in which *flhE* is not part of the *flhBA* operon and displays only a 28–38% homology to the *flhE* gene in the enterics (Stafford & Hughes, 2007), suggests that a role for FlhE as a chaperone is also plausible. While co-localization of FlhE with FlhA was observed, I do not know if FlhE is dedicated to FlhA, or whether it can also interact with FlhB or with more than one of the T3S proteins. Although not much is known about the nature and assembly of flagellar secretion apparatus or of the

proton channels that drive secretion (Paul et al, 2008; Minamino & Namba, 2008), it is attractive to think that FlhE might play a role in promoting optimal interactions among components of the T3S apparatus.

CHAPTER 5: Expression and crystallization of the periplasmic protein FlhE from *S. enterica*

5.1 INTRODUCTION

Flagellar biogenesis has been best studied in *Salmonella enterica* (Macnab, 2003; Chevance & Hughes, 2008; Harshey, 2011). The assembly of flagella begins inside the cell and all flagellar components located beyond the cytoplasmic membrane are exported by the flagellar T3S system using PMF as described in Chapter 1. *flhE* belongs to the *flhBAE* flagellar operon in Enterobacteria (Liu & Ochman, 2007), whose first two members function in T3S secretion. The experiments in Chapter 3 and 4 showed that the absence of FlhE in *S. enterica* and *E. coli* causes cell lysis depending on filament assembly (Figs 3.5, 3.6, 3.7, 4.5) and lowers cytoplasmic pH, indicative of a proton leak (Figs 4.3 and 4.5). Also, FlhE is a periplasmic protein that co-purifies with flagellar basal bodies (Fig. 3.9), and the co-localization assays with fluorescence fusion proteins indicate that FlhE interacts with FlhA (Fig. 4.6), a protein implicated in channeling protons for PMF-driven secretion (Hara et al, 2011). Moreover, the cell lysis phenotype of the *flhE* mutant was similar to that of the *motB* plug-region deletion mutant, which has been demonstrated to leak protons in *E. coli* cells (Hosking et al, 2006) (Fig.4.1). Based on these data, two plausible roles for FlhE are a 'proton plug' and a chaperone for the flagellar T3S system.

X-ray crystallography has elucidated crystal structures of 65 *E. coli* and 2 *Salmonella* periplasmic proteins (these numbers are from the Protein Data Bank (PDB)). Recently, the crystal structure of the MotB plug region was also solved (Kojima et al, 2009). FlhE does not show any homology to proteins collected in the PDB, nor is any primary sequence homology observed by BLASTp analysis. Solving the protein structure of FlhE is therefore the only hope for defining its function in the flagellar assembly pathway. My goal in this Chapter is to attempt to solve the crystal structure of FlhE. To do this, a functional C-terminally 6His-tagged FlhE was overexpressed and purified from the periplasm and screened for crystal formation under several conditions. Of the 384 conditions tested, only one condition produced high quality crystals (diffraction resolution = 2.02 Å).

5.2 RESULTS AND DISCUSSION

5.2.1 Purification of FlhE-6His from *S. enterica* periplasm

The FlhE protein of *S. enterica* consists of 130 amino acids, the first 16 encoding the signal sequence for secretion into the periplasm. To overexpress and isolate protein from the cytoplasm, the 16-amino acid N-terminal signal was deleted and the C-terminus was tagged with 6His-epitope to aid protein purification, When overexpressed from a plasmid and purified from the cytoplasm as described (Wollmann & Zeth, 2006), the yield and purity of this protein were not sufficient for structural studies (data not shown). I therefore purified the FlhE-6His tagged protein from the periplasm as described below. This protein was functional as judged by swarming complementation of a *flhE* mutant. Wild-type FlhE-6His was overexpressed from a plasmid and purified from the periplasm by an osmotic shock procedure (Chen et al, 2004). In the standard osmotic shock, the harvested cells are resuspended by 20-30% sucrose solution, followed by adding EDTA to the final concentration of 1 mM. During these procedures, the osmotic strength from the high sucrose concentration causes cells to shrink. The EDTA treatment increases the outer membrane permeability by chelating divalent cations among lipopolysaccharide (LPS), which are required for LPS stabilization (Hamilton-Miller, 1966). After centrifugation, the cells are resuspended by cold distilled water, which increases cell size rapidly and releases proteins from the periplasm. I chose 30% sucrose concentration in my studies, based on the highest yield of protein at this concentration compared to 20 or

25% sucrose. Also, cold 5 mM $MgSO_4$ solution was used instead of water because it protects the nickel ions of the resins by chelating EDTA possibly contaminated from the previous step. Even though the FlhE-6His expression was high, the yield of FlhE-6His was insufficient (data not shown). To test whether the periplasmic FlhE-6His was leaking out of the cell during suspension in the sucrose solution, supernatants from the sucrose and the $MgSO_4$ solutions were collected and examined by SDS-PAGE gel electrophoresis, followed by staining with SimpleBlue^{TM} SafeStain (Invitrogen). A majority of FlhE-6His was detected in the supernatant of the sucrose suspension (Fig 5.1). Osmotic shock is a popular method for protein purification from the periplasm of *E. coli*, and depends on the permeability of the outer membrane, which is improved by releasing LPS upon adding different concentrations of EDTA. It is not clear whether the release of FlhE-6His into the supernatant after resuspension in the sucrose solution is due to some property of FlhE or of differences in outer membrane structures of *S. enterica* and *E. coli*. When the released and the periplasmic fractions were combined, the yield of FlhE-6His (1 mg l^{-1}) was sufficient for crystallization. The purified protein was concentrated to 7 mg ml^{-1} and used for crystallization.

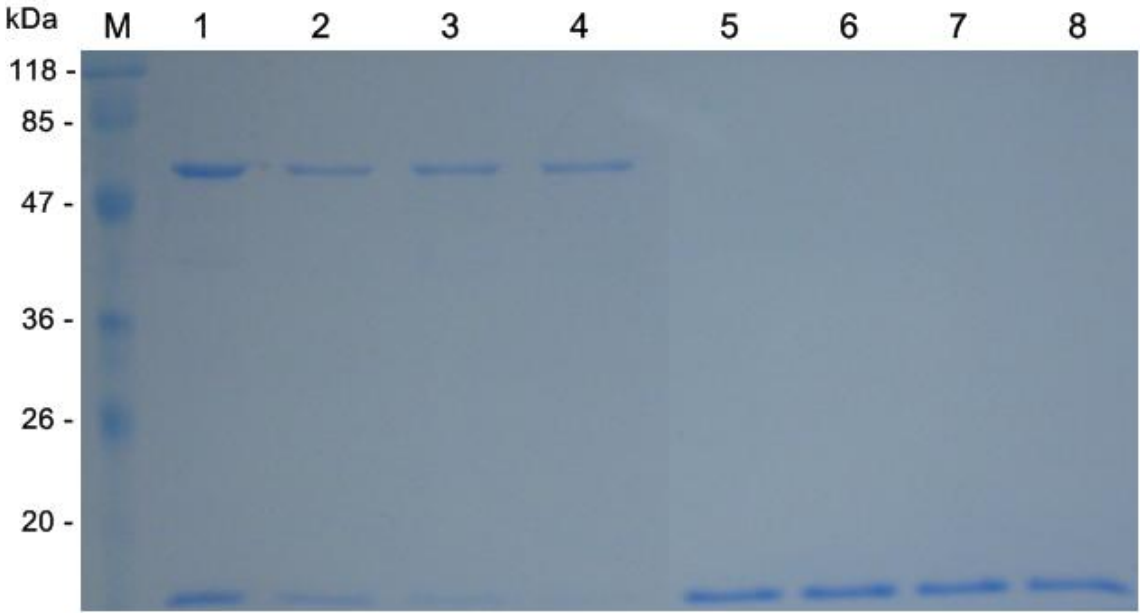

Fig. 5.1. Purification of FlhE-6His from a *S. enterica flhE* mutant (ST004) harboring pTrc99a-*flhE-6His* after 3.5 h induction with the final concentration of 50 µM IPTG at 37^{o}C. The samples were analyzed by 12% SDS-PAGE and stained with SimpleBlue^{TM} SafeStain (see Chapter 2 for detail). Lanes: M, molecular size standard; 1, supernatant collected from 30% sucrose solution, 2, supernatant collected from 5 mM $MgSO_4$; 3-4, flow-through of the Ni-NTA affinity matrix; 5 - 8, FlhE-6His purified by Ni-NTA affinity chromatography. Molecular sizes of the marker are indicated.

5.2.2 FlhE-6His crystal screening

The crystallization experiments were performed at 4^{o}C and at room temperature using the sitting-drop vapor diffusion method with commercially available 96-screening conditions (see Chapter 2 for details). Initially, each protein sample drop was prepared by mixing 0.1 µl reservoir solution with 0.1 µl and 0.2 µl FlhE-6His solution, and stored at 4^{o}C and room temperature, respectively. Each drop was photographed and scored after 2 weeks, and the total scores of each reservoir condition were summed up. Eleven out of 96 reservoir systems, which scored equal or above + 9, were screened for crystal optimization (Table 5.1). Also, it was observed that crystal scores were higher at 4^{o}C and 1:1 ratio in Table 1, respectively. For the optimization, the hanging-drop method was performed with 24-well plates (see Chapter 2 for details). Each drop was set up by mixing 1 µl of reservoir solution with 1 µl of FlhE-6His solution and subsequently stored at 4℃. Micro-crystals were observed on the following 2 conditions: E8 (1.5 M NaCl, 10% ethanol) and E9 (2M NaCl, 0.1 M $CH_3COONa \cdot 3H_2O$, pH 4.6) (data not shown).

To increase the size of crystals, a streak-seeding method was performed. After the fresh protein drops were prepared with the E8 and E9 reservoirs as described above, micro-crystals were streaked on the drops by micro-probes as described in Chapter 2. Crystals large enough (> 0.1 mm in one dimensional size) to be used for data collection grew from E8 reservoir in 24 h (Fig. 5.2). A crystal was collected, briefly transferred to a cyoprotectant solution, mounted in a cryo-loop, and frozen in liquid nitrogen for data collection.

Table 5.1. Crystal screening scores.

Well No.	Reservoir composition	Score				Total score[b]
		4°C		Room temperature		
		1:1[a]	1:2	1:1	1:2	
D9	0.2 M $Zn(CH_3COO)_2•2H_2O$, 18% polyethylene glycol 8000 (w/v), 0.1 M $C_2H_{12}AsNaO_5$ pH 6.5	6	6	9	9	30
F9	0.1 M $NaH_2PO_4•H_2O$, 0.1 M KH_2PO_4, 2.0 M NaCl, 0.1 M MES monohydrate pH 6.5	9	2	9	9	29
E1	2.0 M NaCl, 10% polyethylene glycol 6000 (w/v)	6	6	6	9	27
G8	0.1 M NaCl, 1.6 M $(NH_4)_2SO_4$, 0.1 M HEPES pH 7.5	9	2	9	3	23
G9	2.0 M NH_4HCO_2, 0.1 M HEPES pH 7.5,	9	6	6	0	21
E9	2.0 M NaCl, 0.1 M $CH_3COONa• 3H_2O$ pH 4.6	9	9	0	0	18
A4	2.0 M $(NH_4)_2SO_4$, 0.1 M Tris-HCl pH 8.5	6	2	6	2	16
B3	0.2 M $(NH_4)_2SO_4$, 30% polyethylene glycol 8000 (w/v), 0.1 M $C_2H_{12}AsNaO_5$ pH 6.5	2	2	2	9	15
G12	4.3 M NaCl, 0.1 M HEPES pH 7.5	6	2	2	2	12
E8	1.5 M NaCl, 10% v/v ethanol	7	3	0	0	10
E5	2.0 M $(NH_4)_2SO_4$, 5% 2-propanol (v/v)	9	0	0	0	9

a. Each protein sample drop was prepared in a well by mixing a reservoir solution with FlhE-6His protein solutions with 1:1 and 1:2 ratios (v/v). The plates were stored at 4°C and at room temperature, respectively, for two weeks (See Chapter 2 for details). Crystals were scored by the following score schemes: 0 clear, 1+ phase separation, 2+ precipitate, 3+ grainy precipitate/ microcrystals, 4+ precipitate web, 5+ sherulites, 6+ dusco balls, 7+ needles, 8+ plates, 9+ 3D crystals. **b**. Four different scores from a reservoir condition were summed up. The well no. was listed from the highest to lowest scores.

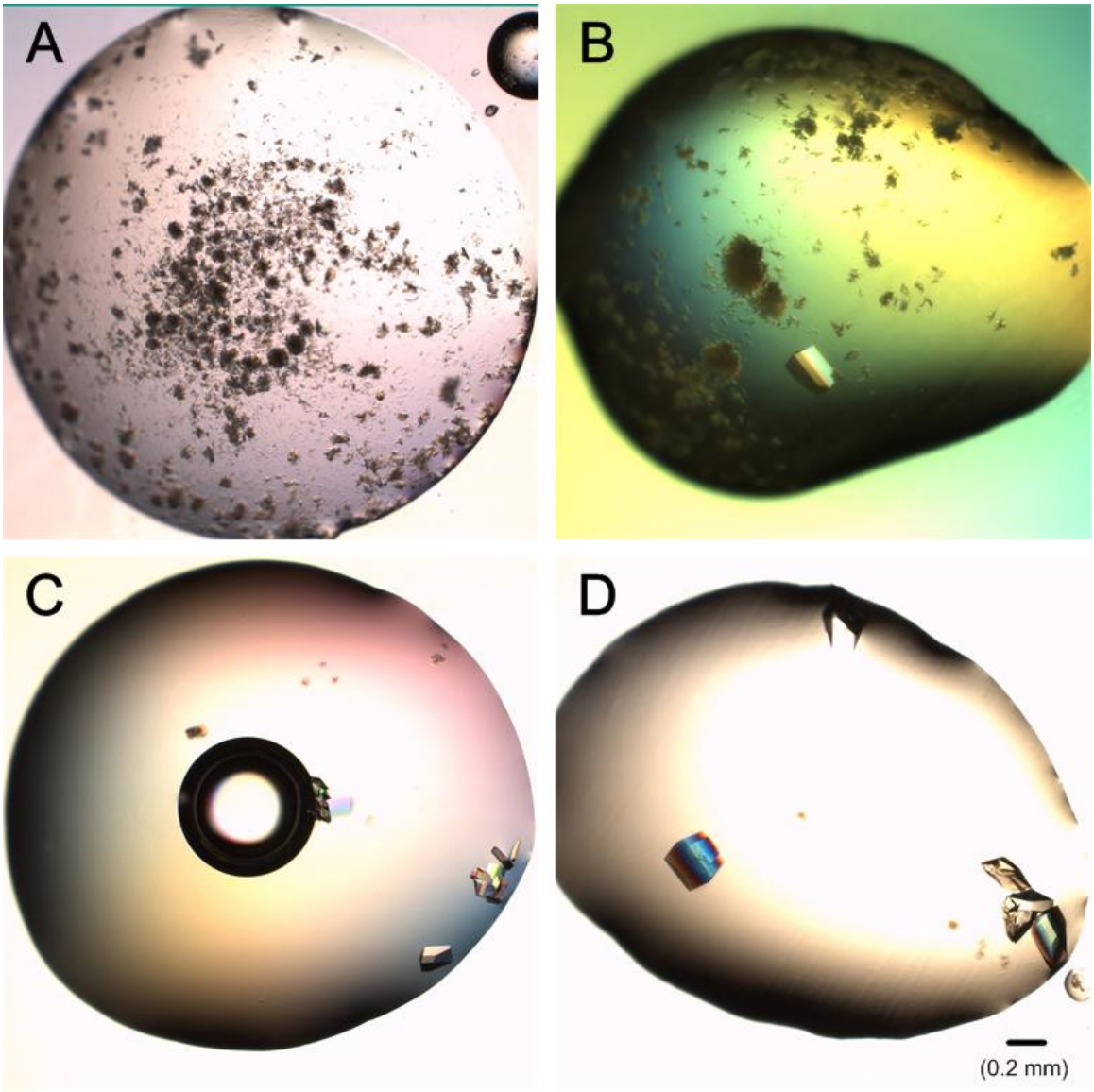

Fig. 5.2. FlhE-6His protein crystals. The micro-crystals (A) were transferred by a streak-seeding method to a fresh protein drop, FlhE-6His crystals were detected in 24 h (B), 3 days (C), and 8 days (D), respectively. For the streak-seeding, a fresh protein drop was prepared by mixing 1 µl of FlhE-6His (7mg ml^{-1}) with 1 µl of E8 reservoir solution (1.5 M NaCl, 10% ethanol). By using a micro-needle (CrystalProbe, Hampton Research), several micro-crystals were streaked on the drop and stored at $4^{o}C$ (see Chapter 2 for details).

5.2.3 X-ray crystallogrphy and data collection

X-ray diffraction data were collected as described in Chapter 2 and crystallogrphic data (Fig. 5.3) are summarized in Table 5.2. FlhE-6His crystals belong to space group $P2_12_12_1$ with cell constants a=25.4, b=36.9, c=108.5 Å and diffracted to 2.02 Å resolution with an R_{merge} of 8.4% and an I/σ_I of 10.2.

To solve the three-dimensional X-ray structure of macromolecules, determining crystallographic phases is a key step. To determine the phases, the derivatization of protein crystals was performed by soaking the crystals in heavy atom solutions. Periplasmic FlhE contains 2 methionine residues (M27 and M53) and 2 cysteine residues (C76 and C80). Because platinum compounds are known to preferentially react with methionine and many mercury compounds specifically target cysteine thiol-groups (Boggon & Shapiro, 2000), FlhE-6His crystals were soaked in 1mM $K_2Pt(CN)_4$ and MeHgAc solutions respectively for 3 days to determine crystal phases after use of the muliple-wavelength anomalous dispersion (MAD) techinique. Even though crystal cracking and dissolution during soaking were not observed, these atoms were not properly incorported to the crystals (data not shown). Also, a NaI solution containg 1 M NaI, 0.5 M NaCl, 10% ethanol, and 20% glycerol was prepared and FlhE-6His crystals were soaked for 15 to 30 min before collecting diffraction data with single-wavelength anomalous dispersion (SAD) because iodide anions easily are diffused into protein crystals during short soaking time and bind to positively charged residues and may also bind in hydrophobic pockets of the protein crystals (Dauter et al, 2000). However, these crystals did not diffract well (data not shown).

Ongoing attempts to solve the phases include trying other Pt and Hg derivatives such as 2 mM of pCMPS (p-chloro-mercuriphenyl sulphonate) and $K_2Pt(Cl)_4$ for crystal soaking. In addition, seleno-methionine labeled FlhE-6His has been expressed at a high yield, and purified similarly to FlhE-6His as before, and is currently set up for crystallization with the E8 reservoir condition in which FlhE-6His crystal was formed before.

Table 5.2. Crystallographic data.

Wavelength (Å)	1.54
Space group	$P2_12_12_1$
Cell constants (Å)	a=25.4, b=36.9, c=108.5
Resolution (Å)	50.-2.02 (2.05-2.02)[a]
R_{merge} (%)	8.4 (22.4)
$I/\sigma_{(I)}$	10.2 (7.3)
Completeness (%)	100.0 (99.7)
Unique reflections	7183
Redundancy	6.5

a. Values in parenthesis correspond to highest resolution shell.

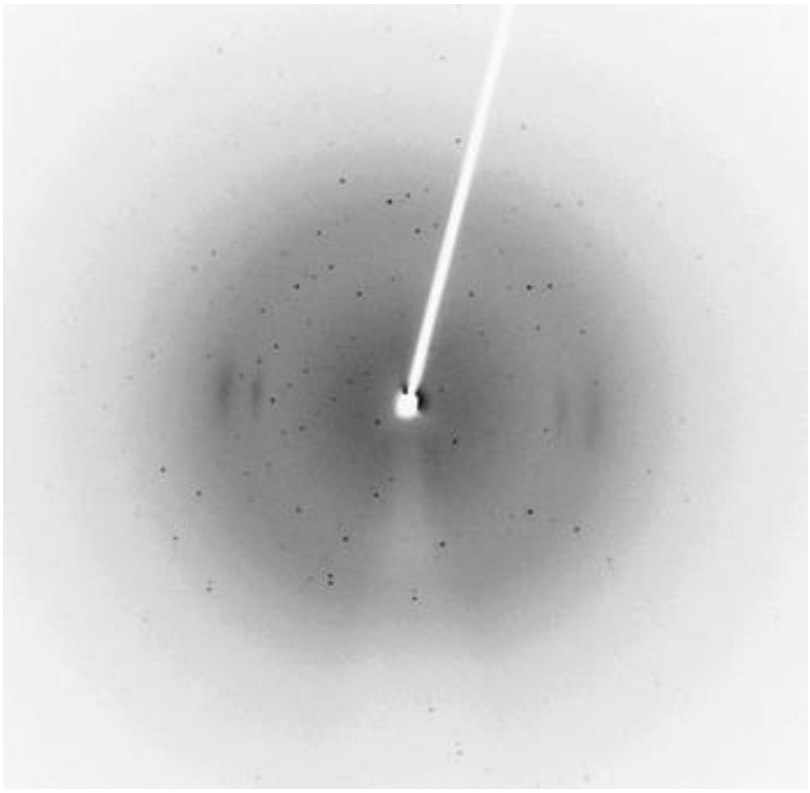

Fig. 5.3. Diffraction image of a FlhE-6His crystal. X-ray diffraction data were collected from the crystal at 100 K on a Rigaku R-AXIS IV++ image plate detector (Rigaku, The Woodlands, TX) with X-rays generated by a Rigaku MicroMax-007 HF rotating anode generator operated at 40 kV, 30 mA.

5.3 FUTURE STUDY

The periplasmic spaces of gram-negative bacteria are particularly exposed to environmental stresses such as detergents, low or high osmolarity, high temperatures, and host immune responses. These stresses are known to impact protein folding. Enteric bacteria such as *E. coli* and *S. enterica* experience extremely low pH during transit through the stomach (Foster, 2004). To survive under these unfavorable growth conditions, bacteria use fine-tuned protein quality control systems (Merdanovic et al, 2011). *E. coli* has around 450 periplasmic proteins and so far the three-dimensional crystal structures of 65 proteins have been elucidated by X-ray crystallography. These structural studies are valuable to determine the function of proteins. For example, the small periplasmic protein Skp consists of 141 residues and forms homotrimers. It was hypothesized to be a chaperone for outer membrane proteins (Harms et al, 2001). After the three-dimensional structure of Skp was elucidated, the structural comparison between Skp and other chaperone proteins validated its function (Korndorfer et al, 2004).

The experiments I have performed to elucidate the role of FlhE (presented in Chapters 3 and 4), suggest two plausible roles of FlhE - proton plug or chaperone - in the flagellar T3S pathway. Because FlhE does not show any homology to the proteins collected in the PBD, elucidation of the three-dimensional structure of FlhE is important if I am to confirm or test the hypothetical roles suggested for FlhE. The advances made in this chapter are very promising toward reaching this goal. The FlhE-6His protein crystallized readily and diffracted at a high resolution (2.02 Å). The only problem that

remains is solving the phase problem. Several concurrent approaches to doing this are ongoing as described above. I am optimistic that a structure of FlhE will soon be at hand, and will suggest new avenues of future research.

References

Aldridge P., Karlinsey J. E., Becker E., Chevance F. F., Hughes K. T. (2006a) Flk prevents premature secretion of the anti-sigma factor FlgM into the periplasm. *Mol Microbiol* **60:** 630-643

Aldridge P. D., Karlinsey J. E., Aldridge C., Birchall C., Thompson D., Yagasaki J., Hughes K. T. (2006b) The flagellar-specific transcription factor, sigma28, is the Type III secretion chaperone for the flagellar-specific anti-sigma28 factor FlgM. *Genes Dev* **20:** 2315-2326

Amann E., Ochs B., Abel K. J. (1988) Tightly regulated tac promoter vectors useful for the expression of unfused and fused proteins in Escherichia coli. *Gene* **69:** 301-315

Attmannspacher U., Scharf B. E., Harshey R. M. (2008) FliL is essential for swarming: motor rotation in absence of FliL fractures the flagellar rod in swarmer cells of Salmonella enterica. *Mol Microbiol* **68:** 328-341

Auvray F., Thomas J., Fraser G. M., Hughes C. (2001) Flagellin polymerisation control by a cytosolic export chaperone. *J Mol Biol* **308:** 221-229

Bennett J. C., Thomas J., Fraser G. M., Hughes C. (2001) Substrate complexes and domain organization of the Salmonella flagellar export chaperones FlgN and FliT. *Mol Microbiol* **39:** 781-791

Block S. M., Blair D. F., Berg H. C. (1989) Compliance of bacterial flagella measured with optical tweezers. *Nature* **338:** 514-518

Boggon T. J., Shapiro L. (2000) Screening for phasing atoms in protein crystallography. *Structure* **8:** R143-149

Bonifield H. R., Hughes K. T. (2003) Flagellar phase variation in Salmonella enterica is mediated by a posttranscriptional control mechanism. *J Bacteriol* **185:** 3567-3574

Brumell J. H., Grinstein S. (2004) Salmonella redirects phagosomal maturation. *Curr Opin Microbiol* **7:** 78-84

Burkart M., Toguchi A., Harshey R. M. (1998) The chemotaxis system, but not chemotaxis, is essential for swarming motility in Escherichia coli. *Proc Natl Acad Sci U S A* **95:** 2568-2573

Butler M. T., Wang Q., Harshey R. M. (2010) Cell density and mobility protect swarming bacteria against antibiotics. *Proc Natl Acad Sci U S A* **107:** 3776-3781

Caiazza N. C., Shanks R. M., O'Toole G. A. (2005) Rhamnolipids modulate swarming motility patterns of Pseudomonas aeruginosa. *J Bacteriol* **187:** 7351-7361

Chen Y. C., Chen L. A., Chen S. J., Chang M. C., Chen T. L. (2004) Modified osmotic shock for periplasmic release of a recombinant creatinase from Escherichia coli. *Biochem Eng J* **19:** 211-215

Chevance F. F., Hughes K. T. (2008) Coordinating assembly of a bacterial macromolecular machine. *Nat Rev Microbiol* **6:** 455-465

Chevance F. F., Takahashi N., Karlinsey J. E., Gnerer J., Hirano T., Samudrala R., Aizawa S., Hughes K. T. (2007) The mechanism of outer membrane penetration by the eubacterial flagellum and implications for spirochete evolution. *Genes & development* **21:** 2326-2335

Chilcott G. S., Hughes K. T. (2000) Coupling of flagellar gene expression to flagellar assembly in Salmonella enterica serovar typhimurium and Escherichia coli. *Microbiol Mol Biol Rev* **64:** 694-708

Datsenko K. A., Wanner B. L. (2000) One-step inactivation of chromosomal genes in Escherichia coli K-12 using PCR products. *Proc Natl Acad Sci U S A* **97:** 6640-6645

Dauter Z., Dauter M., Rajashankar K. R. (2000) Novel approach to phasing proteins: derivatization by short cryo-soaking with halides. *Acta Crystallogr D Biol Crystallogr* **56:** 232-237

DePamphilis M. L., Adler J. (1971) Fine structure and isolation of the hook-basal body complex of flagella from Escherichia coli and Bacillus subtilis. *J Bacteriol* **105:** 384-395

Di Tommaso P., Moretti S., Xenarios I., Orobitg M., Montanyola A., Chang J. M., Taly J. F., Notredame C. (2011) T-Coffee: a web server for the multiple sequence alignment of protein and RNA sequences using structural information and homology extension. *Nucleic Acids Res* **39:** W13-17

Erhardt M., Hughes K. T. (2010) C-ring requirement in flagellar type III secretion is bypassed by FlhDC upregulation. *Mol Microbiol* **75:** 376-393

Erhardt M., Singer H. M., Wee D. H., Keener J. P., Hughes K. T. (2011) An infrequent molecular ruler controls flagellar hook length in Salmonella enterica. *EMBO J* **30:** 2948-2961

Ferris H. U., Furukawa Y., Minamino T., Kroetz M. B., Kihara M., Namba K., Macnab R. M. (2005) FlhB regulates ordered export of flagellar components via autocleavage mechanism. *J Biol Chem* **280:** 41236-41242

Ferris H. U., Minamino T. (2006) Flipping the switch: bringing order to flagellar assembly. *Trends Microbiol* **14:** 519-526

Foster J. W. (2004) Escherichia coli acid resistance: tales of an amateur acidophile. *Nat Rev Microbiol* **2:** 898-907

Francis N. R., Sosinsky G. E., Thomas D., DeRosier D. J. (1994) Isolation, characterization and structure of bacterial flagellar motors containing the switch complex. *J Mol Biol* **235:** 1261-1270

Fraser G. M., Gonzalez-Pedrajo B., Tame J. R., Macnab R. M. (2003a) Interactions of FliJ with the Salmonella type III flagellar export apparatus. *J Bacteriol* **185:** 5546-5554

Fraser G. M., Hirano T., Ferris H. U., Devgan L. L., Kihara M., Macnab R. M. (2003b) Substrate specificity of type III flagellar protein export in Salmonella is controlled by subdomain interactions in FlhB. *Mol Microbiol* **48:** 1043-1057

Fraser G. M., Hughes C. (1999) Swarming motility. *Curr Opin Microbiol* **2:** 630-635

Frye J., Karlinsey J. E., Felise H. R., Marzolf B., Dowidar N., McClelland M., Hughes K. T. (2006) Identification of new flagellar genes of Salmonella enterica serovar Typhimurium. *J Bacteriol* **188:** 2233-2243

Fujime S., Maruyama M., Asakura S. (1972) Flexural rigidity of bacterial flagella studied by quasielastic scattering of laser light. *J Mol Biol* **68:** 347-359

Galan J. E., Wolf-Watz H. (2006) Protein delivery into eukaryotic cells by type III secretion machines. *Nature* **444:** 567-573

Gonzalez-Pedrajo B., Fraser G. M., Minamino T., Macnab R. M. (2002) Molecular dissection of Salmonella FliH, a regulator of the ATPase FliI and the type III flagellar protein export pathway. *Mol Microbiol* **45:** 967-982

Gonzalez-Pedrajo B., Minamino T., Kihara M., Namba K. (2006) Interactions between C ring proteins and export apparatus components: a possible mechanism for facilitating type III protein export. *Mol Microbiol* **60:** 984-998

Guzman L. M., Belin D., Carson M. J., Beckwith J. (1995) Tight regulation, modulation, and high-level expression by vectors containing the arabinose PBAD promoter. *J Bacteriol* **177:** 4121-4130

Gygi D., Rahman M. M., Lai H. C., Carlson R., Guard-Petter J., Hughes C. (1995) A cell-surface polysaccharide that facilitates rapid population migration by differentiated swarm cells of Proteus mirabilis. *Mol Microbiol* **17:** 1167-1175

Hadley M. E., Hruby V. J., Sharma S. D. (1998) Peptides having potent antagonist and agonist bioactivities at melanocortin receptors. *U S Patent* 5731408

Hamilton-Miller J. M. (1966) Damaging effects of ethylenediaminetetra-acetate and penicillins on permeability barriers in Gram-negative bacteria. *Biochem J* **100:** 675-682

Hara N., Namba K., Minamino T. (2011) Genetic characterization of conserved charged residues in the bacterial flagellar type III export protein FlhA. *PLoS One* **6:** e22417

Harms N., Koningstein G., Dontje W., Muller M., Oudega B., Luirink J., de Cock H. (2001) The early interaction of the outer membrane protein phoe with the periplasmic chaperone Skp occurs at the cytoplasmic membrane. *J Biol Chem* **276:** 18804-18811

Harshey R. M. (2003) Bacterial motility on a surface: many ways to a common goal. *Annu Rev Microbiol* **57:** 249-273

Harshey R. M. (ed) (2011) *New insights into the role and formation of flagella in Salmonella*: Caister Academic Press, UK, 163-186pp

Hirano T., Minamino T., Macnab R. M. (2001) The role in flagellar rod assembly of the N-terminal domain of Salmonella FlgJ, a flagellum-specific muramidase. *J Mol Biol* **312:** 359-369

Hirano T., Mizuno S., Aizawa S., Hughes K. T. (2009) Mutations in flk, flgG, flhA, and flhE that affect the flagellar type III secretion specificity switch in Salmonella enterica. *J Bacteriol* **191:** 3938-3949

Hirano T., Yamaguchi S., Oosawa K., Aizawa S. (1994) Roles of FliK and FlhB in determination of flagellar hook length in Salmonella typhimurium. *J Bacteriol* **176:** 5439-5449

Homma M., Fujita H., Yamaguchi S., Iino T. (1984) Excretion of unassembled flagellin by Salmonella typhimurium mutants deficient in hook-associated proteins. *J Bacteriol* **159:** 1056-1059

Hosking E. R., Vogt C., Bakker E. P., Manson M. D. (2006) The Escherichia coli MotAB proton channel unplugged. *J Mol Biol* **364:** 921-937

Hough T., Bernhardt P., Knox R. B., Williams E. G. (1985) Applications of fluorochromes to pollen biology. II. The DNA probes ethidium bromide and Hoechst 33258 in conjunction with the callose-specific aniline blue fluorochrome. *Stain Technol* **60:** 155-162

Hughes K. T., Gillen K. L., Semon M. J., Karlinsey J. E. (1993) Sensing structural intermediates in bacterial flagellar assembly by export of a negative regulator. *Science* **262:** 1277-1280

Ikeda T., Asakura S., Kamiya R. (1989) Total reconstitution of Salmonella flagellar filaments from hook and purified flagellin and hook-associated proteins in vitro. *J Mol Biol* **209:** 109-114

Ikeda T., Homma M., Iino T., Asakura S., Kamiya R. (1987) Localization and stoichiometry of hook-associated proteins within Salmonella typhimurium flagella. *J Bacteriol* **169:** 1168-1173

Ikeda T., Oosawa K., Hotani H. (1996) Self-assembly of the filament capping protein, FliD, of bacterial flagella into an annular structure. *J Mol Biol* **259:** 679-686

Inoue T., Shingaki R., Hirose S., Waki K., Mori H., Fukui K. (2007) Genome-wide screening of genes required for swarming motility in Escherichia coli K-12. *J Bacteriol* **189:** 950-957

Jones C. J., Macnab R. M., Okino H., Aizawa S. (1990) Stoichiometric analysis of the flagellar hook-(basal-body) complex of Salmonella typhimurium. *J Mol Biol* **212:** 377-387

Karlinsey J. E., Tanaka S., Bettenworth V., Yamaguchi S., Boos W., Aizawa S. I., Hughes K. T. (2000) Completion of the hook-basal body complex of the Salmonella typhimurium flagellum is coupled to FlgM secretion and fliC transcription. *Mol Microbiol* **37:** 1220-1231

Katayama E., Shiraishi T., Oosawa K., Baba N., Aizawa S. (1996) Geometry of the flagellar motor in the cytoplasmic membrane of Salmonella typhimurium as determined by stereo-photogrammetry of quick-freeze deep-etch replica images. *J Mol Biol* **255:** 458-475

Kearns D. B. (2010) A field guide to bacterial swarming motility. *Nat Rev Microbiol* **8:** 634-644

Kearns D. B., Losick R. (2003) Swarming motility in undomesticated Bacillus subtilis. *Mol Microbiol* **49:** 581-590

Kihara M., Macnab R. M. (1981) Cytoplasmic pH mediates pH taxis and weak-acid repellent taxis of bacteria. *J Bacteriol* **145:** 1209-1221

Kippert F., Lloyd D. (1995) The aniline blue fluorochrome specifically stains the septum of both live and fixed Schizosaccharomyces pombe cells. *FEMS Microbiol Lett* **132:** 215-219

Kitko R. D., Cleeton R. L., Armentrout E. I., Lee G. E., Noguchi K., Berkmen M. B., Jones B. D., Slonczewski J. L. (2009) Cytoplasmic acidification and the benzoate transcriptome in Bacillus subtilis. *PLoS One* **4:** e8255

Kitko R. D., Wilks J. C., Garduque G. M., Slonczewski J. L. (2010) Osmolytes contribute to pH homeostasis of Escherichia coli. *PloS One* **5:** e10078

Kojima S., Imada K., Sakuma M., Sudo Y., Kojima C., Minamino T., Homma M., Namba K. (2009) Stator assembly and activation mechanism of the flagellar motor by the periplasmic region of MotB. *Mol Microbiol* **73:** 710-718

Konishi M., Kanbe M., McMurry J. L., Aizawa S. (2009) Flagellar formation in C-ring-defective mutants by overproduction of FliI, the ATPase specific for flagellar type III secretion. *J Bacteriol* **191:** 6186-6191

Korndorfer I. P., Dommel M. K., Skerra A. (2004) Structure of the periplasmic chaperone Skp suggests functional similarity with cytosolic chaperones despite differing architecture. *Nat Struct Mol Biol* **11:** 1015-1020

Kubori T., Yamaguchi S., Aizawa S. (1997) Assembly of the switch complex onto the MS ring complex of Salmonella typhimurium does not require any other flagellar proteins. *J Bacteriol* **179:** 813-817

Kutsukake K. (1997) Autogenous and global control of the flagellar master operon, flhD, in Salmonella typhimurium. *Mol Gen Genet* **254:** 440-448

Kutsukake K., Iyoda S., Ohnishi K., Iino T. (1994) Genetic and molecular analyses of the interaction between the flagellum-specific sigma and anti-sigma factors in Salmonella typhimurium. *EMBO J* **13:** 4568-4576

Kutsukake K., Ohya Y., Iino T. (1990) Transcriptional analysis of the flagellar regulon of Salmonella typhimurium. *J Bacteriol* **172:** 741-747

Laubacher M. E., Ades S. E. (2008) The Rcs phosphorelay is a cell envelope stress response activated by peptidoglycan stress and contributes to intrinsic antibiotic resistance. *J Bacteriol* **190:** 2065-2074

Lazova M. D., Butler M. T., Shimizu T. S., Harshey R. M. (2012) Salmonella chemoreceptors McpB and McpC mediate a repellent response to L-cystine: a potential mechanism to avoid oxidative conditions. *Mol Microbiol* **84:** 697-711

Lehnen D., Blumer C., Polen T., Wackwitz B., Wendisch V. F., Unden G. (2002) LrhA as a new transcriptional key regulator of flagella, motility and chemotaxis genes in Escherichia coli. *Mol Microbiol* **45:** 521-532

Li H., Sourjik V. (2011) Assembly and stability of flagellar motor in Escherichia coli. *Mol Microbiol* **80:** 886-899

Lin J., Lee I. S., Frey J., Slonczewski J. L., Foster J. W. (1995) Comparative analysis of extreme acid survival in Salmonella typhimurium, Shigella flexneri, and Escherichia coli. *J Bacteriol* **177:** 4097-4104

Liu R., Ochman H. (2007) Origins of flagellar gene operons and secondary flagellar systems. *J Bacteriol* **189:** 7098-7104

Liu X., Matsumura P. (1994) The FlhD/FlhC complex, a transcriptional activator of the Escherichia coli flagellar class II operons. *J Bacteriol* **176:** 7345-7351

Macnab R. M. (2003) How bacteria assemble flagella. *Annu Rev Microbiol* **57:** 77-100

Matsuyama T., Kaneda K., Nakagawa Y., Isa K., Hara-Hotta H., Yano I. (1992) A novel extracellular cyclic lipopeptide which promotes flagellum-dependent and -independent spreading growth of Serratia marcescens. *J Bacteriol* **174:** 1769-1776

McClelland M., Sanderson K. E., Spieth J., Clifton S. W., Latreille P., Courtney L., Porwollik S., Ali J., Dante M., Du F., Hou S., Layman D., Leonard S., Nguyen C., Scott K., Holmes A., Grewal N., Mulvaney E., Ryan E., Sun H., Florea L., Miller W., Stoneking T., Nhan M., Waterston R., Wilson R. K. (2001) Complete genome sequence of Salmonella enterica serovar Typhimurium LT2. *Nature* **413:** 852-856

Merdanovic M., Clausen T., Kaiser M., Huber R., Ehrmann M. (2011) Protein quality control in the bacterial periplasm. *Annu Rev Microbiol* **65:** 149-168

Minamino T., Iino T., Kutuskake K. (1994) Molecular characterization of the Salmonella typhimurium flhB operon and its protein products. *J Bacteriol* **176:** 7630-7637

Minamino T., Imada K., Namba K. (2008) Mechanisms of type III protein export for bacterial flagellar assembly. *Mol Biosyst* **4:** 1105-1115

Minamino T., Macnab R. M. (1999) Components of the Salmonella flagellar export apparatus and classification of export substrates. *J Bacteriol* **181:** 1388-1394

Minamino T., MacNab R. M. (2000) Interactions among components of the Salmonella flagellar export apparatus and its substrates. *Mol Microbiol* **35:** 1052-1064

Minamino T., Namba K. (2008) Distinct roles of the FliI ATPase and proton motive force in bacterial flagellar protein export. *Nature* **451:** 485-488

Moriya N., Minamino T., Hughes K. T., Macnab R. M., Namba K. (2006) The type III flagellar export specificity switch is dependent on FliK ruler and a molecular clock. *J Mol Biol* **359:** 466-477

Muller H. A., Sinn M. (1977) [Thin-layer chromatography of sugars (author's transl)]. *Clin Chim Acta* **78:** 17-21

Namba K. (2001) Roles of partly unfolded conformations in macromolecular self-assembly. *Genes Cells* **6:** 1-12

Nambu T., Kutsukake K. (2000) The Salmonella FlgA protein, a putativeve periplasmic chaperone essential for flagellar P ring formation. *Microbiol* **146 (Pt 5):** 1171-1178

Nambu T., Minamino T., Macnab R. M., Kutsukake K. (1999) Peptidoglycan-hydrolyzing activity of the FlgJ protein, essential for flagellar rod formation in Salmonella typhimurium. *J Bacteriol* **181:** 1555-1561

Ohnishi K., Ohto Y., Aizawa S., Macnab R. M., Iino T. (1994) FlgD is a scaffolding protein needed for flagellar hook assembly in Salmonella typhimurium. *J Bacteriol* **176:** 2272-2281

Otwinowski Z., Minor W. (1997) Processing of X-ray diffraction data collected in oscillation mode. *Method Enzymol* **276:** 307-326

Parkinson J. S. (1978) Complementation analysis and deletion mapping of Escherichia coli mutants defective in chemotaxis. *J Bacteriol* **135:** 45-53

Parsot C., Hamiaux C., Page A. L. (2003) The various and varying roles of specific chaperones in type III secretion systems. *Curr Opin Microbiol* **6:** 7-14

Patterson-Delafield J., Martinez R. J., Stocker B. A., Yamaguchi S. (1973) A new fla gene in Salmonella typhimurium--flaR--and its mutant phenotype-superhooks. *Arch Mikrobiol* **90:** 107-120

Paul K., Erhardt M., Hirano T., Blair D. F., Hughes K. T. (2008) Energy source of flagellar type III secretion. *Nature* **451:** 489-492

Paul K., Nieto V., Carlquist W. C., Blair D. F., Harshey R. M. (2010) The c-di-GMP binding protein YcgR controls flagellar motor direction and speed to affect chemotaxis by a "backstop brake" mechanism. *Mol Cell* **38:** 128-139

Porter S. L., Wadhams G. H., Armitage J. P. (2011) Signal processing in complex chemotaxis pathways. *Nat Rev Microbiol* **9:** 153-165

Raivio T. L. (2005) Envelope stress responses and Gram-negative bacterial pathogenesis. *Mol Microbiol* **56:** 1119-1128

Rauprich O., Matsushita M., Weijer C. J., Siegert F., Esipov S. E., Shapiro J. A. (1996) Periodic phenomena in Proteus mirabilis swarm colony development. *J Bacteriol* **178:** 6525-6538

Repaske D. R., Adler J. (1981) Change in intracellular pH of Escherichia coli mediates the chemotactic response to certain attractants and repellents. *J Bacteriol* **145:** 1196-1208

Rowley G., Spector M., Kormanec J., Roberts M. (2006) Pushing the envelope: extracytoplasmic stress responses in bacterial pathogens. *Nat Rev Microbiol* **4:** 383-394

Rychlik I., Barrow P. A. (2005) Salmonella stress management and its relevance to behaviour during intestinal colonisation and infection. *FEMS Microbiol Rev* **29:** 1021-1040

Saini S., Brown J. D., Aldridge P. D., Rao C. V. (2008) FliZ Is a posttranslational activator of FlhD4C2-dependent flagellar gene expression. *J Bacteriol* **190:** 4979-4988

Saini S., Floess E., Aldridge C., Brown J., Aldridge P. D., Rao C. V. (2011) Continuous control of flagellar gene expression by the sigma28-FlgM regulatory circuit in Salmonella enterica. *Mol Microbiol* **79:** 264-278

Sauer F. G., Mulvey M. A., Schilling J. D., Martinez J. J., Hultgren S. J. (2000) Bacterial pili: molecular mechanisms of pathogenesis. *Curr Opin Microbiol* **3:** 65-72

Schuch R., Maurelli A. T. (2001) MxiM and MxiJ, base elements of the Mxi-Spa type III secretion system of Shigella, interact with and stabilize the MxiD secretin in the cell envelope. *J Bacteriol* **183:** 6991-6998

Shaner N. C., Steinbach P. A., Tsien R. Y. (2005) A guide to choosing fluorescent proteins. *Nat Methods* **2:** 905-909

Shennawy I. E., Gee D. J., Horobin R. W., Aparicio S. R. (1984) Novel application of aniline blue. Fluorescent staining of glycogen and some protein structures. *Histochem* **81:** 93-98

Shibata S., Takahashi N., Chevance F. F., Karlinsey J. E., Hughes K. T., Aizawa S. (2007) FliK regulates flagellar hook length as an internal ruler. *Mol Microbiol* **64:** 1404-1415

Simm R., Morr M., Kader A., Nimtz M., Romling U. (2004) GGDEF and EAL domains inversely regulate cyclic di-GMP levels and transition from sessility to motility. *Mol Microbiol* **53:** 1123-1134

Smith H. O., Levine M. (1967) A phage P22 gene controlling integration of prophage. *Virol* **31:** 207-216

Sourjik V., Armitage J. P. (2010) Spatial organization in bacterial chemotaxis. *The EMBO J* **29:** 2724-2733

Stafford G. P., Hughes C. (2007) Salmonella typhimurium flhE, a conserved flagellar regulon gene required for swarming. *Microbiol* **153:** 541-547

Stokes J. L. (1956) Enzymatic aspects of gas formation by Salmonella. *J Bacteriol* **72:** 269-275

Takaya A., Erhardt M., Karata K., Winterberg K., Yamamoto T., Hughes K. T. (2012) YdiV: a dual function protein that targets FlhDC for ClpXP-dependent degradation by promoting release of DNA-bound FlhDC complex. *Mol Microbiol* **83:** 1268-1284

Tapley T. L., Franzmann T. M., Chakraborty S., Jakob U., Bardwell J. C. (2010) Protein refolding by pH-triggered chaperone binding and release. *Proc Natl Acad Sci U S A* **107:** 1071-1076

Toguchi A., Siano M., Burkart M., Harshey R. M. (2000) Genetics of swarming motility in Salmonella enterica serovar typhimurium: critical role for lipopolysaccharide. *J Bacteriol* **182:** 6308-6321

Turner L., Zhang R., Darnton N. C., Berg H. C. (2010) Visualization of Flagella during bacterial Swarming. *J Bacteriol* **192:** 3259-3267

Ueno T., Oosawa K., Aizawa S. (1992) M ring, S ring and proximal rod of the flagellar basal body of Salmonella typhimurium are composed of subunits of a single protein, FliF. *J Mol Biol* **227:** 672-677

Van Duyne G. D., Standaert R. F., Karplus P. A., Schreiber S. L., Clardy J. (1993) Atomic structures of the human immunophilin FKBP-12 complexes with FK506 and rapamycin. *J Mol Biol* **229:** 105-124

Wang Q., Frye J. G., McClelland M., Harshey R. M. (2004) Gene expression patterns during swarming in Salmonella typhimurium: genes specific to surface growth and putative new motility and pathogenicity genes. *Mol Microbiol* **52:** 169-187

Wang Q., Mariconda S., Suzuki A., McClelland M., Harshey R. M. (2006a) Uncovering a large set of genes that affect surface motility in Salmonella enterica serovar Typhimurium. *J Bacteriol* **188:** 7981-7984

Wang Q., Suzuki A., Mariconda S., Porwollik S., Harshey R. M. (2005) Sensing wetness: a new role for the bacterial flagellum. *EMBO J* **24:** 2034-2042

Wang Q., Zhao Y., McClelland M., Harshey R. M. (2007) The RcsCDB signaling system and swarming motility in Salmonella enterica serovar typhimurium: dual regulation of flagellar and SPI-2 virulence genes. *J Bacteriol* **189:** 8447-8457

Wang S., Fleming R. T., Westbrook E. M., Matsumura P., McKay D. B. (2006b) Structure of the Escherichia coli FlhDC complex, a prokaryotic heteromeric regulator of transcription. *J Mol Biol* **355:** 798-808

Wilks J. C., Slonczewski J. L. (2007) pH of the cytoplasm and periplasm of Escherichia coli: rapid measurement by green fluorescent protein fluorimetry. *J Bacteriol* **189:** 5601-5607

Winfield M. D., Groisman E. A. (2003) Role of nonhost environments in the lifestyles of Salmonella and Escherichia coli. *Appl Environ Microbiol* **69:** 3687-3694

Wollmann P., Zeth K. (2006) Expression, crystallization and preliminary X-ray analysis of the periplasmic stress sensory protein RseB from Escherichia coli. *Acta Crystallogr Sect F Struct Biol Cryst Commun* **62:** 895-898

Yamamoto S., Kutsukake K. (2006) FliT acts as an anti-FlhD2C2 factor in the transcriptional control of the flagellar regulon in Salmonella enterica serovar typhimurium. *J Bacteriol* **188:** 6703-6708

Yokoseki T., Kutsukake K., Ohnishi K., Iino T. (1995) Functional analysis of the flagellar genes in the fliD operon of Salmonella typhimurium. *Microbiol* **141 (Pt 7):** 1715-1722

Yonekura K., Maki S., Morgan D. G., DeRosier D. J., Vonderviszt F., Imada K., Namba K. (2000) The bacterial flagellar cap as the rotary promoter of flagellin self-assembly. *Science* **290:** 2148-2152